ACTA UNIVERSITATIS SZEGEDIENSIS

ACTA PHYSICA ET CHEMICA

NOVA SERIES

TOMUS XV 19 FASCICULI 1—2

SZEGED, HUNGARIA
1969

ACTA UNIVERSITATIS SZEGEDIENSIS

ACTA PHYSICA ET CHEMICA

NOVA SERIES

TOMUS XV FASCICULI 1—2

SZEGED, HUNGARIA
1969

Adiuvantibus

L. CSÁNYI, D. GÁL, J. I. HORVÁTH, K. KOVÁCS, F. MÁRTA, GY. SIPOS et F. SZÁNTÓ

redigit

ÁGOSTON BUDÓ

Edit

Facultas Scientiarum Naturalium Universitatis Szegediensis de Attila József nominatae

Editionem curant

J. GYULAI, M. HALMOS et I. GALIBA

Nota

Acta Phys. et Chem. Szeged

Szerkeszti

BUDÓ ÁGOSTON

A szerkesztőbizottság tagjai:

CSÁNYI L., GÁL D., HORVÁTH J. I., KOVÁCS K., MÁRTA F., SIPOS GY. és SZÁNTÓ F.

Kiadja

a József Attila Tudományegyetem Természettudományi Kara
(Szeged, Aradi Vértanúk tere 1.)

Szerkesztőbizottsági titkárok:

GYULAI J., HALMOS M. és GALIBA I.

Kiadványunk rövidítése:

Acta Phys. et Chem. Szeged

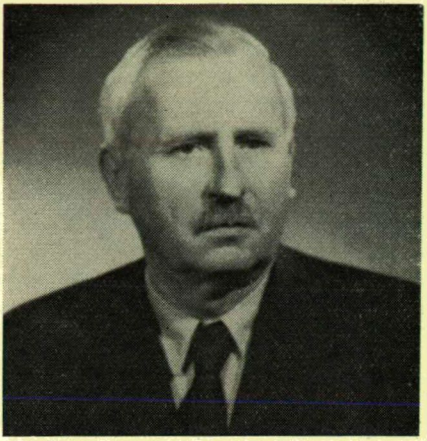

PROFESSOR ÁRPÁD KISS (1889—1968)

Dr. Árpád Kiss, the late Professor of the Institute of General and Physical Chemistry of the University of Szeged, was born in Sárospatak, Hungary, in 1889. Immediately after graduation at the University of Budapest in 1912 he began to work in the Institute of Chemistry No. 3 at the University of Budapest under the guidance of Professor Buchböck. At the beginning, his experiments and scientific publications were connected with radioactivity. Later he became interested in the kinetics of homogeneous gas reactions between nitrogen oxide and chlorine, which was also the topic of his doctoral thesis. Having obtained his PhD degree he continued his scientific work at the University of Budapest.

Unfortunately his valuable scientific work was interrupted by World War I. He was called to the Army, got wounded and fell into captivity at the Eastern Front. During his captivity he worked as a phyto-pathologist and later as a botanist at the Agricultural Experimental Station of Nikolsk-Ussurisk as an employee of the Soviet Geographical Society. In 1920 he returned to Hungary and continued his research work concerning homogeneous gas reactions at the University of Budapest.

His work called international attention and he was invited to the Institute of General and Inorganic Chemistry of the University of Leyden, where he participated in the research work and education as an Assistant Professor between 1922 and 1924. In these years his researches were connected with the investigation of catalytic gas reactions. He established that in the process of nitrozyl-chloride production catalyzed by bromine and nitrogen oxide, respectively, the reaction takes place through intermediate products. Considering the state of development of the theory of gas catalysis at that time, the results obtained in Leyden were of considerable importance.

In 1924 he was invited by the Faculty of Natural Sciences of the university of Szeged as a Professor of Chemistry. He returned to Hungary and henceforth he has been Professor of this University till his retirement in 1962. During this period he was twice the Dean of the Faculty of Natural Sciences and once the President of the University.

During his professorship his scientific work embraced almost every branch

of physical chemistry. In the first period his attention was given to the problems of reaction kinetics, especially to experimental checking of the Brönsted theory, primary and secondary kinetic salt-effect, kinetic effect of complex compounds, *etc.* He and his co-workers carried out pioneering work concerning the temperature dependence of the neutral salt-effect and the influence of salt concentration on activation energy.

In 1931 he directed his efforts towards a new field, the light absorption of electrolyte solutions, investigating the correlations between the light absorption and chemical structure of simple and complex compounds. He and his co-workers succeeded in producing the inner complexes of several metal ions, the existence of which was considered as questionable until then.

He elaborated a theory for the effect of ionization on the absorption spectra and on the solvent effect. Furthermore he improved the theory of oriented light absorption, interpreting the absorption spectra of several polycondensed organic molecules and the effect of the position of subtituents on the absorption spectra. In the recent years he planned to crown his scientific activity by a monograph entitled: „Interpretation of the Absorption Spectra of Coordination Compounds on the basis of the Ligand Field Theory". Death, however, prevented him to complete this monumental work.

Besides his work on the fields mentioned above, the investigation of the electrochemical corrosion of metals has also been started in Hungary under his guidance.

In 1953, as recognition of his remarkable scientific activity, he was elected corresponding member of the Hungarian Academy of Sciences. He also obtained from the Government the honours of Eminent Worker of Higher Education in 1953, the Order of the Labour in 1954, and the Kossuth-Prize in 1955.

Besides the Hungarian Chemical Society he was member of the American Chemical Society, of the Société Chimie de France and of the German Bunsen-Gesellschaft. Since 1945 he had been associate editor of the Zeitschrift für allgemeine und anorganische Chemie, a journal published in the German Democratic Republic.

Reflecting on the events of his life and the way he reacted to them and to other people's esteem, we have to acknowledge that as a scientist and as a man he belonged to the few who never changed and could retain a genuine modesty even when meeting with success and honours of the world, He devoted his life to scientific work and education. Even as a retired Professor he continued this work and he never ceased to give attention and help in problems of his students and his staff. He published his last paper, from the more than 150 written during his long scientific career, shortly before his 79th birthday.

He died the 10th November 1968 in a clinic of the University Medical School of Szeged, mourned by his wife, son, his earlier students and co-workers, and a host of friends throughout the world.

INVESTIGATIONS ON CONNECTIONS BETWEEN DECAY TIME OF FLUORESCENT SOLUTIONS AND OTHER FLUORESCENCE CHARACTERISTICS

By L. GÁTI

Institute of Experimental Physics, Attila József University, Szeged

(Received December 15, 1968)

Solutions of some organic compounds solved in alcohol and water with and without glycerol resp. were studied in order to determine the connection between the decay time τ and other luminescence characteristics, such as quantum yield, degree of polarisation, and intensity of absorption. The decay time was measured with the phase fluorometer built by the author. Our results, more exact in principle than earlier data, enabled us to clear up some of the incertainties found in literature. It could be shown among others that τ as a function of concentration has no maximum, which is at variance with numerous earlier investigations. The cases in which the proportionality between decay time and yield holds have been established. New results were found concerning the dependence of the molecular volume on viscosity of the solvent, and the determination of the decay time from the intensity of absorption.

1. Introduction

The decay time τ of fluorescent solutions depends on numerous factors, for example on constitution [1], [2] and viscosity of the solvent, the latter influencing also the degree of polarisation [3], [4], as well as on temperature and concentration of the solution, this latter considerably affecting also the quantum yeld [5]. Furthermore the dependence of the decay time on layer thickness, caused by secondary luminescence [6], [7], [8], has to be mentioned.

According to theory, τ is closely connected with other luminescence characteristics. Among these, the connection with the luminescence yield was the first to be discovered and the most extensely investigated [5], [9]. According to LEVSHIN [5], in the case of quenching, this connection can be given as follows

$$\frac{\eta}{\eta_0} = \frac{\tau}{\tau_0}, \tag{1}$$

where τ and η refer to the quenched, τ_0 and η_0 to the unquenched fluorescence respectively.

The results of numerous earlier investigations upon the dependence of the decay time on concentration showed considerable deviations from this proportionality (*e. g.* [7], [10]) but also some disturbing effects were found (*e. g.* [7], [11]) which could be ascribed to secondary luminescence. The decay time as a function of concentration, obtained with the method elaborated by BUDÓ and SZALAY [8] in order to eliminate this disturbing effects, as well as the yield values are constant up to the region of concentration quenching.

It has been shown [12] that the relation (1) is valid only in the case of dynamic quenching, *i. e.* if there is no quenching due to inactive absorption by dimers present

at high concentrations. In this case quenching is static and the decay time constant and independent from changes of concentration, whereas the yield value decreases with concentration. Therefore it seemed justified to study concentration quenching in connection with decay time in detail for different dyestuff solutions.

The decay time is also closely connected with the degree of polarisation p of fluorescence. The quantitative relation between p and τ can be expressed by the well-known PERRIN—LEVSHIN-formula [4], [13].

JABŁOŃSKI and SZYMANOWSKI showed in their researches on polarised luminescence [14], [15], [16] that the decay time generally depends on the degree of polarisation of the solution and the angle ϑ enclosed by the electric vector of the partially polarised luminescence light observed and that of the linearly polarised exciting light.

The results of Jabłoński were experimentally controlled by several authors (*e. g.* SZYMANOWSKI [16] and KESSEL [17]), but only qualitative accordance was found. Recently BAUER [18] proved the validity of Jabłoński's theory with very exact fluorometric and polarisation measurements for uranin in different solvents.

With respect to our earlier results [19], [20], which proved the linear Perrin—Levshin-relation to be satisfactorily valid and the fundamental polarisation p_0 as well as the quotient v/τ to be independent of viscosity, our aim was to investigate the dependence of the molecular volume v on the viscosity of the solvent by measuring the decay time τ and the degree of polarisation p.

EINSTEIN's relation [21] between the natural lifetime τ_e and the intensity of absorption (or oscillator strength) holds mainly for resonance radiation or fluorescence processes with very narrow bands of emission and absorption, as shown by the investigations of LADENBURG [22], TOLMAN [23], LEWIS and KASHA [24]. Einstein's relation has been modified by STRICKLER and BERG [25] for substances with broader, less characteristic spectra such as solutions of complex organic dyestuffs; later on BIRKS and DYSON [26] made further refinements, thus obtaining a more exact relation.

FÖRSTER [12], supposing the validity of Blokhintsev's rule of mirror-symmetry, gives another formula for the relation between τ_e and the area below the absorption spectra, involving the intensity of absorption and the so-called mirror-frequency.

Among several further relations (see *e. g.* [27], [28]) we have to emphasize KETSKEMÉTY's modification [29] of NEPÓRENT's formula [30], (see also [31]), involving τ instead of τ_e, as well as the molar extinction coefficient $\varepsilon(\nu)$ and the fluorescence quantum spectrum $f_q(\nu)$ belonging to the frequency ν instead of the integrated absorption spectrum.

In the following we give the formulas mentioned above:

EINSTEIN's modified formula

$$\frac{1}{\tau_e} = \frac{8\pi\nu^2 n^2 \ln 10}{10^{-3} N c^2} \frac{g_i}{g_j} \int_0^\infty \varepsilon(\nu)\, d\nu, \tag{2}$$

where ν is the frequency belonging to the transition $j \to i$, n the refractive index of the solution, g_i and g_j the statistical weights of the lower and the higher (excited) states respectively, $\varepsilon(\nu)$ the decadic molar extinction coefficient and N Avogadro's number.

The expression of BIRKS and DYSON

$$\frac{1}{\tau_e} = \frac{8\pi \ln 10}{10^{-3} N c^2} \frac{n_f^3}{n_a} \frac{g_i}{g_j} \overline{\nu_f^3} \int \frac{\varepsilon(\nu)}{\nu}\, d\nu; \tag{3}$$

here n_f and n_a are the mean refractive indices of the solution over the fluorescence and absorption spectra respectively and

$$\overline{\nu_f^3} = \frac{\int f_q(\nu)d\nu}{\int f_q(\nu)\nu_f^{-3}d\nu},$$

where $f_q(\nu)$ means the normalised quantum spectrum of fluorescence as a function of the frequency ν. In the expression of STRICKLER and BERG [25], instead of n_f^3/n_a in (3) only a factor n^2 is found, for it is assumed that $n_f=n_a=n$, *i.e.* the solution has no optical dispersion.

FÖRSTER's formula

$$\frac{1}{\tau_e} = \frac{8\pi \ln 10}{10^{-3}Nc^2} n^2 \int \frac{(2\nu_0-\nu)^3}{\nu} \varepsilon(\nu)d\nu. \tag{4}$$

ν_0 denoting the mirror-frequency, that it is the frequency belonging to the point of intersection of the absorption and emission spectra of the same height.

KETSKEMÉTY's modification of NEPORENT's formula, wich holds for mirror-simmentry between the absorption and emission spectra,

$$\tau = \frac{c^2 N 10^{-3}\eta_0^2 f_q(\nu)e^{-h(\nu_0-\nu)/kT}}{8\pi n^2\nu^2\eta(\nu)\varepsilon(\nu)\ln 10}, \tag{5}$$

where $\eta(\nu)$ and η_0 are the absolute quantum yield of the fluorescent solution and its maximal value respectively, and $f_q(\nu)$ is the normalised fluorescence spectrum.

Earlier values of τ calculated with the above equations generally resulted to be less than those measured with fluorometric methods, the deviations surpassing the limits of error of the measurements. Besides errors of measurements and spectral factors, these deviations can be interpreted mainly as effects of secondary luminescence due to reabsorption of fluorescence. Namely the decay time observed will be apparently increased by the effect of secondary luminescence [8]. The true decay time τ corrected for secondary luminescence may result considerably less than the directly measured decay time τ'; with other words the fact that the calculated decay times are less than the measured values for must of the dyestuffs studied hitherto is to be attributed at least partly to the effect of secondary luminescence. Therefore we had to examine the measured decay times obtained in our experiments also from this point of view.

2. *Experimental methods and evaluation of results*

a) The phase fluorometer constructed by the authors and described in [32] is based esentially upon the same principle as the apparatus of BAUER and ROZWADOWSKI [33]. The range of measurements with our fluorometer is about 0,1 to 30 nsec, and the absolute error of measurement less than 0,07 nsec for decay times of $\approx$3 to 4 nsec most frequently observed in dyestuff solutions.

In order to check the correct working of our apparatus and to make the necessary corrections, various calibrating tests ewre made. We measured *e.g.* the degree of modulation of the modulating unit, the electron transit time of the photomultipliers as a function of the intensity and wavelength of exciting light and of fluorescence light, *etc.* [32].

b) Measurements of other luminescence characteristics were made with the following methods.

Absorption and emission spectra were measured with a recording spectrophotometer Optica (Milano) type CF 4 DR and the fluorometric attachment constructed for this purpose [34]. Emission spectra were corrected for reabsorption [12]; in this way, provided the necessary conditions given in [35] were fulfilled we obtained the true fluorescence spectra with very good approximation.

The absolute quantum yield was measured with the instrument constructed and described by DOMBI [36]; the true quantum yield was calculated from the observed yield with suitable corrections [35].

Table I

1	2	3	4	5	6
N°	Fluorescent compound	Concentration range (in mole/l)	Solvent	Additive agent	number of solutions studied
1	Fluorescein	$1\times10^{-6}-2\times10^{-2}$	H_2O	2.5×10^{-1} mole/l NaOH	14
2	Fluorescein	$1\times10^{-6}-5\times10^{-2}$	85%EtOH+15%H_2O	10^{-2} mole/l and 2.5×10^{-1} mole/l NaOH	12
3	Fluorescein	1×10^{-4}	0–96% glycerol+water	2.5×10^{-1} mole/l NaOH	9
4	Eosine	$2\times10^{-6}-2\times10^{-2}$	85%EtOH+15%H_2O	10^{-2}, 3×10^{-1} and 5×10^{-1} mole/l NaOH	15
5	Trypaflavine	$1\times10^{-5}-8\times10^{-2}$	85%EtOH+15%H_2O	2%CH_3COOH	10
6	Trypaflavine	2×10^{-4}	0–96% glycerol+water	2%CH_3COOH	10
7	Quinine sulphate	$1\times10^{-5}-1\times10^{-1}$	H_2O	In H_2SO_4	7

The degree of polarisation in viscous solutions was measured with our apparatus described in [37], and partly with its modification [38]. The true degree of polarisation was determined with the method given in [29] and [39] and partly also with our simpler method of correction described in [20].

The viscosity of solutions containing glycerol was measured with Höppler's viscosimeter, the density of the solutions with a picnometric method and the refractive index with Abbe's refractometer.

c) In our investigations upon decay time and other luminescence characteristics we used solutions of organic compounds (trypaflavine, eosine, fluorescein and quinine sulphate) of sufficiently high quantum yield and with absorption and emission spectra lying mainly in the visible range.

The dyestuffs of different provenience were subjected to careful and repeated chemical purification, until the extinction coefficient of the materials proved to be constant.

The compounds, solvents and additional agents used in our investigations and there respective ranges of concentration are given in Table I.

d) The true decay time τ was determined from the measured value τ using BUDÓ and SZALAY's [8] as well as our own method [32]. According to the first method

$$\tau = \tau'(1-\varkappa) \tag{6}$$

where $\varkappa$ is the quotient of the secondary and primary fluorescence sensed by the measuring device, defined by BUDÓ and KETSKEMÉTY in [35]. Using Eq. (6) and an expanded form of the expresion for $\varkappa$, we have given in [32] a simpler method for calculating the true decay time τ which leads to the following approximative formula:

$$\tau = \frac{l_2 l_3 \lg \frac{l_3}{l_2} + l_3 l_1 \lg \frac{l_1}{l_3} + l_1 l_2 \lg \frac{l_2}{l_1}}{\frac{1}{\tau_1'} l_2 l_3 \lg \frac{l_3}{l_2} + \frac{1}{\tau_2'} l_3 l_1 \lg \frac{l_1}{l_3} + \frac{1}{\tau_3'} l_1 l_2 \lg \frac{l_2}{l_1}} \tag{7}$$

where $\tau_i'(i=1, 2, 3)$ are the decay times measured with the corresponding layer thicknesses l_i.

3. *Investigations upon the dependence of decay time and quantum yield on concentration*

The connection between τ and η was studied for three dyestuffs (fluorescein, eosine and trypaflavine) in aqueous and alcoholic solutions. These measurements were made with exciting light of 436 nm wavelength; τ for quinine sulphate was measured with 365 nm exciting wavelength. The layer thicknesses of

the solutions of different concentration (10^{-3} cm—0,5 cm) were chosen with respect to the conditions of applicability of the method of correction for secondary luminescence (for details see [35]).

From our results, Table II shows the dependence on the molar concentration c_M of η_λ and τ measured in aqueous solutions of fluorescein, Table III the values of τ and τ/τ_0 for aqueous solutions of quinine sulphate containing sulfuric acid, with different concentrations and layer thicknesses. The subscript 0 denotes the true yields and decay times obtained with very low concentrations.

Table II

Fluorescein (H_2O, 1% NaOH)

1	2	3	4	5	6	7
N°	c_M (in mole/l)	η_λ	τ (nsec)		η/η_0	τ/τ_0
			calc. acc. to (6)	calc. acc. to (7)		
1.	1×10^{-6}	0.90	3.30	3.32	1.02	0.97
2.	2×10^{-6}	0.89	3.39	3.10	1.01	1.00
3.	5×10^{-6}	0.95	3.37	3.36	1.08	0.99
4.	1×10^{-5}	0.78	3.46	3.59	0.89	1.02
5.	2×10^{-5}	0.80	3.41	3.28	0.91	1.00
6.	5×10^{-5}	0.89	3.29	3.36	1.01	0.97
7.	1×10^{-4}	0.88	3.46	3.37	1.00	1.02
8.	2×10^{-4}	0.86	3.50	3.23	0.98	1.03
9.	5×10^{-4}	0.87	3.46	3.27	0.99	1.02
10.	1×10^{-3}	0.87	3.35	3.12	0.99	0.99
11.	2×10^{-3}	0.74	3.25	3.43	0.85	0.96
12.	5×10^{-3}	0.53	2.58	2.60	0.60	0.76
13.	1×10^{-2}	0.17	1.31	1.33	0.19	0.39
14.	2×10^{-2}	0.05	0.32	0.15	0.06	0.09

Table III

Decay time of quinine sulphate (1n H_2SO_4)

1	2	3	4	5	6	7	8	9	10
c_M (in mole/l)	l (in cm)							mean value	$\frac{\tau}{\tau_0}$
	0.001	0.005	0.01	0.02	0.05	0.1002	0.5001		
	τ (nsec)								
1×10^{-5}						19.76	18.90	19.33	1.00
1×10^{-4}				18.63		19.09	19.87	19.19	0.99
1×10^{-3}			18.29		18.69	19.06	18.47	18.62	0.96
3×10^{-3}		16.90						16.90	0.87
1×10^{-2}	16.42				14.53		14.41	15.12	0.78
5×10^{-2}	9.41							9.41	0.49
1×10^{-2}	6.59		5.91			6.63		6.37	0.33

The curves in Fig. 1 show the dependence on c_M of the quotients η/η_0 and τ/τ_0 for the five solutions studied.

Our investigations performed to check the connections between the true decay time τ and the quantum yield η led to the following results.

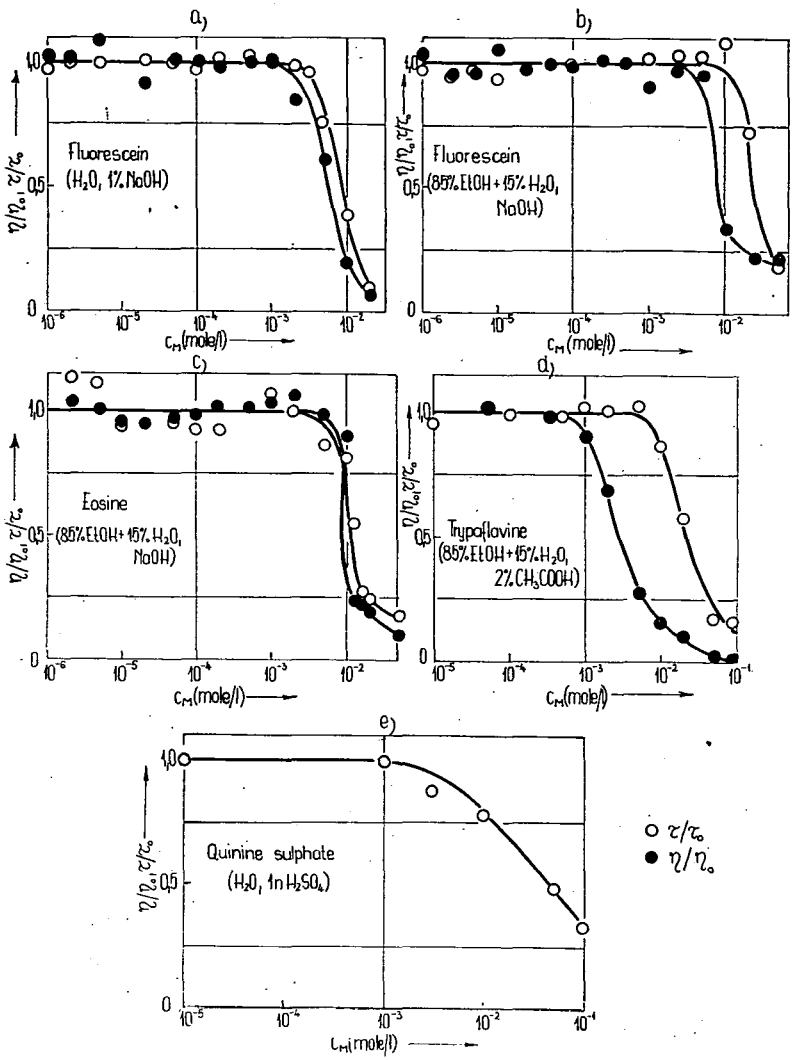

Fig. 1

a) The dependence of η on c_M found in our measurements with aqueous and alcoholic solutions of fluorescein and alcoholic solutions of eosine and trypaflavine confirmed the results of earlier investigations [40], [41].

b) Contrary to earlier results [7], [11], the curves $\tau = \tau(c_M)$ show no rise or maximum, but have a constant value up to the threshold concentration, like the initial portions of the curves $\eta = \eta(c_M)$.

c) The proportionality between $\tau(c_M)$ and $\eta(c_M)$ is approximately fulfilled for aqueous solutions of fluorescein and alcoholic solutions of eosine, in contradiction to results of some earlier investigations [6], [42].

d) This proportionality does not hold for alcoholic solutions of trypaflavine and fluorescein, in which τ/τ_0 begins to decrease at higher concentrations than η/η_0. The fact that no significant changes in absorption spectra were observed in the concentration range studied proves that there occurs no considerable dimerisation in the systems used. Accordingly the divergences from proportionality cannot be ascribed to static quenching produced by dimerisation but are probably due to the circumstance that the exponential law does not hold for the quenching at higher concentrations, as suggested by GALANIN [6], or to the occurence of initial quenching, discussed also by FÖRSTER [12]. Furthermore it may be supposed, according to VIEROSANU [43], that the „deformed" molecules behave like associated dimer molecules with respect to concentration quenching, the presence of both kind of molecules causing inactive absorption.

e) Our experimental results confirm the observation that the directly measured decay times of dyestuff solutions show considerable changes with the layer thickness as a consequence of secondary luminescence.

4. Investigations upon the decay time of viscous dyestuff solutions

In order to clear up the dependence of the molecular volume v on the viscosity of the solvent, we made measurements with aqueous solutions of fluorescein and alcoholic solutions of trypaflavine, both containing glycerol. In these solutions we measured the decay times $\tau^{\parallel}$, $\tau^{\perp}$ and τ_{55} of the components of luminescence light, oscillating in planes with $\vartheta = 0$, 90° and 55° respectively. These measurements were made with layer thicknesses of 0.1 and 0.25 cm for fluorescein, and 0.02, 0.05 and 0.1 cm for trypaflavine. The true decay times were calculated with Eq. (6) and with Eqs. (6) and (7) respectively. The values of τ obtained with both methods were in agreement within the limits of error.

The degree of polarisation for both solutions was measured with the layer thicknesses employed for the measurement of τ; the solutions, held at constant temperature of (30 ± 0.1 °C), were excited with the mercury line of 436 nm wavelength.

Table IV

1×10^{-4} mole/l fluorescein (glycerol + water, 1% NaOH)

1	2	3	4	5	6	7	8	9	10	11	12	13	14
N°	Glycerol cont. (%)	$10^2 \times \eta_v$ (poise)	$1/\eta_v$ (1/poise)	p	$1/p$	r	$1/r$	$\tau^{\parallel}$	τ_{55}	$\tau^{\perp}$	τ (nsec)	$\tau^{\parallel}/\tau$	$\tau^{\perp}/\tau$
1	0	0.90	110.5	0.013	79.05	0.0085	118.08	3.09	3.50	3.27	3.21	0.961	1.019
2	15	1.47	68.0	0.023	43.76	0.015	65.15	3.25	3.48	3.49	3.41	0.954	1.024
3	30	2.68	37.3	0.056	17.72	0.038	26.08	3.21	3.54	3.57	3.44	0.934	1.037
4	45	5.11	19.5	0.097	10.29	0.067	14.94	3.14	3.17	3.44	3.33	0.944	1.034
5	50	6.60	15.1	0.114	8.75	0.079	12.63	3.11	3.17	3.44	3.31	0.940	1.039
6	65	16.50	6.06	0.186	5.38	0.132	7.56	2.95	3.26	3.36	3.19	0.924	1.055
7	75	36.92	2.70	0.269	3.71	0.197	5.07	2.62	3.13	3.41	3.04	0.859	1.121
8	85	107.58	0.92	0.356	2.81	0.269	3.72	2.60	3.03	3.46	3.02	0.861	1.146
9	96	386.29	0.25	0.426	2.35	0.331	3.02	2.66	2.92	3.22	2.86	0.929	1.124

Table IV contains the true degrees of polarisation p obtained from the measurements, the anisotropy of emission r, calculated with the formula $r = 2p/(3-p)$, and their inverse $1/p$ and $1/r$, the true decay times calculated from $\tau^{\parallel}$, $\tau^{\perp}$ and τ_{55} observed in the three directions of oscillation mentioned above, the value of τ calculated with JABŁOŃSKI's [44] equation

$$\tau = \tfrac{1}{3}\left[\tau^{\parallel}(1+2r)+2\tau^{\perp}(1-r)\right] \tag{8}$$

and the quotients $\tau^{\parallel}/\tau$ and $\tau^{\perp}/\tau$ for the aqueous solution of fluorescein containing glycerol.

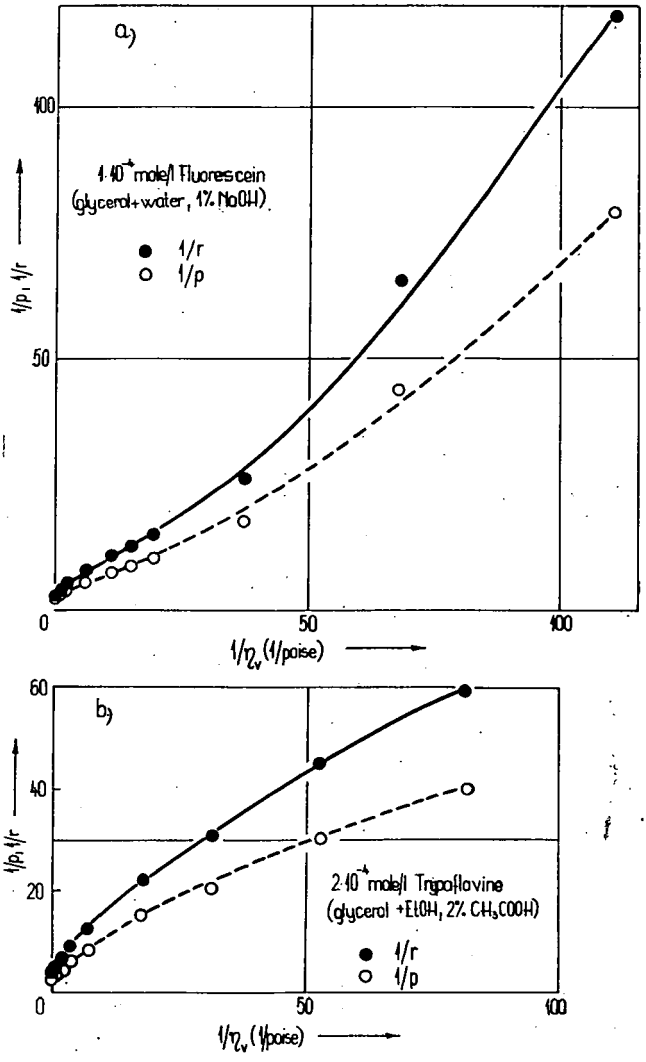

Fig. 2

Fig. 2 shows the values of $1/p$ and $1/r$ for both solutions as a function of $1/\eta_v$ as usual. The trend of deviation from linearity (Fig. 2a) is the same as observed by BAUER and SZCZUREK [45], though the measurements of these authors show greater deviations in consequence of their neglecting the effects of secondary luminescence. In the case of trypaflavine (Fig. 2b) we obtained curves concave from below for both $1/r$ and $1/p$ as a function of $1/\eta_v$, in accordance with measurements of SZALAY [19].

In Fig. 3 the fundamental emission anisotropy r_0, calculated with the method of JABŁOŃSKI [44], the molecular volume v, calculated with the Perrin—Levshin-relation from r_0 and the measured values of r, are given as function of the glycerol content expressed in per cent. The descending section of the curve r_0 for fluorescein solutions with low glycerol content, drawn with a broken line in Fig. 3a, cannot be

considered as reliable because of the errors of measurement. Apart from the section mentioned above, the shape of the curves r_0 and v is similar to those obtained by BAUER [18]. However, in our measurements we found the greatest change in v to be only of one and a half order of magnitude, against the changes of about three orders found by Bauer for both r_0 and v.

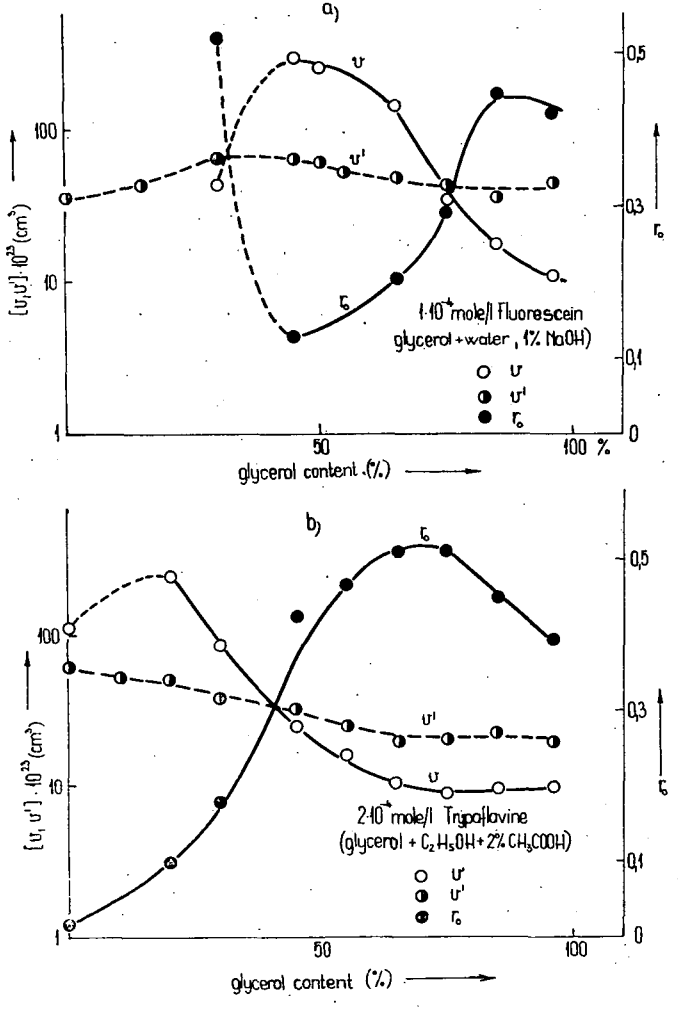

Fig. 3

The molecular volumes were also calculated by substituting the values of r_0 extrapolated for viscosity ∞ ($r_0 = 0.353$ for fluorescein and $r_0 = 0.345$ for trypaflavine) into the Perrin—Levshin-equation. The molecular volumes obtained in this way are shown by the curves marked with v' in Fig. 3. In the case of trypaflavine,

v' lies near to the molecular volumes calculated by SZALAY [19] with a similar method but supposing τ to be constant.

From our investigations on the decay time of polarised luminescence, it can be inferred that the molecular volume of the dyestuffs in solutions of different viscosity, using mixtures of water and glycerol, and of not dehydrated alcohol and glycerol respectively as solvents, increases with the decrease of the glycerol content, *i.e.* in the same direction as suggested by BAUER [18], however in a less extent. JABLOŃSKI and BAUER interpreted this increase with the great solvent capacity of water. Consequently, for our solutions the molecular volume will not be constant with changing τ and r_0, even if the Perrin—Levshin-relation is approximately fulfilled.

5 . Investigations upon the connection between τ and intensity of absorption

These calculations were made on the basis of the relations (3), (4) and (5), using the values of τ and η determined according to the above and the measured absorption and emission spectra.

Table V contains the measured values of τ_M corrected for secondary luminescence, τ_e and $\tau_{calc}(=\eta\tau_e)$, the absolute quantum yield η_λ measured with excitation at 436 nm wavelength, and the refractive index n_D of the solutions, as well as the mean values of the mirror wave numbers $\tilde{\nu}_0$ calculated with different methods. In the case of quinine sulphate τ_{calc} was calculated with the value $\eta_\lambda = 0.54$ taken from [46]. The values of τ_e and τ_{calc}, calculated with different methods, are to be found in columns 8 and 9 of the table in the following order: (F) calculated with Eq. (4), (S—B) with Eq. (3), and (N) with Eq. (5) respectively.

Our investigations led to the following conclusions.

a) The decay times $\tau_{calc}(=\eta\tau_e)$ calculated with FÖRSTER's formula (4) are in better agreement with our own measurements of τ_m (corrected for secondary luminescence) than with the results of earlier workers.

b) Calculations of τ_{calc} with the formulas of STRICKLER and BERG and BIRKS and DYSON respectively (3) are in very good agreement with our measurements for aqueous solutions of fluorescein in the case of not too high concentrations; an approximative accordance was found for fluorescein solutions containing glycerol, whereas solutions of trypaflavine with glycerol and of quinine sulphate showed significant divergences.

c) The values of τ_{calc} obtained with NEPORENT's modified relation (5), were in good agreement with our values of τ_m even in the case of solutions for which the relations mentioned under *a)* and *b)* did not prove valid.

d) For aqueous solutions of quinine sulphate, the results for τ_m calculated with all three relations differred considerably from our measured values. This can be ascribed to the circumstance that for quinine sulphate Blokhintsev's mirror-simmetry relation is not even approximately fulfilled.

It can be stated that the decay times obtained theoretically and the values determined from our measurements with a method more exact in principle than those used earlier are in good agreement in every case when this is to be expected

Table V

1	2	3	4	5	6	7		8	9	10	11
N°	Fluorescent compound; c_M (in mole/l)	Solvent; additive agent	η_λ	$\tilde{\nu}_0 \times 10^{-3}$ (cm^{-1})	$\bar{\tilde{\nu}}^3 \times 10^{-12}$ (cm^{-3})	n		(nsec) τ_e	(nsec) τ_{calc}	(nsec) τ_m	$\frac{\tau_{calc}}{\tau_m}$
1	Fluorescein 1×10^{-4}	water; 1% NaOH	0.88	19.96	6.881	1.3379	F	4.41	3.88		1.11
							S—B	4.06	3.57	3.50	1.02
							N	4.23	3.72		1.06
2	Fluorescein 1×10^{-4}	85% ethanol, 15% water; 1×10^{-2} mole/l NaOH	0.99	19.67	6.569	1.3662	F	4.27	4.23		1.23
							S—B	4.33	4.29	3.43	1.25
							N	3.34	3.31		0.97
3	Fluorescein 1×10^{-4}	96% glycerol; 1% NaOH	0.86	19.68	6.250	1.4678	F	3.77	3.24		1.11
							S—B	4.03	3.47	2.92	1.19
							N	2.53	2.18		0.75
4	Eosine 5×10^{-5}	85% ethanol, 15% water; 1×10^{-2} mole/l NaOH	0.76	18.81	5.681	1.3640	F	3.95	3.00		1.46
							S—B	4.18	3.18	2.06	1.54
							N	3.07	2.33		1.13
5	Trypaflavine 5×10^{-5}	85% ethanol, 15% water; 2% CH_3COOH	0.77	21.05	7.703	1.3605	F	3.64	2.80		0.84
							S—B	3.70	2.84	3.34	0.85
							N	3.96	3.05		0.91
6	Trypaflavine 1×10^{-4}	96% glycerol: 2% CH_3COOH	0.88	20.92	7.276	1.4699	F	3.43	3.02		0.83
							S—B	3.47	3.05	3.63	0.84
							N	4.44	3.91		1.08
7	Quinine sulphate 1×10^{-5}	water; 1n H_2SO_4	0.54	25.30	9.532	1.3387	F	10.17	5.49		0.28
							S—B	9.24	4.99	19.33	0.26
							N	9.33	5.05		0.26

by virtue of the shape and mutual position of the emission and absorption spectra. This result is to be considered as an experimental confirmation of the theories on the decay time.

* * *

The author is indebted to sincere thanks to Prof. A. BUDÓ, director of the Institute for Experimental Physics, for valuable discussions and to Prof. I. KETSKEMÉTY for highly useful suggestions during the measurements and calculations.

References

[1] *Galanin, M. D.:* Dokl. Akad. Nauk SSSR, **57**, 883 (1947).
[2] *Rohatgi, K. K.:* Z. Phys. Chem. **217**, 353 (1961).
[3] *Perrin, F.:* C. R. Acad. Sci., **182**, 219 (1926).
[4] *Perrin, F.:* J. Phys. Rad., **7**, 390 (1926); Ann. Phys. (Paris), **12**, 169 (1929); Acta Phys. Polon. **5**, 335 (1936).
[5] *Levshin, V. L.:* Fotolyuminestsentsia zhidkikh i tverdykh veshchestv (Gosudarstv. Izd. Moskva, Leningrad, 1951).
[6] *Galanin, M. D.:* Trudy FIAN SSSR, **5**, 339 (1950); **12**, 3 (1960).
[7] *Schmillen, A.:* Z. Phys., **135**, 294 (1953); Z. Angew. Phys., **6**, 260 (1954).
[8] *Budó, A.:* Magyar Fiz. Folyóirat, **9**, 269 (1961);
Budó, A., L. Szalay: Z. Naturforsch., **18a**, 90 (1963).
[9] *Vavilov, S. I., V. L. Levshin:* Phys. Zs., **8**, 173 (1922).
[10] *Vavilov, S. I.:* Die Mikrostruktur des Lichtes (Akad.-Verlag, Berlin, 1954).
[11] *Bonch-Bruevich, A. M.:* Uspekhi Fiz. Nauk. SSSR, **58**, 85 (1956); Izv. Akad. Nauk. SSSR, Ser. Fiz., **20**, 591 (1956).
[12] *Förster, Th.:* Fluoreszenz Organischer Verbindungen (Vandenhoeck und Ruprecht, Göttingen, 1951).
[13] *Levshin, V. L.:* Z. Phys., **32**, 307 (1925); Trudy FIAN SSSR, **1**, 19 (1938).
[14] *Jabloński, A., W. Szymanowski:* Nature, **135**, 582 (1935).
[15] *Jabloński, A.:* Z. Phys., **95**, 53 (1935); **103**, 526 (1963); Z. Naturforsch., **16a**, 1 (1961).
[16] *Szymanowski, W.:* Z. Phys., **95**, 440, 450, 460, 466 (1935).
[17] *Kessel, W.:* Z. Phys., **103**, 125 (1936).
[18] *Bauer, R. K.:* Z. Naturforsch., **18a**, 718 (1963).
[19] *Szalay, L.:* Thesis for the Doctor of Physics degree of the Hungarian Academy of Sciences, Szeged, 1964.
[20] *Gáti, L., L. Szalay:* Acta Phys. Chem. Szeged, **4**, 90 (1958);
Gáti, L.: Doctoral dissertation, Szeged, 1958.
[21] *Einstein, A.:* Phys. Zs., **18**, 121 (1917).
[22] *Ladenburg, R. A.:* Z. Phys., **4**, 451 (1921).
[23] *Tolman, R. S.:* Phys. Rev., **23**, 963 (1924).
[24] *Lewis, G. N., M. Kasha:* J. Amer. Chem. Soc., **67**, 994 (1945).
[25] *Strickler, S. J., R. A. Berg:* J. Chem. Phys., **37**, 814 (1962).
[26] *Birks, J. B., D. J. Dyson:* Proc. Phys. Soc., **275**, 135 (1963).
[27] *Neporent, B. S., N. G. Bakhshiev:* Optikai i Spektrosk., **5**, 634 (1958).
[28] *Berlman, J. B.:* Proceedings of the International Conference on Luminescence, 1966. (Akad. Kiadó, Budapest, 1968), Vol. 1., p. 514—519.
[29] *Ketskeméty, I.:* Thesis for the Doctor of Physics degree of the Hungarian Academy of Sciences, Szeged, 1963.
[30] *Neporent, B. S.:* Izv. Akad. Nauk SSSR, Ser. Fiz., **22**, 1372 (1958).
[31] *Budó, A.:* Proceedings of the International Conference on Luminescence 1966. (Akad. Kiadó, Budapest, 1968). Vol. 1, p. 146—159.
[32] *Gáti, L., I. Szalma:* Acta Phys. Chem. Szeged, **14**, 3 (1968).
[33] *Bauer, R. K., M. Rozwadowski:* Bull. Acad. Polon. Sci. Ser. Sci. Math. Astron. Phys., **7**, 365 (1959).
[34] *Török, M.:* Doctoral dissertation, Szeged, 1967.
[35] *Budó, A., I. Ketskeméty:* J. Chem. Phys., **25**, 595 (1956); Acta Phys. Hungar., **7**, 207 (1957).
[36] *Dombi, J.:* Thesis for the Candidate degree of the Hungarian Academy of Sciences, Szeged, 1967.
[37] *Ketskeméty, I., L. Gargya, E. Salkovits:* Acta Phys. Chem. Szeged, **3**, 16 (1957).
[38] *Vize, L.:* Acta Phys. Chem., Szeged, **15**, 27 (1969).
[39] *Budó, A.:* Magyar Fiz. Folyóirat, **9**, 269, (1961);
Budó, A., I. Ketskeméty: Acta Phys. Hungar., **14**, 167 (1962).

[40] *Vavilov, S. I.:* Z. Phys., **31**, 750 (1924).
[41] *Bouchard, I.:* J. Chim. Phys., **33**, 51, 127 (1936).
[42] *Vavilov, S. I.:* Izv. Akad. Nauk SSSR, Ser. Fiz., **9**, 277, 283 (1945).
[43] *Vieroşanu, I.:* Proceedings of the International Conference on Luminescence, 1966, (Akad. Kiadó, Budapest, 1968). Vol. 1., p. 462—467.
[44] *Jabłoński A.:* Lum. of Org. and Inorg. Mat. (J. Wiley & Sons. Inc., 1962); Acta Phys. Polon., **26**, 427 (1964); **28**, 717 (1965).
[45] *Bauer, R., T. Szczurek:* Acta Phys. Polon., **22**, 29 (1962).
[46] *Melhuish, W. M.:* J. Phys. Chem., **64**, 762, (1960); **65**, 229 (1961).

ИЗУЧЕНИЕ ВЗАИМОСВЯЗИ МЕЖДУ ВРЕМЕНИ ЗАТУХАНИЯ И ДРУГИМИ ХАРАКТЕРИСТИКАМИ ФЛУОРЕСЦЕНЦИИ

Л. Гати

Исследовалась взаимосвязь между длительностью флуоресценции τ и другими ее характеристиками, т. е. выходом, степенью поляризации, интенсивностью поглащения у некоторых органических соединений, растворенных в спирте, воде и глицерине.

Время затухания флуоресценции определялось авторами на сконструированном ими фазовом флуорометре.

Полученные результаты, которые теоретически точнее предыдущих, дали возможность выяснить им некоторые неопределенности литературных данных. Установили, что τ как функция концентрации, в отличии от многочисленных предыдущих исследований, не имеет максимума, и также в каких условиях выполняется пропорциональность между временем затухания и выходом люминесценции. Получили новые данные о взаимосвязи объема молекулы от функции вязкости растворителя, и также для определения времени естественного затухания из интенсивности поглащения.

INFLUENCE OF DIFFUSION ON THE ENERGY MIGRATION IN MIXED SOLUTIONS

By Z. VÁRKONYI

Institute of Experimental Physics, Attila József University, Szeged

(Received, November 25, 1968)

The quenching of luminescence of trypaflavine by rhodamine B in aqueous solutions was studied with quencher concentrations from 6×10^{-5} to 2×10^{-3} mole/litre in the viscosity interval 0,01—20 poise and at temperatures between 0 °C and 50 °C. The experimental results are discussed in terms of Förster's and Jabłoński's model. It has been found that the diffusion is not to be neglected in the region of lower viscosities and a quantitative relation taking the diffusion into account is given. The energy transfer proved to be greater even with respect to the diffusion than predicted by the theories of Förster and Jabłoński.

Introduction

According to FÖRSTER's theory of energy migration [1], [2] the probability of energy migration (if the mutual position of excited and quenching molecules is not altered in the excited state) can be expressed as follows:

$$n_{AL} = \frac{1}{\tau_{0A}} \left(\frac{R_0}{R}\right)^6 \tag{1}$$

where τ_{0A}, R and R_0 denote the mean life-time of the excited state of the molecule A in absence of the quenching molecule L, the mean distance between the excited molecule A^* and the quenching molecule L, and the critical distance, respectively.

$$R_0 = \sqrt[6]{\frac{9\overline{\varkappa^2}(\ln 10)^2 c^2 \tau_{0A} I_{\bar{\nu}}}{16\pi^4 n^4 (N')^2 \bar{\nu}_0^2}}\,. \tag{2}$$

Here c is the velocity of light in vacuum, n is the refractive index of solution, $N' = 6.02\times10^{20}$, $\varkappa$ is a constant depending on the mutual orientation of the interacting molecules (in solutions, supposing total randomness, $\overline{\varkappa^2} = 2/3$), $\bar{\nu}_0$ denotes the wave-number of pure electron transition and $I_{\bar{\nu}}$ is the so-called overlap-integral. According to FÖRSTER [3] the following relation exists between the relative yield η/η_0 of the mixed solution and the concentration c of the equimolar solution:

$$\frac{\eta}{\eta_0} = 1 - \sqrt{\pi}\,\frac{c}{c_0}\cdot e^{\left(\frac{c}{c_0}\right)^2}\left[1 - \Phi\left(\frac{c}{c_0}\right)\right] \tag{3}$$

where the constant c_0 is the so-called critical concentration, $\Phi(c/c_0)$ the error-function;

supposing a random distribution of the molecules, c_0 and R_0 are connected by the following relation

$$R_0^3 = \frac{3}{2\sqrt{\pi^3}} \frac{1}{c_0}. \tag{4}$$

Using Eq. (3) and the experimental values of η/η_0, c_0 can be empirically obtained and then R_0 can be calculated with Eq. (4) The comparison of the R_0 values obtained from Eq. (2) and (4) is very useful in examining the validity of Försters's theory. For non-equimolar solutions using FÖRSTER's [3] and KETSKEMÉTY's [4] considerations, R_0 can be calculated with the following relation:

$$R_0^6 = \frac{9\varkappa^2 c^4}{128\pi^4 n^2 N' \tau} \int_0^\infty f_{qA}(\nu) \varepsilon_L(\nu) \frac{d\nu}{\nu^4}. \tag{5}$$

Here $f_{qA}(\nu)$ is the emission quantum spectrum of the donor molecule, and $\varepsilon_L(\nu)$ denotes the decadic molar extinction coefficient of the acceptor molecule. In the systems studied the additivity relation between the spectra of mixed solutions is fulfilled ([5], [6]), the donor does not practically absorb in the overlap region and Beer—Lambert's law is valid. The validity of the restrictions made in Förster's theory has been proved by GALANIN [7], LATT [8], DREXHAGE [9] BOWEN and LIVINGSTONE [10]. They found a good agreement between the values of R_0 determined from the quenching curves and those calculated with Eq. (2) and came to the conclusion that the yield of migration of the excitation energy does not depend substantially on the viscosity of the solvent.

On the other hand, some authors *e.g.* WEINREB [11] and MELHUISH [12] found that the energy transfer is enhanced by an increasing rate of diffusion. Recently several papers [13], [14], [15] point to the fact that the diffusive displacement of the molecules during the life-time of the excited state cannot be neglected. In the modification of Förster's quenching theory by BAGDASARYAN and MULER [13] also the influence of diffusion is taken into consideration. They found that the energy transfer is more effective than it is expected from Förster's theory. FEITELSON [14] obtained similar results for a p-terphenyl-9-methylanthracene system. The quenching process was treated by JABŁOŃSKI [15] on the base of a simplified model of the luminescent centers, which consists of the excited luminescent molecule and the surrounding „active sphere" and may also contain a quenching molecule. Jabłoński came to the following relation:

$$\frac{\eta}{\eta_0} = \frac{1 - e^{-v}}{v}, \tag{6}$$

where $v = nv$, n is the concentration of the quencher and v denotes the volume of the active sphere, which can be determined empirically. Jabłoński's theory [15], [16] has been further developed by HEVESI [17], [18] and BOJARSKI [19], [21]. Taking into consideration the influence of diffusion, Hevesi rewrote Eq. (6) in the following form:

$$\frac{\eta}{\eta_0} = \frac{1 - e^{-ac}}{ac}, \tag{7}$$

where c is the molar concentration of the quencher and $a = N \cdot v$. The volume of the active sphere v is a given function of η_v and of τ. BOJARSKI [19]—[21] completed Jabłoński's theory considering a multilayer luminescent centrum as model and taking into consideration the oscillation in the concentration of quenchers beyond the active sphere.

Composition of the systems and experimental methods

Two dyes (trypaflavine and rhodamine B) were chosen as donor and acceptor, for which the luminescence spectrum of the donor and the absorption spectrum of the acceptor showed a considerable overlap. The viscosity of the solutions was varied in a mixture of glycerol and water by changing the glycerol concentration (0, 60 and 90%) and the temperature (273, 298 and 323 °K). Measurements were made in the viscosity interval from 0.01 to 20 P. The trypaflavine concentration was kept constant (1.25×10^{-4} mole/litre), the concentrations of rodamine B were 6.25×10^{-5}, $1{,}25 \times 10^{-4}$, 2.5×10^{-4}, 5×10^{-4}, 1×10^{-3} and 2×10^{-3} mole/litre, respectively. In order to obtain better solubility of dyes and stabilization of solutions 1×10^{-3} mole/litre HCl was added.

The dyes were purified by recrystallization until constancy of spectra; the glycerol was purified with vacuum distillation.

The spectra and the relative yields were measured using a plane-grating single-beam autocollimating spectrophotometer Optica Milano Type CF 4., with adequate attachments [22]. The temperature was kept constant by a Höppler-type ultrathermostat. The methods described in [23], [6] were used to evaluate the experimental results. Fluorescence spectra were corrected for reabsorption; correction for secondary luminescence could be neglected due to the experimental conditions [24].

Experimental results and discussion

The results are shown in Figs. 1—3. The measured relative yields are plotted as a function of $\log \gamma$, $\left(\gamma = \frac{c}{c_0}\right)$. The quenching curves calculated by using Eq. (3) are drawn with a solid line. It can be seen from the figures that at 273 °K the agreement between the measured and the calculated values is very good; it is less satisfactory at 298 °K, whereas at 323 °K considerable deviations are to be found.

The agreement between calculated and measured data at 273 °K was very good in all sets of solutions at every value of viscosity. This does not mean, however, that the quenching at this temperature does not depend on viscosity. Namely, a comparison of the values of R_F obtained from Eq. (4) using the empirical values of c_0 with the R_0 obtained from the spectra shows that the values of R_0 are much less than those of R_F[1]. Thus it can be only concluded from the figures that Förster's

[1] In the following the critical distances obtained with different methods are marked by different subscripts. R_0 means the critical distance calculated with Eq. (5), R_F that calculated with Eq. (4), R_{BM} the value calculated with Eq. (8) in [13], R_J with Eq. (5) in [16], R_B with Eq. (22) in [20] and R_V calculated with Eq. (9).

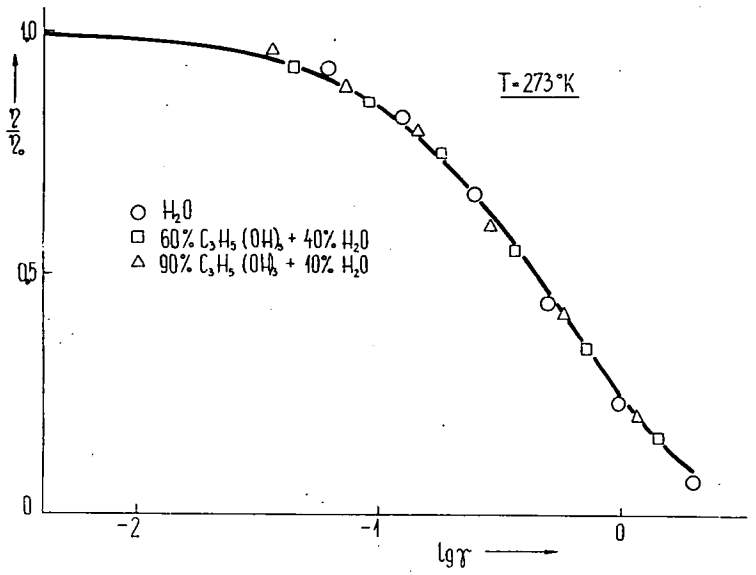

Fig. 1

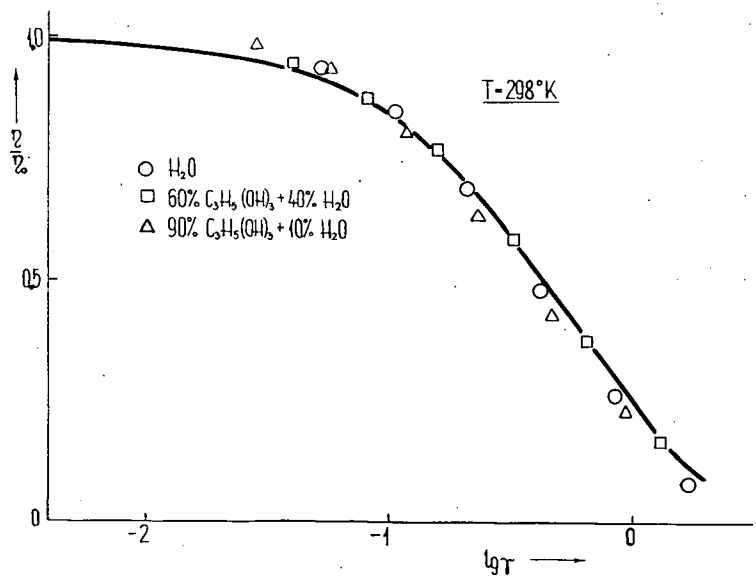

Fig. 2

theory gives a good description of the slope of the quenching curves for the temperature 273 °K.

According to the data of Table I the energy migration is more effective in

Table I

Solution	O_K^T	R_0	R_F	R_{BM}	R_J	R_B	R_V
		Å					
H_2O	273	59.0	75.8	73.4	115.5	75.7	58.4
	298	60.0	72.4	71.0	108.6	72.4	56.6
	323	58.2	61.2	62.5	90.9	63.4	54.9
60% glycerol	273	57.3	68.1	65.3	99.2	69.2	65.3
	298	58.2	66.2	63.4	94.3	66.2	59.3
	323	55.9	59.0	58.7	89.3	61.2	55.2
90% glycerol	273	56.8	63.4	61.4	92.5	64.3	62.5
	298	56.2	59.1	60.0	88.5	63.5	61.1
	323	56.6	57.9	55.5	82.2	60.0	59.9

solutions of lower than in those of higher viscosity. For 323 °K (Fig. 3), Eq. (3) does not give an adequate description of the real shape of the quenching curve (marked by the experimental points in the figure). At low quencher concentrations the experimental points lie systematically above the theoretical curve, at high concentrations below. The data of Table I show a decrease of R_F with viscosity also at this temperature, but the dependence on viscosity is less pronounced here than at 273 °K. Essentially the same was observed for the temperature 298 °K (Fig. 2).

It can also be seen from Table I, that the values of R_0 decrease with increasing

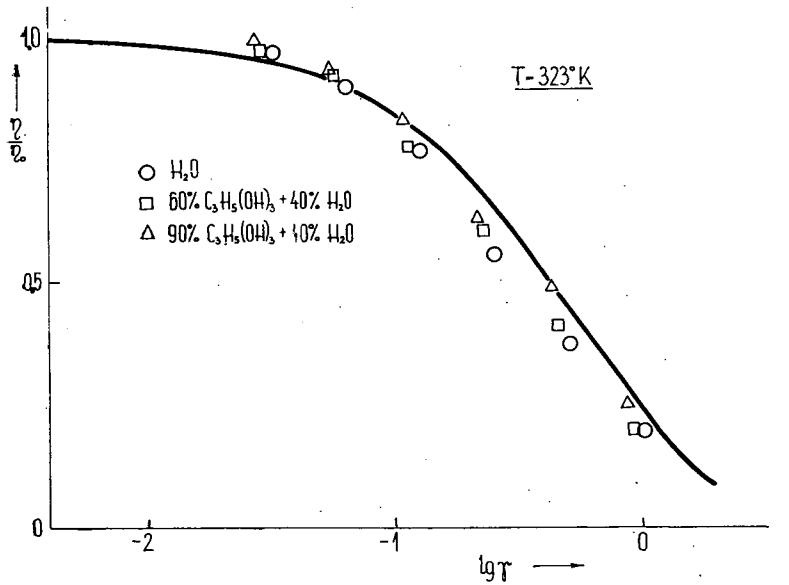

Fig. 3

temperature for the same set of observed solutions. According to the results of SZALAY and KOZMA [25] with glycerol solutions of fluorescein, rhoduline orange and rhodamine B, R_0 is practically the same, whether the energy transfer occurs before or after reaching the vibrational equilibrium. The finding that the R_0 calculated from Eq. (5) and the R_F obtained from Eq. (4) are different (namely $R_0 < R_F$, *i.e.* the energy transfer is more effective than expected from Förster's theory) has been described also is the case of other systems [1], [26], [27].

A better agreement can be obtained if the critical distance is determined with the relations obtained by using the modifications of Förster's theory [13], [15], [16], [17], [20]. These values are also given in Table I. The values R_{BM}, R_J, R_B obtained from the quenching curves were greater for all solutions than those calculated with Eq. (5), despite the refinement of the quenching theories.

In order to ascertain whether the higher rate of energy transfer *i.e.* the difference between R_0 and the experimental R_B is caused by the increase in the duffusion rate, the volume

$$V^* = \frac{4}{3}\pi R_V^{*3} \tag{8}$$

has been substituted instead of the quenching volume V. R_V^* is composed of the radius R_B of the active sphere and of the diffusive displacement determined with the formula $r \equiv (\overline{r_D^2})^{\frac{1}{2}} = \frac{kT\tau}{\pi\eta_v\sigma}$ [21]: $R_V^* = R_B + r$. Here σ is the radius of the excited molecule considered to be spherical. Thus the critical distance is:

$$R_V = \left(\frac{3v}{4\pi N' c_L}\right)^{\frac{1}{3}} - \left(\frac{k}{\pi\sigma}\frac{T}{\eta_V}\right)^{\frac{1}{2}}, \tag{9}$$

where c_L is the concentration of the quencher. According to [20] $R_V = 1.204 R_F$. As it was to be expected, the deviations of R_V from R_B are greater in aqueous solutions at lower viscosities. These deviations are primarily due to the fact that the mean displacements of the molecules in aequous solutions (15.6 Å, 23.1 Å and 27.1 Å) are comparable with the critical distance. The decrease of the distances R_F compared with R_B is so considerable that the values obtained are less then the R_0 calculated with Eq. (4). On the other hand, a good agreement between R_0 and r_V can be obtained, if the latter is calculated with $\sigma = 6$—7 Å, which also seems to be acceptable from a physical point of view, instead of the value $\sigma = 5$ Å used in [28]. In the case of solutions of higher viscosity the values of R_V are not remarkable changed by calculating with Eq. (9), but the inequality $R_0 < R_V$ exists.

It can be inferred from our results that though the diffusion plays a role in energy migration, especially in solutions of low viscosity, the deviation between the critical distances calculated with both methods, *i.e.* with Eq. (5) and from the quenching curves, cannot be explained merely by the neglection of diffusion. Further investigations to clear up the cause of these deviations are in progress.

Appendix

In the following we give some of the relations between the different critical distances characteristic for energy migrations, as well as those obtained in the present paper. BOJARSKI's [31] experimental results based on the shell model $R_J = 1.326R_F$; BOJARSKI's [32] calculations with a refined shell model $R_J = 1.466R_F$; according to BOJARSKI [20] $R_B = 1.204R_F$; SZALAY and SÁRKÁNY [29] calculated $R_J = 1.367R_F$; according to ERIKSEN [30] $R_J = 1.49R_F$ for low concentrations and $R_J = 1.41R_F$ for high concentrations. As a result of our own calculations $R_{BM} = 0.98R_F$, $R_J = 1.474R_F$, $R_B = 1.232R_F$, $R_V = 0.820R_F$ for low viscosities, and $R_V = 0.967R_F$ for high viscosities.

* * *

The author is indebted to thanks to Professor Dr. A. BUDÓ, Director of the Institute, for his interest in this work. Thanks are due to Professor L. SZALAY for his continued help in the course of experiments and to Professor I. KETSKEMÉTHY for his valuable advices.

References

[1] *Förster, Th.:* Z. Naturforsch. **4a**, 321 (1949).
[2] *Förster, Th.:* Z. Elektrochem. **53**, 93 (1949).
[3] *Förster, Th.:* Floureszenz Organischer Verbindungen (Vandenhoeck und Ruprecht, Göttingen, 1951).
[4] *Ketskeméty, I.:* Z. Naturforsch. **17a**, 666 (1962).
[5] *Ketskeméty, I.:* Acta Phys. Hung. **10**, 429 (1959).
[6] *Dombi J.:* Energy transfer processes in luminescent mixed solutions. Thesis for the degree of candidate of physical sciences, Szeged (1967).
[7] *Galanyin, M. D.:* Zs. Exp. Teor. Fiz. 28, 485 (1955).
[8] *Latt, S. A., H. T. Cheung, and E. R. Blant:* J. Ann. Chem. Soc. **87**, 995 (1965).
[9] *Drexhage, K. H., M. M. Zwick and H. Kuhn:* Ber. Bunsenges. f. Phys. Chem. **67**, 62 (1963).
[10] *Bowen, E. J. and R. Livingston:* J. Am. Chem. Soc. **76**, 6300 (1954).
[11] *Weinreb, A.:* J. Chem. Phys. **35**, 91 (1961).
[12] *Melhuish, W. H.:* J. Phys. Chem. **67**, 1681 (1963).
[13] *Bagdasaryan, H. C., A. L. Muler:* Opt. i Spektr. **18**, 990 (1965).
[14] *Feitelson, J.:* J. Chem. Phys. **44**, 1497 (1966).
[15] *Jabłoński, A.:* Acta Phys. Polon. **13**, 175 (1954).
[16] *Jabłoński, A.:* Bull. Acad. Polon. Sci. Ser. Sci. Math. Phys. Astron. **6**, 663 (1958).
[17] *Hevesi, J.:* Quenching of the photoluminescence of viscous dye-stuff solutions by foreign substances. Thesis for the degree of candidate of physical sciences, Szeged (1965).
[18] *Hevesi, J.:* Acta Phys. et Chem. Szeged **8**, 15 (1962).
[19] *Bojarski, C.:* Acta Phys. Polon. **19**, 631 (1960).
[20] *Bojarski, C.:* Acta Phys. Polon. **30**, 169 (1966).
[21] *Bojarski, C.:* Proceedings of the International Conference on Luminescence, 1966. (Akadémiai Kiadó, Budapest, 1968) Vol. 1. p. 446.
[22] *Ketskeméty, I., J. Dombi, J. Hevesi, R. Horvai und L. Kozma:* Acta Phys. et Chem. Szeged, **7**, 88 (1961).
[23] *Ketskeméty, I.:* Physical basis of the luminescence of solutions. Thesis for the degree of doctor of physical sciences, Szeged (1964).
[24] *Budó, A.:* Magyar Fizikai Folyóirat **9**, 269 (1961).
[25] *Szalay, L., L. Kozma:* Acta Phys. Hung. **20**, 389 (1966).
[26] *Szvesnyikov, B. Ja., P. I. Kudrjasov, L. A. Lumerova:* Opt. i Szpektr. **9**, 203 (1960).
[27] *Weinreb, A.:* J. Chem. Phys. **35**, 91 (1961).

[28] *Szalay, L.:* Investigations on fluorescence polarization of solutions. Thesis for the degree of doctor of physical sciences, Szeged (1964).
[29] *Szalay, L., B. Sárkány:* Acta Phys. et Chem. Szeged **8**, 23 (1962).
[30] *Eriksen, E. L.:* Phys. Norvegica **2**, 189 (1967).
[31] *Bojarski, C.:* Ann. Phys. **12**, 253 (1963).
[32] *Bojarski, C.:* Acta Phys. Polon. **25**, 179 (1964).

ВЛИЯНИЕ ДИФФУЗИИ НА ПЕРЕДАЧУ ЭНЕРГИИ В СМЕШАННЫХ ЛЮМИНЕСЦИРУЮЩИХ РАСТВОРАХ

З. Варкони

Исследовалось тушение флуоресценции трипофлавина родамином в глицеринно-водном растворе, при концентрации $6 \cdot 10^{-5}$—$2 \cdot 10^{-3}$ м/л тушителя, в области вязкости раствора 0.01—20 пз. и в интервале температуры 0—50 °C. Полученные экспериментальные данные интерпретируют по модели Ферстера и Яблонского.

Установили, что при низких значениях вязкости следует учитывать влияние диффузии, дали количественное соотношение этого явления. Степень передачи энергии с учетом диффузии больше, чем можно было бы ожидать на основе теории Ферстера и Яблонского.

A POLARIZATION SPECTROFLUORIMETER

By L. VIZE

Institute of Experimental Physics, Attila József University, Szeged

(Received December 2, 1968)

With the apparatus described, polarization spectra, polarization of emission, and diagrams of polarization can be measured. The apparatus, containing an electro-magnes wich allows to adjust the twist of the polarizator with great accuracy, is suitable to measure signals of 10^{-15}. A with a signal to noise ratio = 100 in the wavelength interval from 360 nm to 800 nm. The apparatus can also be used or measuring excitation and emission spectra.

Introduction

Examination of the polarization of luminescence, together with other luminescence-characteristics, can give valuable informations concerning the structure of molecules [1], migration of energy [2] and interactions between the molecule capable of luminescence and the solvent [3]. It seemed therefore justified to build an apparatus, wich can be considered as more accurate than those constructed earlier [4—9], using some recent results of experimental technics.

1. *The principle of measurements* is based on the following definition given *e.g.* in [10]. Let us consider a part of the solution to be studied, contained in a volume element ΔV of parallelepiped form in a system of co-ordinates $OXYZ$, so that O be comprised in ΔV, the edges of ΔV being parallel to the corresponding axes of the system. Let the solution in ΔV be irradiated with monochromatic, linearly polarized light, the electric vector of which is parallel to the X-axis. Let us consider a narrow beam of fluorescence-light of wavelength λ', emitted parallel with the Z axis and passing through a polarizator, the intensities of the beams with electric vectors parallel to the X and Y axis being denoted by I_1 and I_2 respectively. The degree of polarization $p(\lambda, \lambda')$ expressed in terms of I_1 and I_2 is then given by the following formula:

$$p = \frac{I_1 - I_2}{I_1 + I_2}. \tag{1}$$

It would however be inexact to make measurements on a quantity of solution of such a little volume, because the conditions in the volume-element ΔV would be altered among others by surface effects. In order to obtain the true degree of polarization given by Eq. (1) from the measured degree of polarization p' determined in the same way from the intensities I_1 and I_2 measured on macroscopic quantitites of solution (p' being therefore not generally to be considered as true degree of polarization), the measurements are to be corrected according to [10]. One of the

conditions necessary for this correction is to comply with the conditions of excitation and observation described in [10] during the measurement of p'. Therefore we took care that in our instrument the sample could be excited on a surface of 0.01 cm², and the luminescence beam emitted under a beam angle of 0.05 rad could be observed on a surface of about 0.80 cm².

2. *Optical arrangement.* The plane of reference of the apparatus serving to measure successively the intensities I_1 and I_2 is the plane determined by a_1 and a_2 the axis of the cone of exciting light and that of observed radiation respectively (see Fig. 1). In Fig. 1 L denotes a high-pressure xenon arc. lamp (type Osram XBO 450); L' a high pressure mercury lamp (type Osram HBO 500), or a halogen (iodine) lamp of 150 W; M_1 and M_2 are monochromators (type Zeiss SPM-2) L_1, L_2, L_3 and L_4 fused silica lenses for projection; C_1 and C_2 cells containing $CuSO_4$ solution for absorbing heat radiation; F_1 is a Schott-filter absorbing most part of the exciting light, F_2 an interference filter transmitting the band selected from the spectrum of L'; S_1 and S_2 metal mirrors; *Em* is an electro-magnet serving to adjust the polaroid filter P_1 around axis a_1 with high accuracy; H_1 and H_2 are handles to turn the sample-holder and the polaroid filter P_2 in the desired position; *CH* is the sample-holder; V a dc amplifier (Clamann—Grahnert, type MV-4); *DV* a digital voltmeter (EMG 1361) which can be coupled with a printing recorder; *Th* denotes an ultra-thermostat; V_1 the vacuum pump; D_1, D_2 and D_3 are diaphragms; *Ph* a photo-multiplier (EMI 9558 a). Concerning the part of Fig. 1 enclosed by a broken line see part 4.

In *adjusting the apparatus*, the first step was to determine the plane (a_1, a_2). This was performed with a cathetometer for observing the light beam from a pinhole source of light in the sample holder passing through diaphragms of small aperture placed in the channels of excitation and observation. The electric vector **E** of the exciting light was adjusted in position I, perpendicular to the plane (a_1, a_2), with a Sénarmont-prism. The electric vector **E** can be brought from position I into the plane (a_1, a_2) (position II) with the electro-magnet *Em*, this method being more convenient and giving better reproducibility. In order to secure practical immobility of the projection on the cell of the exit slit of the monochromator M_1 when turning the polarizator P_1, this latter must be plane-parallel within some minutes and perpendicular to axis a_1. After projecting the light of the halogen lamp P_2 with the aid of a metal mirror placed in the position of the xenon lamp L, the polaroid P_2 was turned around a_2, until the instrument coupled with the photo-multiplier *Ph* indicated a minimal value. This operation could be performed with the aid of the range-switch of the dc amplifier with a mean relative error of about 0.1%.

In the *course of measurements* the vector **E** of exciting light was brought first into position I perpendicular to plane (a_1, a_2), then into position II parallel to it with the aid of the electro-magnet *Em*, and the intensities $I'_{\parallel}$ and $I'_{\perp}$ of the luminescence light corresponding to positions *I* and *II* of **E**, passing through the fixed polaroid P_2 in the direction of a_2, were measured. The light from monochromator M_1 being partially polarized and its degree of polarization depending on the wavelength λ, the intensities I_{I} and I_{II} passing P_1 in position *I* and *II* are generally different. To take into account this fact in measuring the degree of polarization, the quotient $c(\lambda) = I_{\text{II}}(\lambda)/I_{\text{I}}(\lambda)$ is to be measured. To this end a metal mirror was put in the place of the cell and parchment paper before the diaphragm D_1; P_2 thus obtained always

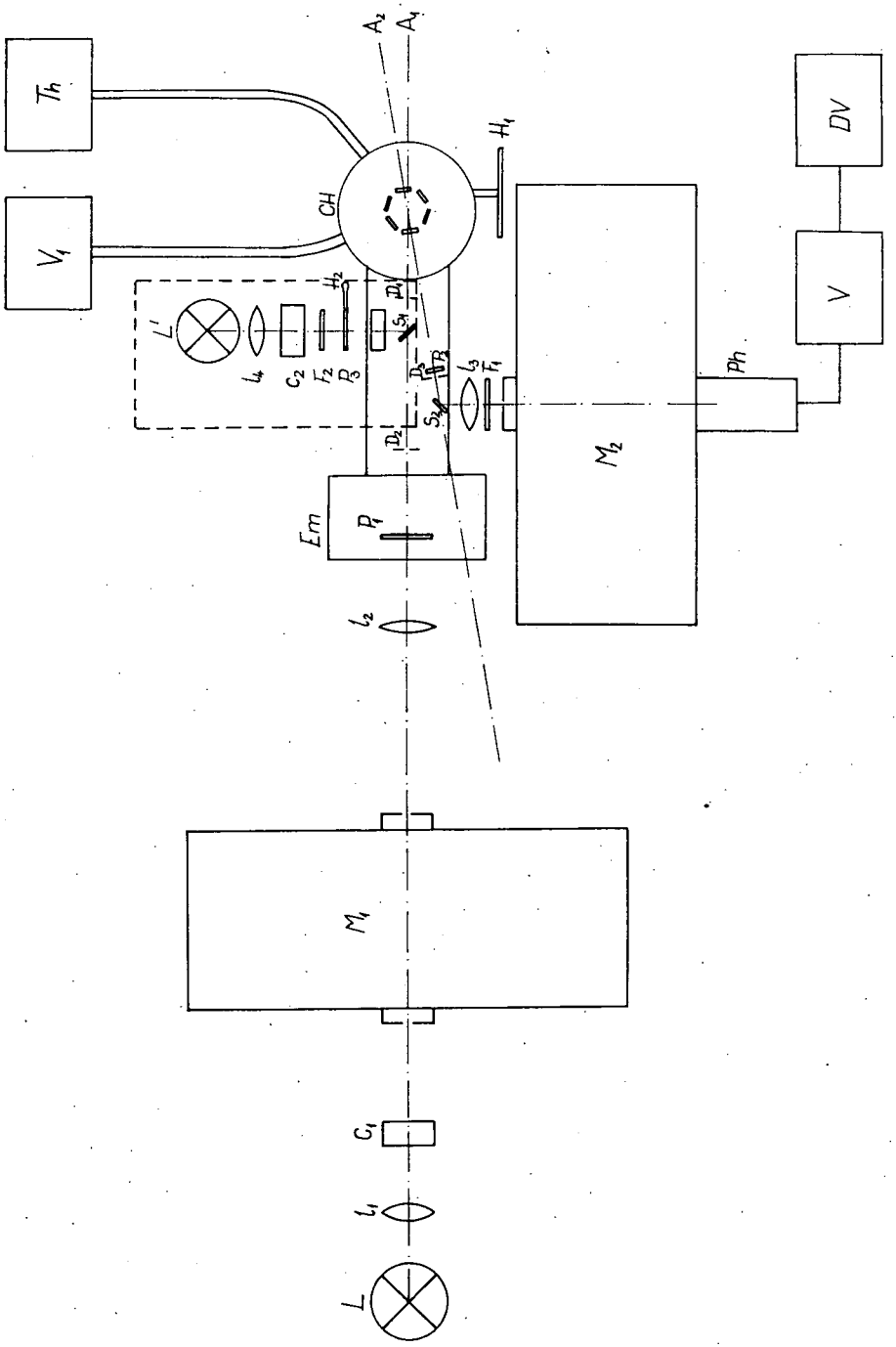
Th
V1
A2
A1
H1
CH
DV
V
L'
L4
C2
F2
B3
H2
D1
S1
D3
B2
L3
F1
S2
D2
Ph
M2
Em
P
L2
M1
C1
L1
L

Fig. 1

natural light. The measured degree of polarization p' (which is not generally to be considered identical with p defined in Eq. (1)) can be calculated from the intensities $I'_{\parallel}$ and $I'_{\perp}$ measured directly (provided that the intensity of dispersed light can be neglected against I' and $I'_{\perp}$) with the following formula:

$$p'(\lambda, \lambda') = \frac{I'_{\parallel} c(\lambda) - I'_{\perp}}{I'_{\parallel} c(\lambda) + I'_{\perp}}. \qquad (2)$$

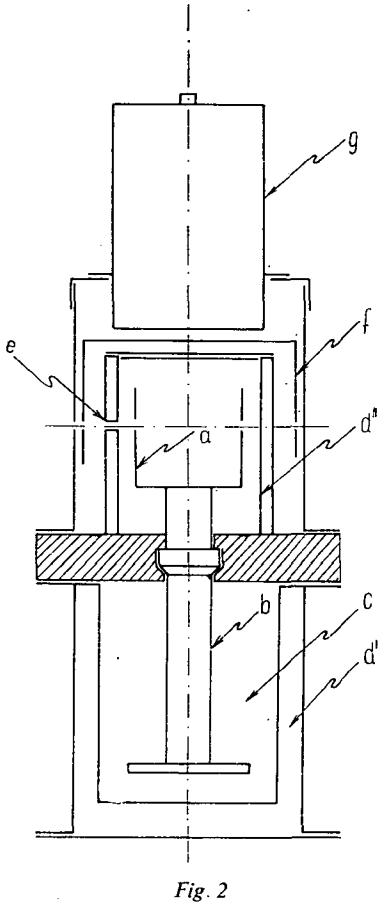

Fig. 2

If the intensities $I_{\parallel d}$ and $I_{\perp d}$ of the dispersed light cannot be neglected in comparison with $I'_{\parallel}$ and $I'_{\perp}$, the solution is to be replaced by a solution of chinese ink which has the same absorption at wavelength λ; then p' can be calculated from the measured intensities $I_{\parallel d}$ and $I_{\perp d}$, with the following formula (the intensities of disper sed light including the dark current of the multiplier):

$$p'(\lambda, \lambda') = \frac{(I'_{\parallel} - I_{\parallel d}) c(\lambda) - (I'_{\perp} - I_{\perp d})}{(I'_{\parallel} - I_{\parallel d}) c(\lambda) + (I'_{\perp} - I_{\perp d})}. \qquad (3)$$

We had also to check the linearity of the dc amplifier, the error of which was found to be less than 0.5%. For this measurement the digital voltmeter was used.

3. The degree of polarization depends, besides the wavelengths λ and λ' of exciting and observed light, also on the *temperature of the sample*. The sampleholder *CH*, together with the thermostat *Th* and the vacuum-pump V_1, an electric heater in the sample-holder and a thermocouple measuring the temperature serve to ensure constancy of the temperature desired. The rod *b* of the revolving cell-holder *a* made of metal (see Fig. 2), capable of receiving 6 cells simultaneously and mounted on a plastic plate, was immersed in liquid air (or water) in the container *c* (or flowing through it). The spaces *d'* and *d''* could be evacuated. The exciting light passing through the double window *e* made of glass (or of fused silica) fell on the solutionr and the luminescence light through the same window on the polaroid P_2. The cylinde-*f* of the easily demountable mechanical phosphoroscope was rotated by the electro, motor *g*.

The electromagnet *Em* serves to adjust the position of the polaroid P_1 fitted with high accuracy in a mild-iron holder. In order to obtain the angles 0°, 90°, 180° and 270°, and for measurements according to [4], also 45°, 135°, 225° and 315°, between **E** and the vector **E'** of the observed light, **E** has to be adjusted in the angles 0°; 45°30′; 90°; 134°30′; 180°; 224°30′; 270°; 314°30′ with respect to position I, as can be shown by trigonometrical calculation. (These angles are determined by

the condition that for measurements according to [4], the components in the directions I and II of E, which encloses the angle α with position I, viewed from the direction of the axis a_2 enclosing an angle of 10° with axis a_1, have to be equal.)

4. *The sensitivity of the apparatus* is determined by the sensitivity of the photomultiplier (EMI 9558 a, which is 200 μA/lumen for the photocatode) and that of the Clamann—Grahnert dc amplifier (type MV 4, with an input resistivity of 17 MΩ and bandwidth of about 0.5 Hz) which is 10^{-12} A. According to our measurements the fluctuation of the dark current amounts to about 10^{-12} A. The quantum yield of the photocathode of the multiplier is about 0.1 for blue and green light, the gain can be estimated to 10^5 with the anode voltage 1200 volts employed, thus our observing system indicates quantum current densities of 10^3 photon/cm^2 sec. For reliable measurements a signal to noise ratio of ~ 100 is necessary, *i.e.* luminescence light fluxes down to 10^5 photon/cm^2 sec can be measured.

When measuring solutions of high concentration, highly quenched solutions or solutions of low-yield by themselves, the desired signal to noise ratio from the monochromator M_1 cannot be secured. In these measurements the light of source L' is to be projected on the sample along a shorter path, through an interference filter, with the aid of mirror S_1 (see the part enclosed by a broken line in Fig. 1). The beam angle of the exciting light cone is then 1 rad.

Accuracy of the apparatus. Using an iodine lamp, which practically shows no fluctuations, as exciting light source, the relative error of the measured degree of polarization *vs.* degree of polarization is shown by curve *A* of Fig. 3; according to this the relative error is 3% for 10% degree of polarization and 30% for 1% degree of polarization. If xenon-arc or mercury lamps must be used for excitation, the accuracy of the apparatus will be impaired, the fluctuation of the light flux from the lamps amounting to 1—1.5%, (see curve *B* in Fig. 3). In this case the random error due to the fluctuation of the light flux can be diminished by increasing the time constant of the observing system to 3 sec by a condensator shunted with the working resistance of the multiplier, then compensating $I'_\perp$ with a simple compensator of great resistance and measuring $I'_\parallel - I'_\perp$ directly in position *I* of the polaroid P_1, after increasing the amplification in a small but known degree. Curve *C* in Fig. 3 shows that the error of measurement can be considerably reduced in this way. As an example the very low ($\sim 0.6\%$) degree of polarization of an aqueous fluorescein solution of 10^{-4} mole/litre concentration has been measured with and without compensator, five times in each position of P_1 and for all six positions of the cell holder, *i.e.* 120m easurements were made with and without compensator, respectively. Our results are shown in Fig. 4, where the ordinate *y* gives the number of the results in the corresponding interval divided by the total number of measurements.

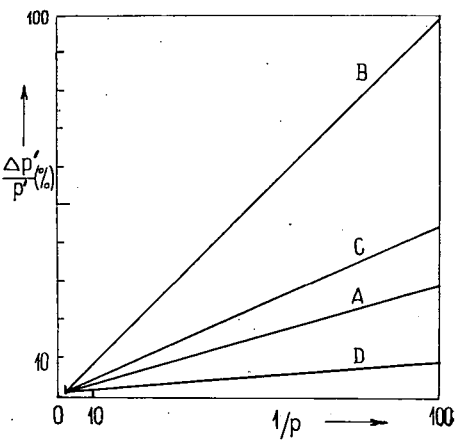

Fig. 3

Whereas the half-width of this function measured with compensator is only about 0.4% (in degrees of polarization), it is 1.2% without compensator.

The accuracy of measurements can be also defined as the error $\Delta\bar{p}'$ in determining the mean value $\bar{p}'$ of a sequence of measurements concerning the quantity studied, divided by $\bar{p}'$. According to our measurements, this relative error amounts to $\sim 0.1\%$, and is due partly to the imperfect linearity of the observing system,

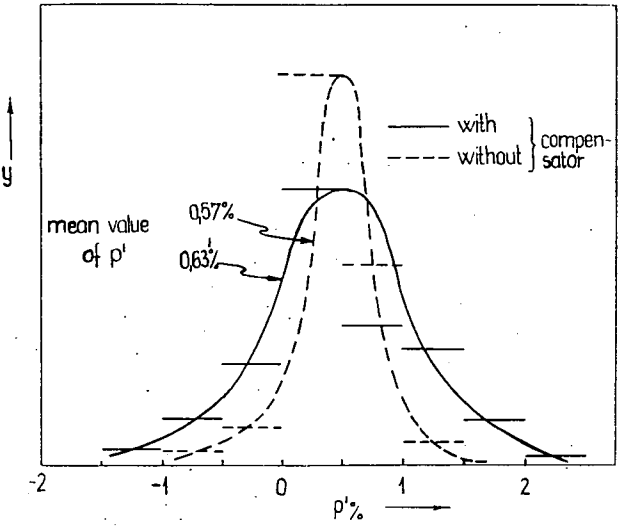

Fig. 4

partly to imperfections in regulation of the polaroids. The accuracy of our apparatus in this sense is shown by curve *D* of Fig. 3. In determining the accuracy of a measuring device according to this definition, two conditions have to be fulfilled: 1. The speed of measurements has to be high enough, and 2. the distribution has to correspond to a distribution function, characteristic for the apparatus, with adequate accuracy. With our apparatus these requirements are fulfilled, as the results of measurements show Gaussian distribution with an error of less than 10%.

The speed of measurements is about 1 result per second. The measurement of a polarization spectrum consisting of 20 points takes about 30 minutes.

Changes of more than 0.2 sec duration can be well studied with an oscilloscope of adequately low frequency (*e.g.* EMG type 1546) coupled with the amplifier.

Among the corrections to be made on the measured degree of polarization p', the correction for secondary luminescence has already been mentioned. If the exciting and observed light beam is not sufficiently parallel and monochromatic, corrections for parallelism and band width are to be made.

The field of application of the apparatus includes measurements of polarization spectra, polarization of emission, excitation and emission spectra as well as diagrams of polarization in the wavelength interval from 360 to 800 nm in a temperature

range which can be changed from about the temperature of liquid air to that of boiling water, as well as investigations on changes taking place in more than 0.2 sec in fluorescence and phosphorescence phenomena alike.

* * *

The author wishes to express his sincere thanks to Prof. A. BUDÓ, Director of the Institute, as well as to Professors I. KETSKEMÉTY and L. SZALAY for their interest during the work and for valuable remarks.

References

[1] *Memming, R.:* Z. Phys. Chem. **28**, 168 (1961).
[2] *Szalay, L.:* Ann. Physik **14**, 221 (1964).
[3] *Vize, L.:* Acta Phys. et Chem. Szeged **14**, 13 (1968).
[4] *Ketskeméty, I., L. Gargya, E. Salkovits:* Acta Phys. et Chem. Szeged **3**, 16 (1957).
[5] *Bauer, R., M. Rozwadowski:* Optik **18**, 37 (1961).
[6] *Ainsworth, S., E. Winter:* Applied Optics **3**, 371 (1964).
[7] *Monnerie, L., J. Néel:* J. Chem. Phys. Physico-Chimie Biologique **62**, 504 (1965).
[8] *Dehler, J., F. Dörr:* Z. angew. Phys. **19**, 147 (1965).
[9] *Lippert, E., F. Aurich:* Spectrochimica Acta **22**, 1073 (1966).
[10] *Budó, Á., I. Ketskeméty, E. Salkovits, L. Gargya:* Acta Phys. Hung. **8**, 181 (1957).

ПРИБОР ДЛЯ ИЗМЕРЕНИЯ СТЕПЕНИ ПОЛЯРИЗАЦИИ ЛЮМИНЕСЦЕНЦИИ

Л. Визе

На описанном приборе можно измерять поляризационный спектр, спектр поляризации; получить диаграммы поляризации. Прибор, в котором с помощью электромагнита с большой точностью можно поворачивать поляризатор, пригоден для измерения сигнала 10^{-15} А, при соотношении сигнал/шум-100, в области от 360 до 800 нм. длины волны. На нем можно снимать спектр люминесценции и спектр возбуждения.

TEMPERATURE DEPENDENCE OF THE GRÜNEISEN PARAMETERS OF SOME CUBIC METALS

S. K. SANGAL and P. K. SHARMA
Physics Department, University of Allahabad, Allahabad, India

(Received September 1, 1968)

The temperature dependence of the Grüneisen parameters of cubic metals sodium, potassium, copper, silver, gold and aluminium is studied from the experimentally measured pressure derivatives of elastic constants, using Bhatia's electron gas model. Formidable integrals over the phonon wave vectors are evaluated from Houston's six-term interpolation procedure. The calculated γ values are compared with available experimental data. The agreement of the theoretical values with experiments is satisfactory for silver, but not in the case of other metals.

1. *Introduction*

The effect of anharmonicity on thermal expansion of crystals is usually expressed in terms of a dimensionless parameter γ, called the Grüneisen parameter, defined by the relation

$$\gamma = \frac{\beta V}{\chi C_v}, \tag{1}$$

where β is the volume thermal expansion coefficient, χ the compressibility, V the volume and C_v the specific heat at constant volume. This quantity is related to the variation of lattice vibration frequencies with volume. GRÜNEISEN's theory [1] assumes γ to be a constant, independent of temperature and lattice frequency.

Recent experimental and theoretical investigations on thermal expansions of crystals have shown inadequacy of Grüneisen's theory. The experiments of RUBIN *et al.* [2], WHITE [3], and CARR *et al.* [4] on thermal expansions of metals at low temperatures show that γ varies with temperatures. BLACKMAN [5] and BARRON [6] have made detailed calculations of γ for ionic crystals by using idealized models for their lattice dynamics and have found that drastic variation in γ values occure at temperatures about 0.3Θ (Θ: Debye temperature). Since then many calculations on the temperature variation of γ of cubic metals have been carried out, notably by SHEARD [7], HORTON [8], COLLINS [9] and TOYA [10].

In the present paper, we report a calculation of temperature dependence of Grüneisen parameter for some cubic metals on the basis of BHATIA's model of electron-lattice interaction [11, 12]. It has been shown by JOSHI and HEMKAR [13, 14] that this model offers a fairly reasonable decription of vibration spectra and heat capacities of alkali and noble metals. In a recent study [15], we found thet this model provides a plausible explanation of gross features of temperature variation of Debye—Waller factors and resistivities of these metals. It was therefore thought proper to use this model to compute the thermal expansion of some cubic metals.

The results for sodium, potassium, copper, silver, gold and aluminium, for which data on pressure dependence of elastic constants are available, are presented in this paper and compared with available experimental values.

2. *Theory*

The volume thermal expansion coefficient β of a solid is given by the relation

$$\beta = -\chi \frac{\partial^2 F}{\partial V \partial T}, \tag{2}$$

where F is the Helmholtz free energy. In the quasi-harmonic approximation, the temperature dependence of the Free energy can be written as [16]

$$F = kT \sum_{\mathbf{q},j} \ln\left[1 - \exp(-\hbar\omega_{\mathbf{q}j}/kT)\right] + E_0, \tag{3}$$

where E_0 is the cohesive energy at absolute zero including the zero point energy, $\omega_{\mathbf{q},j}$ the angular frequency of lattice waves of wave vector $\mathbf{q}$ and polarization j, k the Boltzmann constant and the summation over $\mathbf{q}$ is taken over all the normal modes of the crystal. Combining Eqs. (2) and (3), we get

$$\frac{\beta V}{k\chi} = \sum_{\mathbf{q},j} \gamma_{\mathbf{q},j} E(\hbar\omega_{\mathbf{q},j}/kT), \tag{4}$$

where $E(x)$ is the Einstein specific heat function and

$$\gamma_{\mathbf{q},j} = -(\partial \ln \omega_{\mathbf{q},j}/\partial \ln V)_T. \tag{5}$$

The formula (4) gives the Grüneisen parameter γ as

$$\gamma = \frac{\beta V}{\chi C_v} = \frac{\sum_{\mathbf{q},j} \gamma_{\mathbf{q},j} E(\hbar\omega_{\mathbf{q},j}/kT)}{\sum_{\mathbf{q},j} E(\hbar\omega_{\mathbf{q},j}/kT)}. \tag{6}$$

Replacing the summation over allowed values of $\mathbf{q}$ within the first Brillouin zone by integrations over $\mathbf{q}$ and solid angle Ω in the wave vector space, Eq. (6) can be written as

$$\gamma(T) = \frac{\sum_j \int_\Omega d\Omega \int_0^{q_{max}} dq\, \gamma_j(q) E(\hbar\omega_j(q)/kT) q^2}{\sum_j \int_\Omega d\Omega \int_0^{q_{max}} dq\, E(\hbar\omega_j(q)/kT) q^2}. \tag{7}$$

3. *Numerical calculations*

The Grüneisen parameter at different temperatures is calculated using the expression (7). To evaluate the integrals, we have employed HOUSTON's method, as developed by BETTS *et al* [17]. The integration over q was performed numerically and the integration over Ω was carried out by using modified Houston's spherical six-term integration procedure. The applicability of Houston's method for evaluating various physical properties of a crystal has been discussed by several authors [18—20]. In this method, the integrand which is invariant under the operations of the complete cubic symmetry is expanded in cubic harmonics and the series is averaged analytically over the complete solid angle. The six directions used in the calculation are: [100], [110], [111], [210], [211] and [221].

To use HOUSTON's integration method, the secular equations determining the vibration frequencies of body-centred and face-centred cubic metals [11, 12] were solved for q vectors lying along the above six directions. The quantities $\gamma_j(q)$ were obtained in terms of the elastic constants C_{ij} and their pressure derivatives $\partial C_{ij}/\partial P$. In the calculation we took account of the variation of elastic constants and lattice parameters with temperature. In high temperature regions, these were obtained by extrapolation from the existing measurements.

4. *Results and Discussion*

The calculated values of the Grüneisen parameters for sodium, potassium, copper, silver, gold and aluminium, for which data on pressure derivatives of elastic constants are available have been plotted as a function of reduced temperature (T/Θ_0) in Figs. 1—4. Here Θ_0 is the Debye temperature deduced from the elastic constants. For comparison, the values of γ derived from experiments on thermal expansions have also been shown. The values of the pressure derivatives of elastic constants along with sources of the temperature variation of elastic constants and thermal expansion data needed in the calculation are listed in Table I. The lattice parameter values at different temperatures were obtained from PEARSON [21].

A survey of Figs. 1—4 shows that the agreement between theory and experiment is reasonably satisfactory for silver throughout the temperature range studied, for potassium at temperatures neither very low nor very high, for copper and aluminium at low temperatures only, and for gold at a particular temperature at which experimental value is known. In view of nonavailability of sufficient experimental data for sodium, potassium and gold, no definite conclusions can be drawn for these metals. The marked discrepancies in the case of sodium are probably caused by large uncertainties in the values of elastic constants reported by QUIMBY and SIEGEL [22] and also by the change in crystal structure. In our calculation we have taken no account of the fact that sodium undergoes martensitic type of phase transformation [23, 24] from a *bcc* to a mixture of *bcc* and *hcp* phases at about 37 °K. In potassium, the anharmonic effects are quite predominant because of low melting point. Hence a good agreement between theory and experiment is not possible at higher temperatures. For copper, the disagreement at high temperatures is due to the fact that BHATIA's theory gives a poor representation of frequency distribution of this metal in the high frequency region. The discrepancies in the case of aluminium

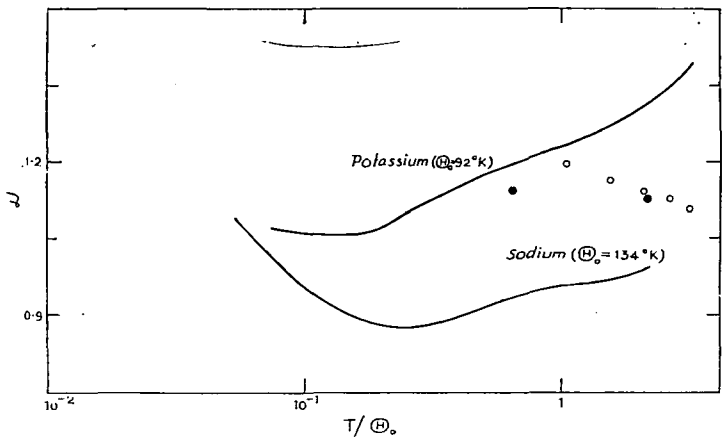

Fig. 1. Variation of γ with temperature for sodium and potassium. Experimental data: 0 potassium; sodium

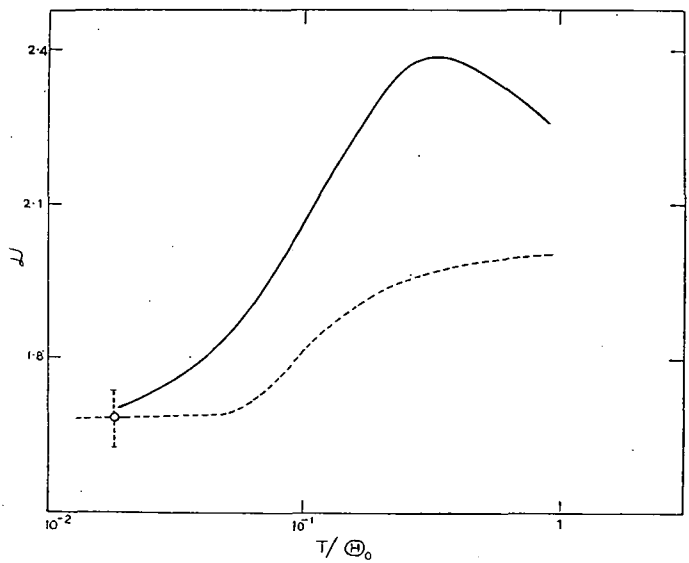

Fig. 2. Variation of γ with reduced temperature for copper ($\Theta_0 = 331$ °K). The solid curve shows present calculations and the broken curve corresponds to experimental measurements

are not unexpected and may be attributed to the approximate description of electron--lattice interaction and to the assumption of short range interionic interaction in the theory.

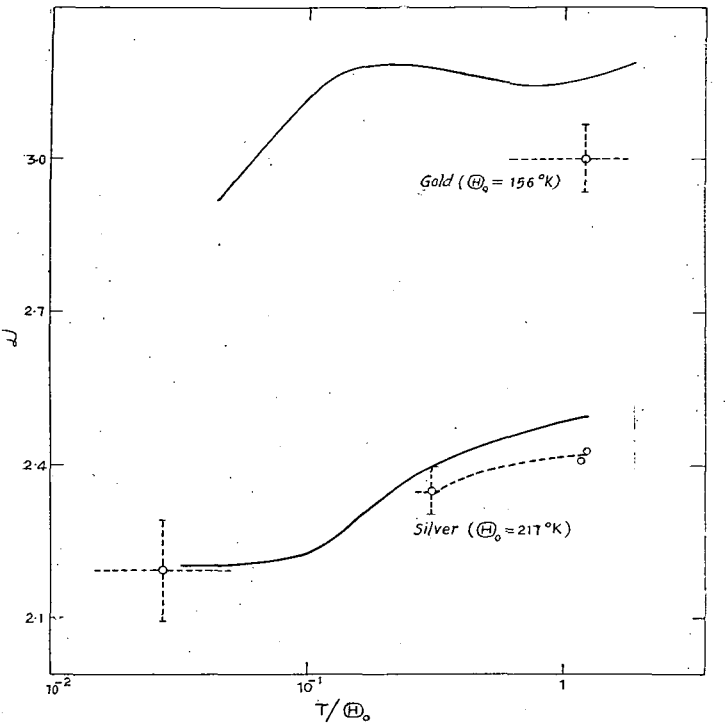

Fig. 3. Variation of γ with reduced temperature for silver and gold. Circles show experimental values

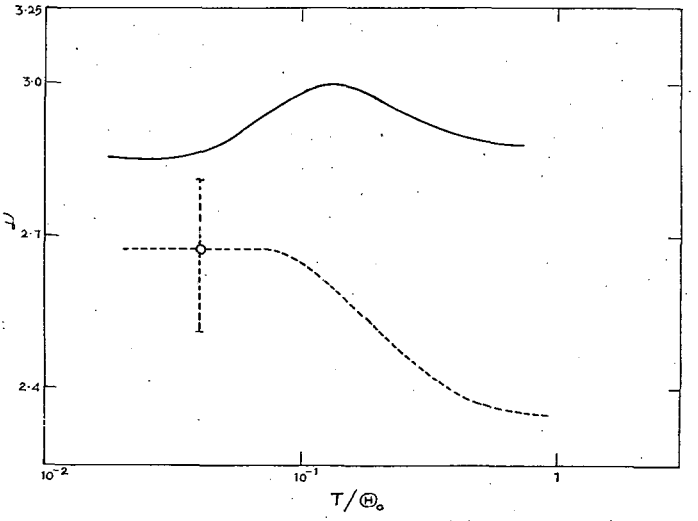

Fig. 4. Variation of γ with reduced temperature for aluminium (Θ_0=407 °K). The solid curve is based on present calculations and the dashed curve shows experimental measurements

Table I

Material	Pressure derivatives of elastic constants			Reference for pressure derivative	Reference for elastic constants	Reference for thermal expansion
	$\partial C_{11}/\partial P$	$\partial C_{12}/\partial P$	$\partial C_{44}/\partial P$			
Sodium	3.901	3.449	1.630	Daniels [a]	Quimby and Siegel [e]	Corruccini and Gniewek [j]
Potassium	4.305	3.803	1.620	Smith and Smith [b]	Marquardt and Trivisonno [f]	Monfort and Swenson [k]
Copper	6.363	5.203	2.350	Daniels and Smith [c]	Overton and Gaffney [g]	Rubin et al. [l]
Silver	7.032	5.754	2.310	Daniels and Smith [c]	Neighbours and Alers [h]	Corruccini and Gniewek [j]
Gold	7.014	6.138	1.790	Daniels and Smith [c]	Neighbours and Alers [h]	Vorruccini and Gniewek [j]
Alumí-nium	7.350	4.110	2.310	Schmunk and Smith [d]	Sutton [i]	Corruccini and Gniewek [j]

[a] *W. B. Daniels:* Phys. Rev. **119**, 1246 (1960).
[b] *P. A. Smith, C. S. Smith:* J. Phys. Chem. Solids **26**, 279 (1965).
[c] *W. B. Daniels, C. S. Smith:* Phys. Rev. **111**, 713 (1958).
[d] *R. E. Schmunk, C. S. Smith:* J. Phys. Chem. Solids **9**, 100 (1959).
[e] *S. L. Quimby, S. Siegel:* Phys. Rev. **54**, 293 (1938).
[f] *W. R. Marquardt, J. Trivisonno:* J. Phys. Chem. Solids **26**, 273 (1965).
[g] *W. C. Overton, J. Gaffney:* Phys. Rev. **98**, 969 (1955).
[h] *J. R. Neighbours, G. A. Alers:* Phys. Rev. **111**, 707 (1958).
[i] *P. M. Sutton:* Phys. Rev. **91**, 816 (1953).
[j] *R. J. Corrucinni, J. J. Gniewek:* Thermal Expansion of Technical Solids at Low Temperatures (National Bureau of Standards, Washington, 1961).
[k] *C. E. Monfort, C. A. Swenson:* J. Phys. Chem. Solids **26**, 291 (1965).
[l] *T. Rubin, H. W. Altman, H. L. Johnston:* J. Amer, Chem. Soc. **76**, 5289 (1954).

* * *

The authors are thankful to the University Grants Commission, New Delhi for financial assistance and to the computer centre, Roorkee for providing the facilities of IBM 1620 computer.

References

[1] *Grüneisen, E.:* Handbuch der Physik (Springer–Verlag, Berlin 1926), Vol. 10.
[2] *Rubin, R., H. W. Altman, H. L. Johnston:* J. Phys. chem. **65**, 65 (1961).
[3] *White, G. K.:* Phil. Mag. **6**, 1425 (1961); Proceedings of VIII International Conference on Low Temperature Physics (Butterworths, London, 1963), p. 394.
[4] *Carr, R. H., R. D. McCammon, G. K. White:* Proc. Roy Soc. **A280**, 72 (1964).
[5] *Blackman, M.:* Proc. Phys. Soc. (London) **B70**, 827 (1957); Phil. Mag. **3**, 831 (1958); Proc. Phys. Soc. (London) **B74**, 17 (1959).
[6] *Barron, T. H. K.:* Phil. Mag. **46**, 720 (1955); Ann. Phys. (USA) **1**, 77 (1957).
[7] *Sheard, F. W.:* Phil. Mag. **3**, 1381 (1958).
[8] *Horton, G. K.:* Canad. J. Phys. **39**, 263 (1961).
[9] *Collins, J. G.:* Phil. Mag. **8**, 323 (1963).

[10] *Toya, T.:* J. Res. Inst. Catalysis, Hokkaido Univ. **9**, 178 (1961).
[11] *Bhatia, A. B.:* Phys. Rev. **97**, 363 (1955).
[12] *Bhatia, A. B., G. K. Horton:* Phys. Rev. **98**, 1715 (1955).
[13] *Joshi, S. K., M. P. Hemkar:* J. Chem. Phys. **34**, 1458 (1961); Phys. Rev. **122**, 12 (1961); Physica **27**, 793 (1961).
[14] *Hemkar, M. P., S. K. Joshi:* J. Phys. Soc. Japan **17**, 754 (1962).
[15] *Sangal, S. K., P. K. Sharma:* unpublished.
[16] *Slater, J. C.:* Introduction to Chemical Physics (McGraw-Hill, New York, 1939).
[17] *Betts, D. D., A. B. Bhatia, M. Wyman:* Phys. Rev. **104**, 37 (1956).
[18] *Horton, G. K., H. Schiff:* Proc. Roy. Soc. **A250**, 248 (1959).
[19] *Ganesan, S., R. Srinivasan:* Canad. J. Phys. **40**, 91 (1962); Proc. Roy. Soc. **A271**, 154 (1963).
[20] *Gupta, R. P., P. K. Sharma:* J. Chem. Phys. **48**, 2451 (1968).
[21] *Pearson, W. B.:* A. Handbook of Lattice spacings and structures of Metals and Alloys (Pergamon Press, New York, 1958).
[22] *Quimby, S. L., S. Siegel:* Phys. Rev. **54**, 293 (1938).
[23] *Martin, D. L.:* Proc. Roy. Soc. **A254**, 433 (1960).
[24] *Barret, C. S.:* Acta Cryst. **9**, 671 (1956).

ELECTROCHEMICAL STUDIES ON THE INHIBITION OF THE CORROSION OF IRON AND STEEL IN METAL-HYDROGEN SULPHIDE-WATER TERNARY SYSTEMS. II

Investigation of the synergetic effect of some organic corrosion inhibitors and hydrogen sulphide

A. RAUSCHER, L. HACKL, J. HORVÁTH, F. MÁRTA

Institute of General and Physical Chemistry, Attila József University, Szeged

(Received December 10. 1968)

The aim of this paper is to evaluate, on the basis of laboratory experiments, the applicability of cationic organic inhibitors in acidic aqueous systems containing hydrogen sulphide. Experimental results obtained by intermittent galvanostatic polarization suggest that the inhibiting effect of dicyclohexylamine — used as a model compound — is due to a synergetic effect, as supposed by JOFA and HACKERMAN.

Introduction

According to the principles of electrochemical kinetics the effect of organic corrosion inhibitors as surface active agents upon the corrosion reaction is associated with the change in the structure of the electric double-layer, caused by their adsorption. This change has considerable influence on the exchange current and on the overvoltage of the electrochemical corrosion reactions.

The schematic diagram shown in Fig. 1 shows the polarization behaviour of a corroding metal in oxygen-free aqueous solutions. The construction of the diagram has been based on the assumption that two oxidation-reduction systems are involved in the corrosion reaction and that the potential of the $Me \rightleftharpoons Me^{++} + 2\,e^-$ equilibrium is more negative than that corresponding to the $2\,H^+ + 2\,e^- \rightleftharpoons H_2$ equilibrium. Under such conditions the dissolution of the metal proceeds with simultaneous hydrogen evolution. Under steady state conditions the potential of the corroding metal is represented by ε_{corr}. At this potential the rate of the anodic dissolution of the metal ($Me \rightarrow Me^{++} + 2\,e^-$) expressed in current density is equal to the rate of the hydrogen ion discharge ($2\,H^+ + 2\,e^- \rightarrow H_2$). Heavy lines on Fig. 1 represent the polarization curves obtainable by externally applied polarizing current; β_a and β_c are the Tafel slopes of the anodic and cathodic polarization curves.

The effect of corrosion inhibitors on the polarization characteristics of the corroding metal is shown by Fig. 2. It can be established that the decrease of the corrosion current density from i_{corr_1} to i_{corr_2} is due to the decrease in the exchange currents of the anodic and cathodic reactions (i_{0_H} and $i_{0_{Me}}$) and also to the increase in the Tafel slopes β_a and β_c. In Fig. 2 the increase of β_a is somewhat higher than that of β_c, accordingly, on addition of the inhibitor the corrosion potential shifts towards the positive potential region. As seen in Figs. 1 and 2 the value of the corrosion currents can be established by extrapolating the anodic and cathodic Tafel-

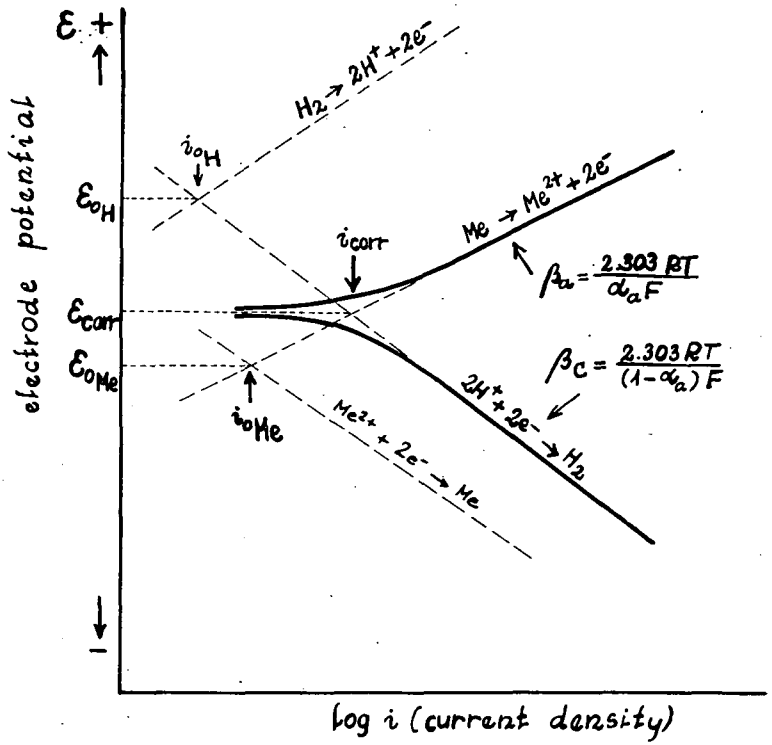

Fig. 1. Schematic polarization diagram for a corrosion reaction involving two redox systems

lines towards the corrosion potential ε_{corr}. Similar curves can be obtained by intensiostatic (galvanostatic), intensiokinetic and also by potentiostatic or potentiokinetic methods. Thus the effect of inhibitors on the corrosion rate can be studied on the basis of polarization diagrams obtained by the above methods, provided that the polarization curves obey the Tafel equation within one order of magnitude of current density.

Polarization curves obtained by step-wise or continuously increased polarizing current, however, cannot provide information about the change of the overvoltage of the anodic or cathodic reaction in time. For the study of this problem the intermittent galvanostatic polarization method may be used with advantage. The electrode potential — time diagram obtained by this method is essentially a series of subsequent galvanostatic charging curves, providing a stripe the width of which represents the potential difference between the corrosion potential and the polarization potential developed by the polarizing current i_{pol}. This difference is characteristic of the overvoltage of the anodic and cathodic reaction. The correlation between the polarization data obtained by different methods are shown in Fig. 3.

For the sake of better comparison Fig. 3 has been constructed to represent a special case where the decrease of the corrosion current density in the presence of adsorption inhibitor does not involve the change of the corrosion potential ε_{corr}.

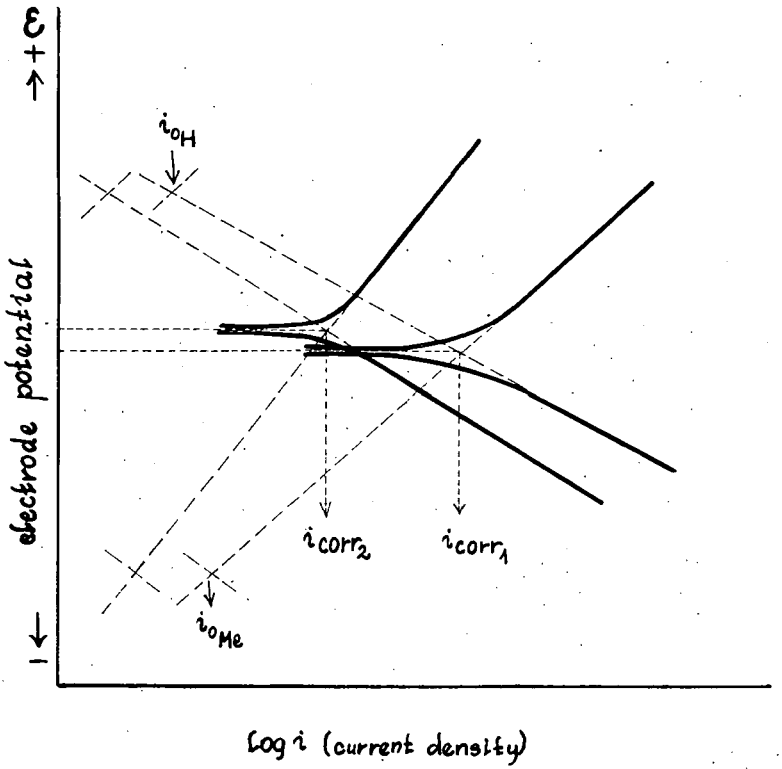

Fig. 2. Demonstration of the effect of an adsorption inhibitor by schematic polarization diagrams

Comparing the corrosion currents in Fig. 3 in the absence (i_{corr_1}) and presence (i_{corr_2}) of the inhibitor with the potential difference between ε_{corr} and the potential developed by the polarizing current density i_{pol} it is seen that the decrease of the corrosion current density is proportional to the increase of this potential difference, provided that the same electrode reactions are taking place in both cases with different overoltages. This suggests that under relatively simple conditions, *i.e.* if the anodic and cathodic polarization curves obey the Tafel equation and concentration or resistance overvoltage or new electrode reactions do not complicate the picture, intermittent galvanostatic polarization can provide a useful method for the study of the effect of corrosion inhibitors on the overvoltage of anodic and cathodic reactions and of the change of their effectiveness in time.

Applicability of dicyclohexylamine as adsorption inhibitor

Considering the inhibitor efficiency of organic amines HACKERMAN and MAKRIDES [1] supposed, that the interaction between the nitrogen atom of the amine group and the unoccupied *d*-orbitals of the metal surface is an acid-base interaction of the

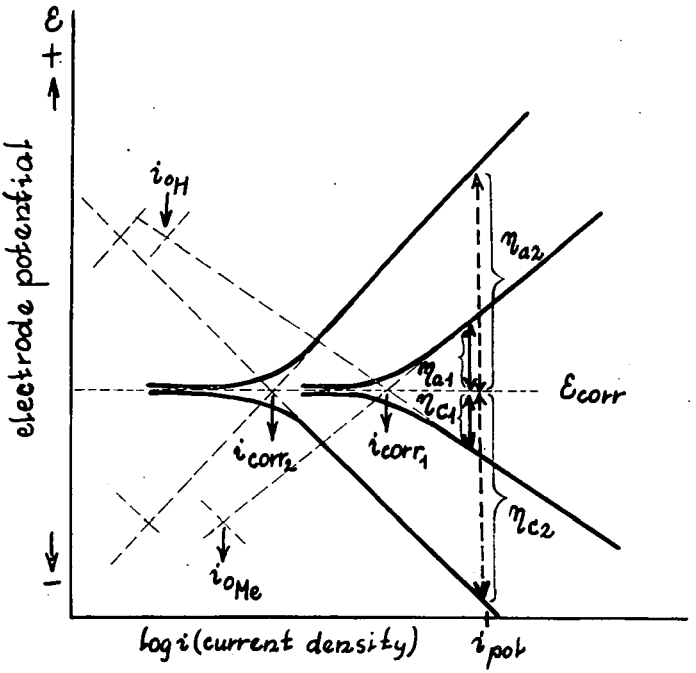

Fig. 3. Correlation between polarization data obtainable with continuous galvanostatic and intermittent galvanostatic polarization

Lewis-type. KAESCHE and HACKERMAN [2] furthermore suggested that the adsorption or rather chemisorption of the inhibitor is by means of the free amine. Recently, however, JOFA *et al.* [3, 4], FISCHER [5, 6] and HACKERMAN [7] have found that in the presence of halide anions and HS^- the adsorption of amines and of some other organic compounds takes place in the form of onium cations. Considering the characteristics of organic corrosion inhibitors it can be concluded that among other factors the basicity of the amines is important from the point of view of corrosion inhibitor efficiency. For the experiments described in this paper we have selected dicyclohexylamine as a model compound. Being a secondary amine with saturated rings, DCHA is a strong base with a relatively high electron density on the nitrogen atom. Considering the extreme forms — the free amine and the cationic form — in acidic solutions the equilibrium is shifted towards the cationic form. In the presence of H_2S the following equilibrium can be suggested:

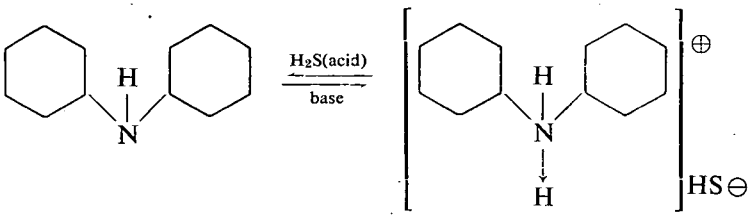

(1)

Considering the basicity of DCHA, it can be supposed that in the presence of H_2S in aqueous solutions the amine is predominantly present in the form of onium cations, producing a water-soluble salt with H_2S. By increasing pH and decreasing H_2S content the equilibrium shifts towards the free amine form. The solubility of DCHA is relatively low in aqueous solutions, very good in mineral oils and organic solvents like alcohols [8]. These properties should be considered for determining the applicability of DCHA in complex systems encountered *e. g.* in the petroleum industry.

Experimental

To investigate the effect of DCHA on the overvoltage of the anodic and cathodic reactions, measurements were carried out by steady-state and intermittent galvanostatic polarization. This method was first applied by NAGEL, LANGE and OHSE [9, 10] for the investigation of the equilibrium potentials of electrode processes taking place in metal/water binary systems. Recently the method was applied by the authors for the investigation of Me—S—H_2O ternary systems [11]. Theoretical aspects of the method have been discussed in details by LANGE and GÖHR [12]. A detailed description of the experimental cell and the block scheme of the measuring equipment is given in a previous paper of the authors [11]. Registration of the curves was carried out by a Metrohm Potentiograph Type E-336. The stock solution contained 5% Na_2SO_4. Acidic and alkaline pH values were set by addition of H_2SO_4 and NaOH (Reanal, of p. a. quality). Saturation with H_2S was carried out by bubbling H_2S gas through the solution, previously de-areated with nitrogen. The inhibitor was first dissolved in 10 ml methyl alcohol, then added to the experimental solution. Results described in this paper were obtained in stagnant solution, at 25 C°. Working electrodes were forged from mild steel and electrolytic iron. Cylindrical surface area was about 2 cm^2. Prior to the experiments, electrode surfaces were polished with different grades of emery paper, degreased in acetone and pickled at room temperature in a solution containing 15% HNO_3 and 5% HF. Pickling was followed by rinsing in distilled water and in the experimental solution.

Results and discussion

In 0.1 N H_2SO_4 solution containing 5% Na_2SO_4 the overvoltage of the anodic dissolution of iron and that of the cathodic hydrogen evolution is relatively low, as seen on Fig. 4. a. The corrosion potential is between $-0{,}25$ and -0.26 V (NHS). On addition of 0.01 M/l DCHA there is only a slight increase in the overvoltage of the anodic dissolution of iron. The increase in the overvoltage of the cathodic reaction, however, is definitely higher. This behaviour can be explained by the predominantly cationic nature of DCHA in acidic solutions. As it was pointed out by ANTROPOV [13], the action of organic corrosion inhibitors, determined by their adsorption, is strongly dependent on the surface charge of the metal and consequently on the position of the steady-state corrosion potential (or of the potential of an electrode polarized anodically or cathodically) relative to the zero charge point. Differential capacitance measurements carried out in H_2SO_4 solutions show that for

iron $\varepsilon_{q=0}$ is between $-0{,}33$ and $-0{,}37$ V (NHS) [14, 15]. This value was recently confirmed by the crossed wires method [16]. Considering -0.37 to be the zero charge potential, the corrosion potential of the iron surface on the Φ scale is:

$$Fe_{\Phi_{corr}} = Fe_{\varepsilon_{corr}} - Fe_{\varepsilon_{q=0}} \qquad (2.\,a.)$$

$$Fe_{\Phi_{corr}} = -0.25 - (-0.37) = 0.12\ V\ (NHS) \qquad (2.\,b.)$$

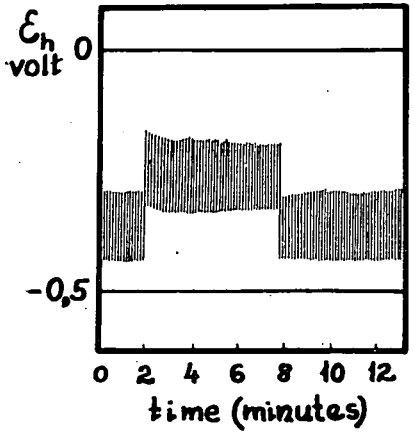

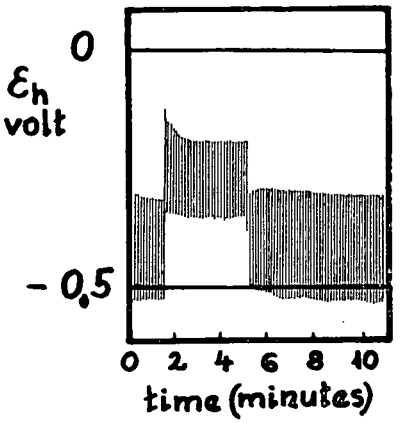

Fig. 4a. Electrode potential — time diagram obtained by intermittent galvanostatic polarization with iron electrode immersed into 0,1 N H_2SO_4 containing 5% Na_2SO_4. The upper and lower line series have been obtained by anodic and cathodic polarization, respectively. Current density: 1 mA/cm².

Fig. 4b. Potential — time diagram obtained in the same solutiou as in Fig. 4a. after addition of 0,01 M/1 DCHA. C.d.: 1 mA/cm².

It follows that under the experimental conditions discussed above the iron surface is positively charged. This charge hinders the adsorption of organic cations and promotes that of anions. For this reason at the corrosion potential $DCHA^+$ cations cannot adsorb on the iron surface. This is in good agreement with the experimental results of JOFA *et al.* [3, 4], who established that organic compounds of the cationic type are only weakly adsorbed on the iron surface from solutions of H_2SO_4. On anodic polarization the adsorption of cations is even less probable. The very slight increase in the overvoltage of the anodic dissolution of iron may be due to chemisorption of the free amine by the unshared electrons of its nitrogen atom. Since the concentration of the free amine is very low in acidic solutions, its effect on the overvoltage of the anodic dissolution may not be considerable. On the other hand, if the electrode is polarized towards the negative potential region from the corrosion potential, the adsorption of cations on a negatively charged metal surface will be possible. Thus on a cathodically polarized iron surface $DCHA^+$ ions can adsorb and inhibit the hydrogen ion discharge process. This is a possible explanation for the polarization behaviour shown in Fig. 4*a* and *b*.

The effect of H_2S on the anodic dissolution of iron and on the cathodic reduction of hydrogen ions is shown in Fig. 5*a*. It is seen that the overvoltage of the anodic

and cathodic reaction is considerably decreased, as compared to Fig. 4*a*. It has been shown by JOFA and TOMASHOVA [17] that the stimulating action of H_2S on the corrosion of iron increases with the increase of H_2S concentration in the solution.

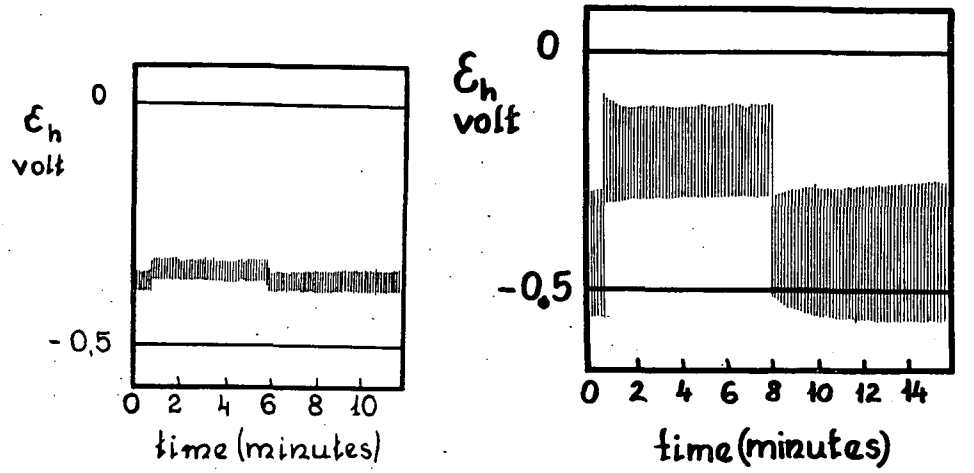

Fig. 5a. Potential — time diagram obtained in acidic solution saturated with H_2S. C.d.: 1 mA/cm²
Fig. 5b. Potential — time diagram obtained in acidic solution saturated with H_2S after the addition of 0.01 M/1 DCHA. C.d.: 1 mA/cm².

Similar results were obtained by HORVÁTH [18] in aqueous culture media inoculated with sulphate-reducing bacteria. The shift of the corrosion potential towards the negative region can be attributed to a decrease in the overvoltage of the anodic reaction giving rise to higher corrosion rate. In an earlier paper the accelerating action of H_2S on electrochemical reactions was attributed by JOFA [19] to the development of a negative adsorption potential ψ_1 as a result of HS^- adsorption on a positively charged metal surface. Recently JOFA [3] advanced the hypothesis that the action of H_2S is due to the formation of a surface catalyst acting in a similar manner as proposed by FRUMKIN [20] for OH^- ions. For iron the formation of this hypothetical catalyst has been described by JOFA et al. [3] by the following equations:

$$Fe + H_2S + H_2O \rightleftharpoons (FeHS^-)_s + H_3O^+ \tag{3}$$

The concentration of the catalyst may be given by

$$(FeHS^-)_s = K\frac{[H_2S]}{[H_3O^+]} \tag{4}$$

It follows that the anodic charge transfer reaction should be the oxidation of the surface catalyst:

$$(FeHS^-)_s \longrightarrow FeHS^+ + 2e^- \tag{5}$$

followed by the hydrolysis of the $FeHS^+$ ion or by the formation of FeS, depending on the pH of the solution. On the basis of equation (4) it can be expected that by lowering pH the concentration of the catalyst decreases parallel to the decrease of the stimulating effect of H_2S.

Fig. 5*b* demonstrates the synergetic effect of H_2S and DCHA in acidic solutions. It is seen that the overvoltage of both the anodic and cathodic reaction is highly increased. According to HACKERMAN [7] the synergism of the effect of anions and organic cations in corrosion inhibition can be attributed to the stabilization of the adsorbed or chemisorbed anion layer by organic cations. Considering that H_2S promotes the inhibiting effect of DCHA, it is reasonable to assume that in the presence of dissolved H_2S an ionic or dipole compound is formed on the iron surface — which may be considered as a surface catalyst — oriented with its negative end towards the solution. Then the negatively charged surface may promote tha adsorption of $DCHA^+$ cations, which in turn stabilize the $(FeHS^-)_s$ surface compound formed according to equation (3). In the case of cathodic polarization the explanation of the increased overvoltage may be similar to that given previously for the H_2S-free system.

References

[1] *Hackerman, N., A. C. Makrides:* J. Phys. Chem. **59**, 707 (1955).
[2] *Kaesche, H., N. Hackerman:* J. Elektrochem. Soc. **105**, 192, (1958).
[3] *Jofa, Z. A., V. V. Batrakov, Cho-Ngok-Ba:* Electrochim. Acta **9**, 1945, (1964).
[4] *Jofa, Z. A.:* Proceedings European Symposium on Corrosion Inhibitors, Annali Univ. Ferrara, Nuova Serie, Sez. V. 93, (1966).
[5] *Fischer, H., W. Seiler:* Proceedings European Symposium on Corrosion Inhibitors, Anali Univ. Ferrara, Nuova Serie, Sez. V. 19, (1966).
[6] *Lorenz, J. W., H. Fischer:* Proceedings European Symposium on Corrosion Inhibitors, Annali Univ. Ferrara, Nuova Serie, Sez. V. 81, (1966).
[7] *Hackerman, N., E. S., Snavely, J. S. Payne:* J. Electrochem. Soc. **113**, 679, (1966).
[8] *Cerveny, L.:* Proceedings European Symposium on Corrosion Inhibitors, Annali Univ. Ferrara, Nuova Serie, Sez. V. 701 (1966).
[9] *Nagel, K., R. Ohse, E. Lange:* Z. Elektrochem. **61**, 795, (1957).
[10] *Lange, E., R. Ohse:* Naturwissenschaften, **45**, 383, (1958).
[11] *Horváth J., L. Hackl:* Corros. Sci. **5**, 525 (1965).
[12] *Lange, E., H. Göhr:* Thermodynamische Elektrochemie, (Hüthig, Heidelberg, 1962).
[13] *Antropov, L. I.:* „Inhibitors of metallic corrosion and the phi-scale potentials." Ist International Congress on Metallic Corrosion, London, 1961.
[14] *Ajazjan, E. O.:* Dokl. Akad. Nauk. SSSR. **100**, 437 (1955).
[15] *Frumkin, A. N.:* Svensk Kemisk Tidskrift, 77:**6**—7, 300 (1965).
[16] *Voropaeva, T. N., B. V. Derjagin, B. N. Kabanov:* Izv. Akad. Nauk, 257 (1963).
[17] *Jofa, Z. A., J. N. Tomashova:* Zhur. Fiz. Khim. **34**, 1036, (1960).
[18] *Horváth J.:* Acta Chim. Hung. **25**, 65, (1960).
[19] *Kuznetzov, V. A., Z. A. Jofa:* Zhur. Fiz. Khim. **31**, 201, (1947).
[20] *Kabanov, B., R. Burstein, A. N. Frumkin:* Disc. Faraday Soc. **108**, 732, (1961).

ЭЛЕКТРОХИМИЧЕСКОЕ ИЗУЧЕНИЕ ИНГИБИЦИИ КОРРОЗИИ ЖЕЛЕЗА И СТАЛИ В ТЕРНИРНЫХ СИСТЕМАХ МЕТАЛЛА—СЕРЫ—ВОДЫ. II.

Изучение совместного действия органических коррозионных ингибиторов и сероводорода

А. Раушер, Л. Хакл, И. Хорват, Ф. Марта

Цель настоящей работы на основе лабораторных экспериментальных данных оценивать возможностей применения органических соединений как коррозионных ингибиторов катионного типа в кислых растворах, содержащих сероводород. Экспериментальные данные, полученные при помощи прерывной гальваностатичной поляризации указывают, что эффективность дициклогексиламина, употребленного в качестве модельного соединения приписывается совместному действию H_2S и ингибитора, предположенному авторами Иофа и Гаккерман.

SIMULTANEOUS DETERMINATION OF PEROXYSULPHURIC ACID AND CERIUM(IV) IONS

By I. PÉNZES and L. J. CSÁNYI

Institute of Inorganic and Analytical Chemistry, Attila József University, Szeged

(Received December 10, 1968)

Both components of a peroxysulphuric acid and cerium (IV) reaction mixture can be determined when cerium (IV) ions are precipitated by sodium acetate and sodium fluoride quenching solution. On the macro scale after iodometric titration of peroxysulphuric acid the cerium (IV) fluoride precipitate is dissolved in sulphuric acid, then the liberated iodine titrated with thiosulphate. On the micro scale the estimation of peroxysulphuric acid is carried out spectrophotometrically by measuring the absorption of iodine formed at 351 nm, while cerium (IV) is determined by its own colour at 320 nm after dissolution of the precipitate.

Recently it has been described [1] that in presence of cerium(IV) ions peroxysulphuric acid decomposes rapidly. The amount of oxygen evolved during the decomposition is somewhat greater than expected according to the equation $H_2SO_5 = 1/2\ O_2 + H_2SO_4$ and a part of cerium(IV) ions is also reduced. Because the measurement of oxygen evolved furnishes only meagre data for the elucidation of the mechanism of this rather involved reaction, it was necessary to find an appropriate method for the simultaneous determination of peroxysulphuric acid and cerium(IV) ions.

Peroxysulphuric acid and cerium(IV) ions represent not only potentially but also kinetically strong oxidizing agents. Considering the possibilities, it was expected that arsenous acid could be used as selective reagent, because it reduces peroxysulphuric acid quickly while its reaction with cerium(IV) ions, in the absence of catalysts, is very slow. However, in dilute solutions the peroxysulphuric acid cannot be instantaneously reduced by arsenous acid, consequently, it is not suitable for quenching the fast decomposition reaction.

Substances like iron(II), reacting instantaneously with both partners are suitable to stop the reaction and for the determination of the total oxidizing capacity, but the individual concentrations of the partners cannot be estimated.

Neither chelating agents can be used to this purpose, since most of them react rather quickly with peroxysulphuric acid as well as with cerium(IV) ions.

It would be expected that the simultaneous determination of the mentioned substances can be carried out by precipitation of the cerium(IV) ions, since precipitation is generally satisfactorily fast and thus suitable for quenching the reaction.

It is known that cerium(IV) ions hydrolize at pH's as low as 1 forming hydroxide or basic salt precipitate, but the addition of alkali to the reaction mixture may result in the partial decomposition of peroxysulphuric acid. Besides, another source of error may arise, because during the reaction between peroxysulphuric acid and

cerium(IV) ions, cerium(III) ions are also formed, which can be oxidized in presence of alkali either by molecular oxygen or by the remaining peroxysulphuric acid.

Although the precipitation of cerium(IV) by phosphate ions is quantitative, the forthcoming iodometric determination of peroxysulphuric acid will be erroneous. Namely, a part of the phosphate precipitate is of colloidal dimension, which will be dissolved by iodide and liberates iodine.

The separation of cerium(IV) ions can be carried out by fluoride ions. Since hydrogen fluoride is a fairly weak acid, the buffering of the solution is necessary. In presence of an acetate buffer cerium(IV) ions can be quantitatively precipitated by fluoride. According to the analysis the precipitate obtained has a composition of $Na_2[CeF_4(OH)_2]$. The precipitate proved to be resistant towards iodide, thus its separation is unnecessary. Reliable results can be obtained when acetate is used in cca. 2.5 fold and fluoride in cca. 25 fold excess with respect to the quantity of acid and cerium(IV) ions present, resp. Under such conditions the pH of the solution is about 4.5—4.8, which has two advantages. Firstly, at such pH the fluoride is

Table I

Taken		Found*		Percentage error	
H_2SO_5 mg	Ce(IV) mg	H_2SO_5 mg	Ce(IV) mg	H_2SO_5	Ce(IV)
10.67	9.15	10.69	9.13	+0,19	−0.22
7.84	9.00	7.83	9.00	−0.13	0
7.46	9.15	7.49	9.13	+0.40	−0.22
5.49	9.00	5.48	9.08	−0.18	+0.89
5.33	9.15	5.28	9.13	−0.94	−0.22
5.26	19.16	5.26	19.21	0	+0,26
4.09	—	4.05	—	−0.98	—
3.92	9.00	3.96	9.00	+1.02	0
3.68	9.58	3.65	9.67	−0.82	+0.94
3.19	9.15	3.18	9.13	−0.31	−0.22
2.63	4.79	2.60	4.83	−1.14	+0.83
2.36	9.00	2.38	8.99	+0.85	−0.11
2.05	9.61	2.03	9.70	−0.98	+0.94
1.57	1.92	1.57	1.93	0	+0,52
1.06	9.15	1.07	9.13	+0.94	−0.22
1.03	4.80	1.02	4.85	−0.97	+1.04
0.79	9.00	0.79	9.00	0	0
0.52	0.96	0.52	0.97	0	+1.04
0.41	1.92	0.40	1.90	−2.45	−1.04
0.20	0.96	0.19	0.97	−5.00	+1.04

* Data of single measurements.

less aggressive, so glassware can also be used, secondly, the iodometric determination of the peroxysulphuric acid is not interferred with dissolved oxygen. If the sample is added to the mentioned precipitating mixture, the reaction immediately stops as it can be seen in Table I. Data enlisted here were obtained by adding cerium(IV) to the quenching acetate and fluoride solution containing also peroxysulphuric acid of known quantity.

The iodometric determination of peroxysulphuric acid is followed by estimation of the cerium(IV) content. On acidifying the titrated solution with dilute sulp-

phuric acid saturated with boric acid, the precipitate is quickly dissolved and iodine is liberated by cerium(IV) ions. Boric acid is applied to convert hydrogen fluoride formed into tetrafluoroborate to damp the aggressiveness of the reaction mixture. Based on the foregoing the following procedure can be recommended for the simultaneous determination of peroxysulphuric acid and cerium(IV) ions.

Procedure

Under vigorous shaking the sample is pipetted to a solution containing as many ml of 2.5 M sodium acetate as acid equivalents are present and sodium fluoride in 25 fold excess with respect to cerium(IV). Then 0.5 g of potassium iodide is added to the solution containing the precipitate and after 3 minutes the iodine formed is titrated with thiosulphate by using starch as indicator. After the titration of peroxysulphuric acid cca. 1 g of marble chips is added and the solution is gently acidified with 20% sulphuric acid saturated with boric acid. When the acid concentration is about 0.1 M, the precipitate dissolves rapidly and the iodide will be oxidized by the cerium(IV) ions. After 3 minutes iodine is titrated again with thiosulphate. The interference of oxygen dissolved is prevented by carbon dioxide. By this method 0.7—70 mg of peroxysulphuric acid and 1.5—40 mg of cerium(IV) ions can be determined with about ± 1 % relative error.

Spectrophotometric analysis of the reaction mixture

By the above procedure solutions with concentrations lower than 10^{-4} M cannot be determined with sufficient accuracy. According to our experiences the reaction between peroxysulphuric acid and cerium(IV) ions can be satisfactorily stopped by using acetate and fluoride even in very dilute solutions. Only the formation of well-coagulated precipitate takes a longer time. Since in the presence of cerium(IV) fluoride precipitate peroxysulphuric acid can be kept for hours without any decomposition, no error is caused by waiting for recrystallization of the precipitate. For spectrophotometric analysis of the components the precipitate must be separated. To this end the precipitate is collected on a sintered glass filter of G5 porosity and washed thoroughly with cca. 0.1 M sodium acetate solution. The filtrate is collected in a graduated flask and 5 ml of cca. 2% potassium iodide solution added. The flask is filled up with 0.1 M acetate solution. After 10—15 minutes the iodine liberated is measured spectrophotometrically at a wavelength of 351 nm. As blank a solution having the same composition (acid, sodium acetate, sodium fluoride and potassium iodide) is to be used.

The precipitate is then redissolved in a graduated flask by 0.4 M sulphuric acid saturated with boric acid. Before filling the flask, potassium-aluminium-sulphate is added in a quantity to obtain about 0.01 M concentration with respect to aluminium. The flask is then filled up with 0.4 M sulphuric acid and the absorbance of cerium(IV) measured against 0.4 M sulphuric acid as blank solution at 320 nm. The addition of aluminium ions is necessary to prevent the bleaching effect of BF_4^- ions on the light absorption of cerium(IV). By this method $1\times10^{-6}-1\times10^{-4}$ M peroxysulphuric acid and $1\times10^{-6}-5\times10^{-4}$ M cerium(IV) can be estimated with ± 2.5% relative error as it is seen in Table II.

If the knowledge of the total cerium concentration is also required, cerium(III) ions are oxidized by peroxydisulphate according to WILLARD and YOUNG [2] and then the absorbance is measured at 320 nm.

Table II

Taken		Found*		Percentage error	
H_2SO_5 mg	Ce(IV) mg	H_2SO_5 mg	Ce(IV) mg	H_2SO_5	Ce(IV)
0.521	4.79	0.524	4.70	+0.58	+1.88
0.484	4.77	0.489	4.68	+1.03	+1.89
0.339	3.81	0.344	3.88	+1.47	+1.84
0.312	3.83	0.318	3.77	+1.92	−1.56
0.242	2.86	0.245	2.89	+1.24	+1.05
0.156	1.91	0.156	1.87	0	−2.10
0.145	1.91	0.148	1.95	+2.06	+2.10
0.052	0.48	0.054	0.47	+3,86	−2.08
0.049	0.48	0.048	0.47	−2.04	−2.08

* Data of single measurements.

References

[1] *Csányi, L. J., F. Solymosi:* Anal. Chim. Acta **15**, 501 (1956).
Csányi, L. J., F. Solymosi, I. Szücs: Naturwissenschaften **10**, 353 (1959).
Csányi, L. J., L. Domonkos: Acta Chim. Hung. **34**, 383 (1962).
[2] *Willard, H. H., P. Young:* J. Am. Chem. Soc. **50**, 1379 (1928).

СОВМЕСТНОЕ ОПРЕДЕЛЕНИЕ ПЕРОКСИСЕРНОЙ КИСЛОТЫ И ЦЕРИЯ(IV)

И. Пензеш и Л. Й. Чани

Определение обоих компонентов реакционной смеси состоящей из пероксисерной кислоты и церия(IV) проведено путём осаждения ионов церия(IV) стопорным раствором ацетата натрия и фтористого натрия. В макро-количестве после йодометрического титрования пероксисерной кислоты осадок фтористого церия(IV) растворен в серной кислоте, а йод титрован тиосульфатом. В микро-количестве пероксисерная кислота определяется спектрофотометрически, путём измерения поглощения света образующегося йода при 350 нм. При определении церия(IV) измерили свой цвет при 320 нм после растворения осадка.

MICRO-DETERMINATION OF CERIUM

By I. PÉNZES and L. J. CSÁNYI

Institute of Inorganic and Analytical Chemistry, Attila József University, Szeged

(Received December 10, 1968)

Copper(II) phtalocyanine, methylene blue and iron(II) have been recommended for the micro-determination of cerium(IV) in the presence of cerium(III). — Optical interaction between cerium(IV) and cerium(III) has been observed when cerium(IV) is present in form of hydroxo complexes.

There are many useful volumetric macro methods for the determination of cerium(IV) ions, but these are not precise enough on micro scale [1]. For this reason it was necessary to find better ways for the estimation of cerium(IV) in minute quantities.

1. *Determination of cerium(IV) based on its own colour*

It is well known that cerium(IV) ions strongly absorb the light at 320 nm, in 0,4 M sulphuric acid, $\varepsilon = 5540$ l. mole^{-1} cm^{-1}. This behaviour makes possible the spectrophotometric determination of cerium(IV) [2]. The estimation based on the absorbance, however, can be carried out only under strictly defined experimental conditions. Namely, cerium(IV) ions hydrolize even at low pH values, cerium(IV) hydroxide or basic salts being precipitated. This can be avoided by adjusting the sulphuric acid concentration at least to 0.4 M.

When cerium(IV) ions are present in form of hydroxo complexes and the solution contains cerium(III) ions as well, an optical interaction can be observed. From this follows that the amount of cerium(IV) ions determined spectrophotometrically depends on the concentration of cerium(III) present. The extent of the optical interaction is the greatest in presence of perchloric acid, while somewhat smaller in nitric acid and the smallest in a sulphuric acid medium.

Reliable analytical data for cerium(IV) ions can be obtained only in absence of cerium(III). The measurement can then be carried out in the following way: The acid concentration is adjusted to 0.4 M by sulphuric acid and the absorbance measured at 320 nm. The Lambert—Beer law holds in the range of $10^{-6} - 10^{-4}$ M and the concentration of cerium(IV) can be calculated by using the value of the extinction coefficient given above.

2. *Determination of cerium (IV) by oxidation of different dyestuffs*

When the solution to be analysed contains cerium(III) ions, too, other ways are to be looked for to determine the cerium(IV) ions. To this end a series of dyestuffs was tested. The following were found suitable for the determination based on the bleaching effect of cerium(IV).

a) *Determination with the aid of copper (II) phtalocyanine complex*

The copper(II) complex of phtalocyanine is readily soluble in water, the obtained blue solution absorbs the light at 620 nm, and its extinction coefficient is as high as 42 000 l. $mole^{-1}$ cm^{-1}. The complex reacts with cerium(IV) ions rapidly. On adding the oxidizing agent to the dye solution, transitorily a red colour is developed, the disappearence of which takes a longer time especially when the concentration of cerium(IV) is relatively high. This phenomenon may be ascribed either to a multistep oxidation process or to the disproportionation reaction of the red intermediate. For the analysis the following procedure may be suggested:

Adjust the acid concentration of the solution to be analysed to 0.4 M by sulphuric acid and add the aqueous solution of the copper(II) phtalocyanine reagent drop by drop in a quantity to obtain a dye concentration of about 2.10^{-5} M. After having filled the graduated flask, measure the absorbance at 620 nm. If proceeding so, the dyestuff will be rapidly oxidized on the effect of cerium(IV) to the final state and thus the measurement can be carried out immediately. By this method 0,03—0,3μM cerium(IV) can be determined with $\pm 3\%$ relative error. Cerium(III) ions present do not interfere with the analysis, while strong oxidizing reagents do.

The aqueous solution of the reagent can be stored without any decomposition for a longer time. — It is necessary to call attention to the fact that the absorbance of the dye markedly depends on temperature.

b) *Determination of cerium (IV) by methylene blue*

The reaction between methylene blue and cerium(IV) ions may also be applied to analytical purposes [3]. In 1 M sulphuric acid methylene blue has a high absorption peak at 755 nm (the extinction coefficient is 52 600 l. $mole^{-1}$ cm^{-1}) and the Lambert—Beer law holds. Under such experimental conditions the dye instantaneously reacts with cerium(IV) ions, 1 mole methylene blue and cca. 4.5 mole cerium(IV) being involved in the reaction.

In neutral solutions, however, depending on the dye concentration, rather involved association equilibria exist, which result in a great change in the absorbance of the dye.

According to our experiences reliable data can be obtained by the following procedure:

The sample to be analysed is pipetted into a graduated flask of 25 ml containing 3—4 ml of 10^{-4} M methylene blue solution and sulphuric acid sufficient, taking into account also the acid content of the sample, to attain 1 M total acid concentration at the end volume. The flask is then shaken thoroughly and filled up to the mark. The absorbance of the solution is measured at 755 nm by using 1 M

sulphuric acid as blank. The drop in the absorbance caused by cerium(IV) is proportional to its concentration. By this method 0,1—1,0 μM of cerium(IV) can be estimated with $\pm 1{,}5\%$ relative error.

c) *Determination of cerium(IV) by iron(II) ions*

The interference of cerium(III) can also be avoided by reducing cerium(IV) ions with iron(II) and measuring the light absorption of the iron(III) formed. At about 0.8 M acid concentration the reaction is instantaneous. For determination the following procedure may be suggested. Pour the sample in a graduated flask of 25 ml containing 10 ml of 10^{-2} M $FeSO_4$ and sulphuric acid in a quantity to get 0.4 M acid concentration at the end volume. The flask is filled up to the mark, then the absorption of iron(III) is measured at 304 nm. The estimation of 1.2—12.5 μM cerium(IV) can be carried out with $\pm 2\%$ relative error. It should be mentioned that cerium(III) ions also absorb the light at 304 nm, the extinction coefficient is, however, only 26 $l\,mole^{-1}\,cm^{-1}$. Consequently, cerium(III) does not interfere heavily when its concentration is commensurable with that of cerium(IV).

Ferroin was also applied to the determination of cerium(IV) but, contrary to literature, [4] no reliable results were obtained.

References

[1] *Brukl, A., A. Faessler:* Handbuch der analytischen Chemie Bd. III. a/III. b., 317. (Springer Verlag Berlin, 1956).
Eremin, Yu. G., L. A. Lavrova, V. V. Raevskaya, P. N. Romanov: Zav. Lab. **30** (12) 1427 (1964).
[2] *Boyle, J. W.:* Radiation Research **17**, 427 (1962).
Blatz, L. A.: Anal. Chem. **33**, (2) 249 (1961).
[3] *Goto, H., Y. Kakita:* J. Chem. Soc. Japan, Pure Chem. Sect. **79**, (12) 1524 (1958).
[4] *Culkin, F., J. P. Riley:* Anal. Chim. Acta **24**, (2) 167 (1961).

МИКРО-ОПРЕДЕЛЕНИЕ ЦЕРИЯ(IV)

И. Пензеш и Л. Й. Чани

Для определения микро-количеств церия(IV) в присутствии церия(III) авторами рекомендовались фталоцианин меди(II), метиловый голубой и железо(II). Если церий(IV) имеется в виде гидроксо комплексов, оптическое взаимодействие между цериями (IV) и (III) было наблюдено.

MIXED COMPLEXES OF CU(II)PAN WITH CHLORIDE AND BROMIDE IONS

By J. A. SZABÓ and V. NIKOLASEV

Institute of Organic Chemistry, Attila József University and Institute of Pathophysiology, University Medical School, Szeged

(Received November 30, 1968)

Cu-PAN-Cl and Cu-PAN-Br complexes have been prepared and their structure and composition studied.

Introduction

An orange red dye 1-(2-pyridylazo-)-2-naphtol (PAN) as a valuable indicator has been introduced by CHENG and his co-workers [1—5] in the complexometric titrations of copper, zinc, cadmium and indium solutions with ethylenediaminetetraacetic acid. Recently the stability constants of complexes of Ni, Co, Zn, and Mn ions with PAN in some aqueous-organic mixtures were calculated. The extraction mechanisms of PAN complexes of the metals mentioned above have not been sufficiently studied, but it is evident that in the case of extraction of indium, iron(III), cobalt(III), yttrium, palladium(II), rhodium(III) or iridium with PAN [9—13], mixed complexes are formed with outer anion to produce uncharged complexes. The structures of complexes extractable in chloroform or other organic solutions have not been investigated so far. The aim of the present paper is to study the problem of Cu(II) PAN yielding uncharged mixed complexes with bromide and chloride ions.

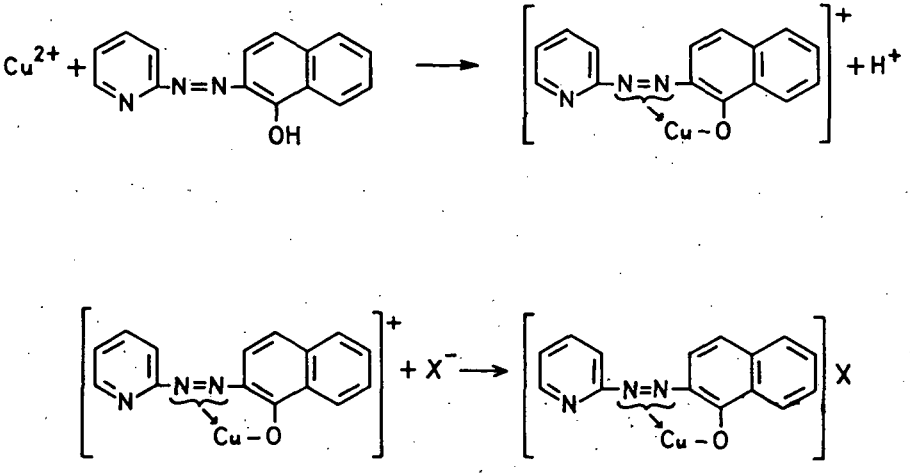

$X^- = Cl^-$ or Br^-

Experimental

Materials: $CuSO_4 \cdot 5\,H_2O$ KBr, KCl, p. a. PAN, (REANAL). IR Spectra were taken with an UNICAM SP 200 Spectrometer. Samples were prepared in Merck UVASOL KBr. Preparation of complexes: 2 ml of aqueous 10^{-1} M $CuSO_4 \cdot 5\,H_2O$ was added to 2 ml of ethanolic solution, saturated with PAN, then 2 ml of 5 M aqueous KBr or 2.5 M aqueous KCl was added. Within some minutes a violet red precipitate was formed which after centrifugation was dried over anh. $CaCl_2$ and P_2O_5.

Results

Microanalitical combustion method was used to determine the carbon-, hydrogen, and nitrogen-content. After fuming the complexes with H_2SO_4—$HClO_4$ mixture, copper was determined volumetrically by the iodide-thiosulphate method. Halide was determined gravimetrically as silver halide. The results were as follows:

Cu-PAN-Cl, found: Cu 17.95 C 50.85 N 3.88 H 3.10 Cl 9.76 O 14.44, calc: Cu 18.05 C 51.13 N 3.98 H 3.12 Cl 10.05 O 13.63%.

Cu-PAN-Br, found: Cu 15.95 Br 19.90 O 13.10 N 3.62 H 2.99 C 44.50. calc: Cu 16.04 Br 20.18 O 12.40 N 3.52 H 2.80 C 45.45.

Infrared spectra have been taken. From the curves the following could be established.

In the spectrum of PAN the following peaks appear: 755 cm^{-1} and 841 cm^{-1} aromatic ring, 1215 cm^{-1} (strong) ($\nu C-O$), 1510 cm^{-1} ($\nu N=N$), 1603 cm^{-1} pyridine aromatic ($\nu C{=}{-}C$), further 1563, 1572, 1625 cm^{-1} aromatic ($C{=}{-}C$), 2200 cm^{-1}, 3650 cm^{-1} broad associated OH. In the case of Cu-PAN-Br and Cu-PAN-Cl the OH peak does not appear and the 1510 cm^{-1} strong azo peak can be found at a considerably smaller wave number at 1375 cm^{-1}, in consequence of a metal-ion bond being formed.

No significant change was found with the wave numbers, of the aromatic groups except the peaks appearing about 1600 cm^{-1} which essentially gave two maxima at 1592 cm^{-1} and 1610 cm^{-1}.

Bromide and chloride ions have no influence on infrated spectra in the region measured. According to our assumption the formation of Cu-PAN, Cu(II)PAN-Br and Cu(II)PAN-Cl can be described as follows, Fig. 1. In our opinion the effect of substances accelerating the extraction of Cu(II)PAN into an organic phase can be explained by the formation of a neutral mixed complex.

References

[1] *Cheng, K. L.:* Anal. Chem. **27**, 1582 (1955).
[2] *Cheng, K. L.:* Anal. Chem. **30**, 243 (1958).
[3] *Cheng, K. L.:* Anal. Chem. **1027**, 243 (1958).
[4] *Cheng, K. L., R. H. Bray:* Anal. Chem. **27**, 782. (1955).
[5] *Cheng, K. L., T. R. Williams:* Chem. Anal. **44**, 96 (1955).
[6] *Burton, F., M. B. Williams:* Anal. Chem. **31**, 1044 (1959).
[7] *Corsini, A., I. May-Syng Yik., Q. Fernando, H. Freiser:* Anal. Chem. **34**, 1090 (1962).
[8] *Betteridge, A., Q. Fernando, H. Freiser:* Anal. Chem. **35**, 294 (1963).

[9] *Zolotov, Yu. A., I. V. Serjakova, G. A. Vorobyeva:* Talanta, **14**, 737 (1967).
[10] *Shibata, S.:* Anal. Chim. Acta **125**, 348 (1961).
[11] *Goldstein, G., D. L. Manning, O. Menis:* Anal. Chem. **31**, 192 (1959).
[12] *Busev, A. I., L. V. Kiseleva:* Vestnik Mosk. Univ. Ser. II, Khim. **4**, 179 (1958).
[13] *Stokely, I. R., W. D. Jacobs:* Anal. Chem. **35**, 149 (1963).

СМЕШАННЫЕ КОМПЛЕКСЫ Cu(II) PAN с ИОНАМИ ХЛОРИДА И БРОМИДА

Й. А. Сабо и В. Николашев

Авторы готовили комплексы Cu(II) PAN Cl и Cu(II) PAN Br и изучали их строение и содержание.

LOCATION OF THE COMPONENTS IN CHROMATOGRAMS BY MEASUREMENT OF THE THERMAL GRADIENT ARISING FROM THE HEAT OF ADSORPTION

By L. MÉSZÁROS and GY. SCHÖBEL

Institute of Applied Chemistry, Attila József University Szeged,

(Received November 30, 1968)

Measurement of the heat of adsorption of the individual components along the axis of a chromatoraphic column makes possible the exact location of the respective components. The measurement is accomplished by means of a micro thermocouple; the technique possesses high sensitivity and is particularly advantageous when the usual optical methods fail, *e.g.* in the case of colourless substances or a coloured adsorbent.

There exist several, well-known techniques for the detection and location of components, *e.g.* along a chromatographic column. These methods are usually based on optical observation or visualization, *e.g.* by irradiation with ultraviolet light [1, 2], of the components. Unfortunately, the principle implies the restriction that the components to be separated must be coloured or have to le visualized in some way [3—11] in order to distingvish them from each other as well as from the adsorbent itself.

We wish to report here an essentially new technique for the location of the components separated in a chromatogram. The technique is based on the known facts that migration of a component along the column consists of continous adsorption and desorption processes, and that both adsorption and desorption processes are accompanied by thermal changes. Measurement of these, extremely minute, thermal changes, *i.e.* the thermal gradient, along the axis of the chromatographic column was found suitable for the location of the adsorbed components.

The thermal gradient was measured with the aid of a micro thermocouple (1—5 mg), simply constructed by welding together the ends of an iron and a constantan wire. It was found that the welded wires need not be isolated, as the minute voltage of a few millivolts induced by the thermal gradient was not affected by the presence of metal powders or carbon adsorbent either. The omission of the usual insulation, consisting of two ceramic tubes, considerably reduced the heat capacity of the detector and thus increased the sensitivity.

The free terminals of the thermocouple were connected either to a millivoltmeter with temperature scale or rather to a compensograph. The welded joint of the couple was then moved up and down along the axis of the column by means of an electric motor and the voltage generated in the thermocouple on passing through the adsorption zones was continuously recorded. Plotting the voltage against the position of the welded joint in the adsorbent, the exact location of the separated components in the column could be immediately obtained.

Description of the apparatus

Figure 1 shows a schematic illustration of the apparatus. The iron [2] — constantan (3) thermocouple (4) tightened by spring (7) and led by pulleys (6) is drawn up and down by electric motor (10). The movement is reversed by the device (11) as soon as the welded joint (4) has left the space filled with adsorbent. The free terminals (8) of the thermocouple are connected to compensograph (9).

A characteristic curve obtained in case of two components is also given in the figure.

Examples

a) *Examination of leaf pigments*

Dried spinach leaves were extracted with benzenemethanol (6:4) and the extract passed through a column of 20 cm height and 26 mm inner diameter filled with precipitated $CaCO_3$. Subsequent to the development of the chromatogram an iron — constantan thermocouple of 0.2 mm. diameter was passed along the axis of the column with a rate of 1 cm/sec. The chromatographic column was made of a double-walled glass-tube and water of 20 °C was circulated in the jacket. In Fig. 1 both the apparatus and the temperature — displacement curve are shown, the latter in a shortened form to fit the length of the tube. A strict correlation was found between the sites of the individual components separated, as shown by their colour, and the sites of maxima observed in the compensogram.

In another experiment the adsorbent was mixed with 20(w)% black glass-powder, so that the visual evaluation of the chromatogramm was not possible. The thermal gradient, measured just as in the preceding description, indicated a decrease in the height of the maxima and simultaneously an increase in their relative distance. The adsorbent was then pushed out of the tube, cut to pieces according to the compensogram the sections were extracted with ethyl alcohol separately and each chromatographed on separate $CaCO_3$ columns. Each column showed then only one coloured component, proving the reliability of our method.

b) *Separation of the components of the product of a vapour-phase heterogeneous catalytic reactor*

In the course of a continuous procedure of the author (12) for the large-scale oxidative transformation of furfurol to furan, *via* 2-furoic acid, it was necessary to separate the two main components of the reaction product, namely furan and carbon dioxide. This was done by adsorption on charcoal filled in a chromatoggraphic tube, the elution being carried out by steam. The site of adsorption of furan could easily be recognized in all cases, as the heat of adsorption was so high that it could be sensed merely by hand. Application of the present technique, however, revealed the presence of another adsorption zone, namely that of carbon dioxide. Disregarding of the existance of this adsorption zone had caused serious difficulties earlier; as a matter of fact if the evaluation was started before complete removal of carbon dioxide, the latter carried along part of the furan, too, thus decreasing the yield.

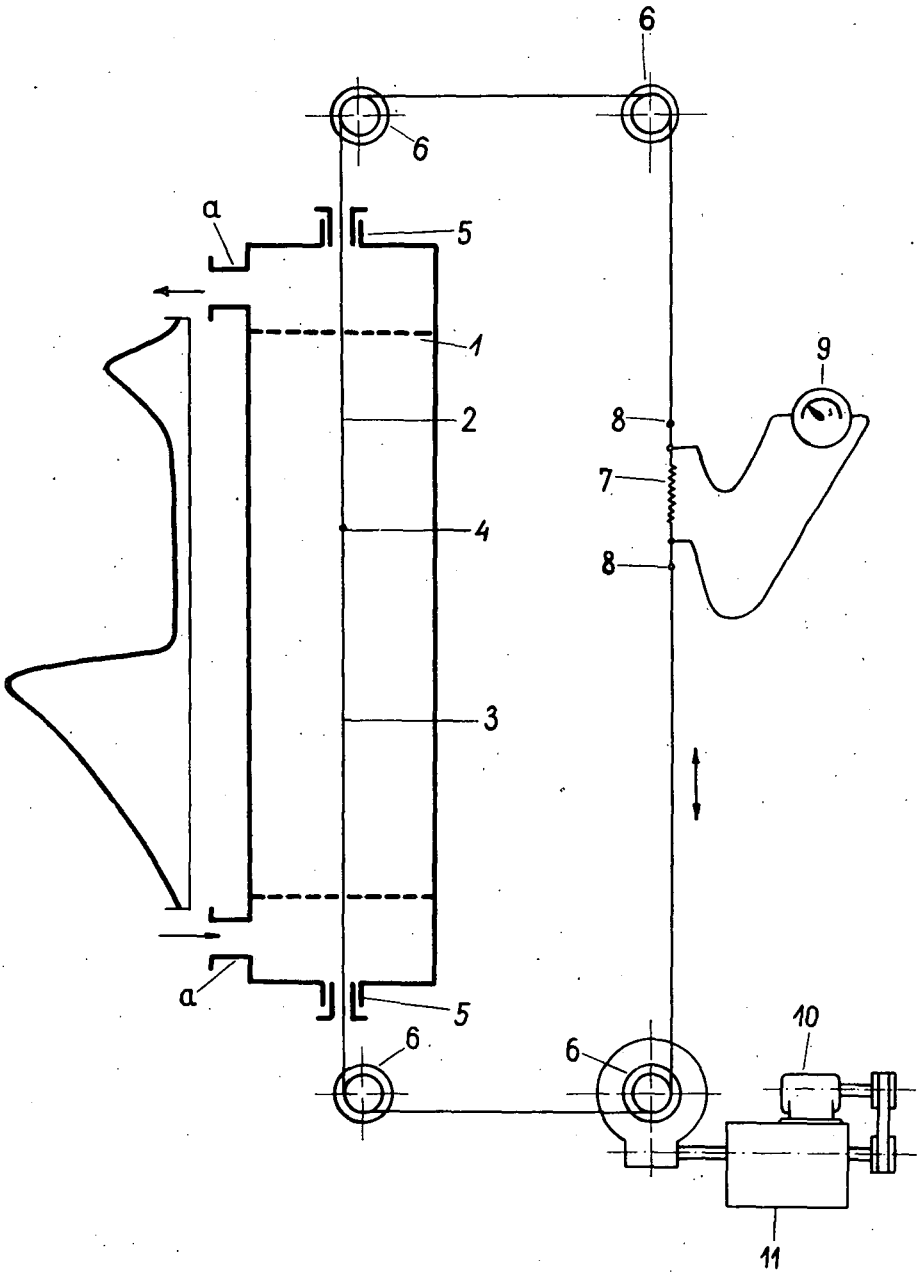

Fig. 1

Discussion

The above technique is just the reverse of that used in gas-chromatography. While in gas-chromatographs the detector is fixed and the changing medium passes through it, in our method the medium is standing (or at least almost standing) and the detector is moving. This offers wide possibilities for various technical applications both in laboratory work and in industry [13].

References

[1] *Zechmeister, L., L. Cholnoky:* Principles and Practice of Chromatography 2nd Ed. (Reinhold, New York, 1943).
[2] *Almasy, F.:* Biochem. Z. **291**, 421 (1937).
[3] *Zechmeister, L., L. Cholnoky, B. Újhelyi:* Bull. Soc. Chim. Biol. **18**, 1885 (1936).
[4] *Brockmann, H., F. Volpers:* Ber. **80**, 77 (1947).
[5] *Brown, J. A., M. M. Marsh:* Anal. Chem. **25**, 1865 (1953).
[6] *Sease, J. W.:* J. Am. Chem. Soc. **70**, 3630 (1948).
[7] *Graff, M. M., E. L. Skau:* Ind. Eng. Chem., Anal. Ed. **15**, 340 (1943).
[8] *Sylvester, N. D., A. N. Ainsworth, E. B. Hughes:* Analyst **70**, 295 (1945).
[9] *Rodewald, M., L. Zechmeister:* Enzymologia **15**, 109 (1951).
[10] *Valentin, J., G. Kirchübel:* Arch. Pharm. **284**, 114 (1951).
[11] *Oshchakowskii, V. V.:* Zhur. Anal. Him. **11**, 606 (1956).
[12] *Mészáros, L.:* Acta Phys. et Chem. Szeged **8**, Suppl. 1 (1962).
[13] *Mészáros, L.:* Unpublished results.

УСТАНОВЛЕНИЕ МЕСТ КОМПОНЕНТОВ ХРОМАТОГРАММА ИЗМЕРЕНИЕМ ТЕМПЕРАТУРНОГО ГРАДИЕНТА ТЕПЛА АДСОРБИРОВАНИЯ

Л. Месарош и Д. Шебел

Термоэлемент был приготовлен из железных и константановых проволок что они сварились таким образом что проволоки стали одной нитью. Проволока переходит через химические реакторы, газовой хроматограф или жидкой хроматограф с часовым механизмом и место пайки идёт по прямой линии. Включая в компенсограф, измеряется попутной тепловой градиент из которого в случае гетерогенных каталитических трубчатых печей в газовой фазе предполагается где именно химический процесс имеет место.

В случае хроматограммов определяются хроматограммы бесцветных веществ на цветных абсорбентах и потом они изолируются.

Присутствие абсорбированного фурана и углекислоты обнаружено этим методом, а десорпция фурана осуществляется после элюирования слоя углекислоты.

Термоэлемент применяя без оболочки является детектором температуры с тысячей, десятью тысячей большей тепловой инерцией.

По нашим опытам электрическое закорочивание не влияет на точность измерения.

VERWENDUNG VON FURFUROL, XII

Untersuchungen von Reaktoren für exotherme-katalytischer Prozesse. I

Von L. MÉSZÁROS und S. A. GILDE

Institut für Angewandte Chemie der Attila-József-Universität, Szeged

(Eingegangen am 30. November 1968)

Die Volumvergrößerung der Rohröfen haben wir unter Beibehaltung der ursprünglichen Höhe durch Eintragen von Katalysatoren zwischen parallele Oberflächen gelöst. Die Entfernung der Flächen voneinander wurde geringer gewählt als der Umfang des Rohrofens. Durch dieses System der Volumvergrößerung wurden die spezifischen Produktionswerte nicht beeinträchtigt, während die Vergrösserung des Apparates durch lineare Berechnungen erreichbar war. Diese Methode kann verallgemeinert werden. In Verbindung mit anderen Arbeiten hatten wir auf diese Weise aus unserem Fadenreaktor Band- und Gardinenreaktoren, und aus unserem Zerstäuber Spaltzerstäuber bzw. Kreis-Spaltzerstäuber entwickelt. Aus unseren Planparallelreaktoren haben wir dann Scheibenreaktoren hergestellt und mit 5, die Reaktionsgase aus- und einführenden, perforierten, bogenfürmigen Röhren versehen. Eine Automatik sorgte für den Wechsel der Ein- und Ausföhrstellen, wodurch die entstehendenlokalen Übererwärmungen ihren schädlichen Einfluß nicht entfalten konnten, weil sie kontinuierlich auf immer andere Punkte des Apparates verlagert würden. Die Brauchbarkeit der Apparate-Familie haben wir mit der Reaktion der Furanherstellung aus Furfurol erprobt und erwiesen, welche eine sehr hohe Reaktionswärme aufweist.

Wir haben uns mit der Dimensionierung von Reaktoren für exotherm-katalytische Reaktionen, bzw. ihrer idealen Gestaltung mit Zugrundelegung der Furfurol—Furan-Reaktion beschäftigt und dabei Ergebnisse erhalten, die sich verallgemeinern lassen.

Im Laboratoriumsausmaß durchgeführte Operationen sind oft nur schwer auf industrielle Maßstäbe zu übertragen, wenn die Vergrößerung der Ausmaße auch durch wirtschaftliche Faktoren beeinflußt oder beschränkt wird [1, 2].

In Kenntnis der Theorie der untersuchten Prozesse kann mit Hilfe statistischer Methoden, sowie unter Verwendung der Ähnlichkeitstheorie die Zahl der erforderlichen Versuche wesentlich verringert und mit kleineren Apparaten gearbeitet werden, und die erhaltenen Ergebnisse sind auf eine ganze Reihe anderer, ähnlicher Vorgänge zu verallgemeinern. Das gleiche Ziel verfolgten mit anderen Begriffen P. BENEDEK und A. LÁSZLÓ mit der Einführung des Freiheitsgrades der einzelnen Systeme [3].

Die Praxis des Chemikers und des Chemieingenieurs wendet jene Gesetze der Hydrodynamik und der Wärmeübertragung systematisch an, die sich mit den Methoden der Ähnlichkeitstheorie auf Grund von Versuchsdaten verallgemeintern lassen; während zur Lösung ausgesprochen chemisch-technologischer Probleme die Ähnlichkeitstheorie bisher nur wenig Verwendung gefunden hat. Die technologischen Prozesse der chemischen Industrie sind überaus verwickelt und infolgedessen sind auch die Ahnlichkeitsbedingungen kompliziert so daß sie an Modellen schwer zu verwirklichen sind.

Im Laufe unserer Arbeit trachteten wir durch Klärung der Fragen der stufenweisen Dimensionsvergrößerung von dem als „eindimensional" zu betrachtenden, dünnen Rohrreaktor zu eine dreidimensionale Vergrößerung zulassenden Reaktortypen zu gelangen. Unser Ziel ist demgemäß die Untersuchung der Intensivierung der chemischen Reaktion auf Grund von Modellreaktoren und eine jeweils vervollkommnete Lösung def automatischen Steuerung der Apparate.

Diese Aufgaben stehen in enger Beziehung zu den Bestrebungen von M. KORACH und der ungarischen chemisch-technologischen Schule [4].

Wärmeverteilung in Rohrreaktoren

Bei exotherm-katalytischen Reaktionen bedeutet die Ableitung der freiwerdenden Wärme, bzw. die Konstanterhaltung der Temperatur des Reaktors eines der heikelsten Probleme der Planung und Bemessung. Somit ergab sich als erstes Ziel, die Wärmegradienten im Reaktorquerschnitt innerhalb enger Wertgrenzen zu halten.

Zur Untersuchung dieser Frage sollen Rohrreaktoren verschiedener Weite dienen, die mit Katalysatorkörnenen von 0,1 mm Durchmesser gefüllt werden. Die Reaktorwand werde auf einer Temperatur von T_0 °C gehalten, die Beschaffenheit und die auf 1 cm² Querschnitt bezogene Raumgeschwindigkeit der durchströmenden Stoffe sei konstant. Unsere untersuchten Reaktoren haben Durchmesser von 1, 3, 10, 30 bzw. 100 mm. Setzen wir nun die Reaktion in Gang, d. h. beginner wir die Reaktionskomponenten — z. B. Furfurol und Luft — in stöchiometrischen Mengen einzuspeisen, u. zw. *a* mg Furfurol pro cm² und Stunde. Die Untersuchung der äquithermalen Oberflächen in Abhängigkeit von der Zeit (Abb. 1, links von der Ebene *y*, *z*) ergibt immer mehr gestreckte Paraboloide. — Untersuchen wir die axialen Temperaturgradienten in Abhängigkeit vom Durchmesser (Abb. 1, rechts von der *y*, *z*-Ebene), die mit guter Näherung auch jetzt Paraboloide darstellen. Aus Abbildung 1 ist ersichtlich, daß in dem Reaktor von 1 mm lichter Weite die Differenz zwischen äußerer und innerer Temperatur gering, und das System technisch isotherm ist. Wird der Durchmesser erweitert, so nimmt die Temperaturdifferenz zwischen Reaktorwand und Mittellinie allmählich zu. Bei einem Durchmesser von 30 mm erreicht die Temperaturdifferenz einen solchen Wert, daß bei noch weiter zunehmender Temperatur das Material schon verbrennt und die Produktion steil absinkt.

Im Falle des in Abb. 1 dargestellten Versuches läuft die Reaktion am vorteilhaftesten in Reaktoren von 10, 3 und 1 mm lichter Weite ab, da die isothermalen Reaktionsbedingungen mit der Abnahme des Durchmessers immer besser angenähert werden. Hierbei ist jedoch das Füllen und Entleeren des Katalysators sehr umständlich; man bedenke nämlich, welche Wanddicke und Rohrbündelzahl ein Reaktor haben muß, wenn der Prozeß auf einen Katalysatorraum von 1 m³ bemessen werden soll. Bei großen Abmessungen setzt also das Verbrennen des Reaktionsgemisches und des Katalysators, bei kleinen dagegen die Kostspieligkeit und Umständlichkeit der Behandlung Grenzen; es müssen zwischen beiden die optimalen Maße gesucht werden. Nach unseren experimentellen Befunden haben die entsprechendsten oxydativen Reaktoren 20—30 mm Durchmesser, und im Falle stark exothermer Prozesse dürfen die Reaktoren elemente beliebig großer Betriebe 2—2,5 m Länge

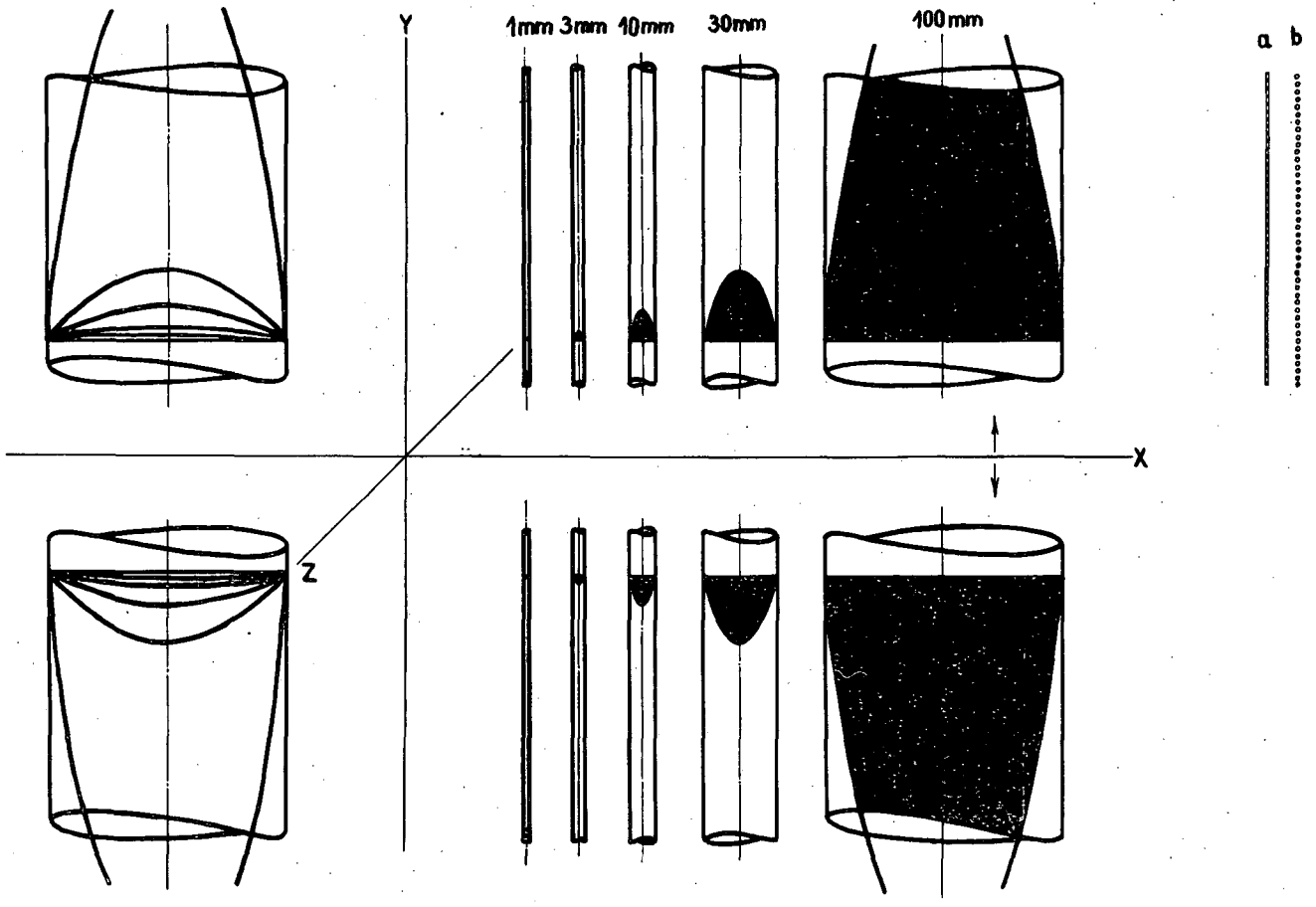

Abb. 1. Darstellung der Wärmegradienten in Rohreaktoren von verschiedenem Durchmesser

nicht überschreiten. Im Falle gleicher Reaktordurchmesser können die Bedingungen der optimalen Betriebsmäßigkeit innerhalb gewisser Grenzen auch durch Änderung der Wärmeleitfähigkeit des Latalysators bestimmt werden.

Der Wärmeaustausch verläuft um so schneller, je größer die Wärmeleitfähigkeit und die spezifische Wärme des Katalysatorenträgers ist. Bei oxydativen Prozessen ist daher z. B. die Verwendung von Aluminiumgrießträgern vorteilhaft. Natürlich sind die Wärmegradienten auch innerhalb der Katalysatorkörnchen beträchtlich. Wir haben bei unseren Versuchen auch in den großen Reaktoren Katalysatorenträger von 0,1 mm ∅ benutzt, um die Gradientenveränderung an der Katalysatoroberfläche vernachlässigen zu können und um zu verhüten, daß in den dünnen Reaktoren Gänge entstehen, welche die Ähnlichkeit des Strömungswiderstandes erheblich gefährden. In der Praxis haben sich Katalysatorkörnchen gut bewährt, deren Abmessungen 1/20 des Reaktordurchmessers betragen, dich besteht natürlich eine obere Grenze, die bei etwa 10 mm liegt.

Bei den Rohrreaktoren ist zu berücksichtigen, daß Wärmegradienten sich nicht nur in zur Reaktorachse senkrechten Querschnitten — in Gestalt von konzentrischen Kreisen — ausbilden, vielmehr ändern sich diese auch längeder Achse; deshalb sind die Gradienten dem gesamten Reaktor entlang oft derart, daß chemisch optimale Reaktionsverhältnisse nur in 10—20% des Reaktorraumes gesichert sind.

Entwicklung neuer Reaktortypen

Der für eine gegebene Reaktion als gut befundene Katalysator muß in Rohrreaktoren von verschiedenem Durchmesser und verschiedener Länge ausprobiert werden, um die optimalen Reaktorabmessungen experimentell entwickeln zu können. Bedient man sich des Prinzips der in Abb. 2 dargestellten Zylinderringselemente, so ist dieses Ziel leicht zu erreichen. Die Methode ist billiger, als der Bau besonderer Reaktoren für jede Abmessung. Mit Hilfe des „Metallbaukasten-Prinzips" können auch Profile mit beliebig verengertem oder erweitertem Querschnitt ausprobiert werden.

Die als optimal befundenen Reaktorabmessungen seien z. B. die Höhe l und der Radius r. Die industriellen Betriebe bauen nun zahlreiche, aus Rohren von Radius r und Länge l, d. h. aus optimal befundenen Reaktorelementen bestehende Reaktorrohrbündel in einem gemeinsamen Wärmeaustauschbad mit Wärmeregulierung.

Wir haben jedoch versucht, andere Wege zur Vergrößerung zu finden. Früher hatten wir nämlich bereits untersucht, wie Apparate für elektrolytische Herstellung gewißer Stoffe unter Verwendung konzentrischer Elektroden bequem vergrößert werden können.

Als Modellreaktion diente die Herstellung von Dihydrodimethoxy-Furan aus Clausen Class-Furan mittels elektrolytischer Alkoxylierung.

Der äußere Radius der zylindrischen Elektroden war R, der innere Radius r, und ihre Höhe l (Abb. 3).

Das Ergebnis der Arbeit war, daß bei Verwendung von Elektroden der Höhe l und einem Elektrodenabstand $R-r$ eine quasi unendlich breite *planparallele* Elektrode entstand. Die Strömungsverhältnisse einer entsprechend breiten planparallelen Elektrode in einer gegebenen vertikalen Ebene werden nämlich durch

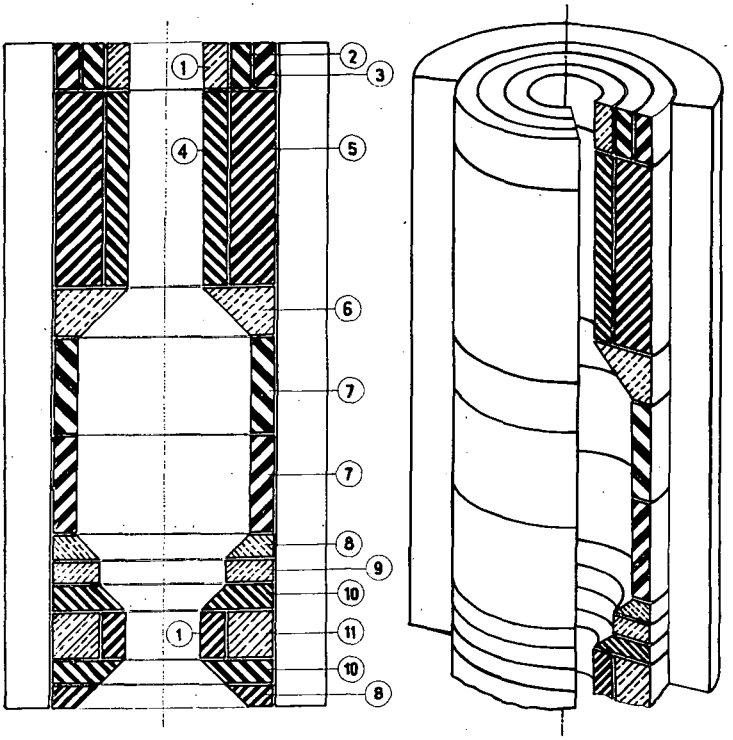

Abb. 2. Reaktor-Baukasten

den Umstand, ob die Entfernung zwischen Zentrum und Rand der Elektrode 20—30 cm, oder aber mehrere 100 Meter beträgt, nicht mehr verändert. Zu bemerken ist, daß außer der bequemen betriebsmäßigen Ausgestaltung nach unseren Versuchen die Verwendung einer doppelten Stromdichter möglicht wurde. Außerdem läßt sich auch die Pt-Oberfläche doppelt ausnutzen, wenn auch an der anderen Seite der Anode eine Kathode angebracht wird. Die geometrischen Beziehungen dieser Ergebnisse konnten bei den Vergrößerungsverschen des Planparallelreaktors erfolgreich verwendet werden.

Die Vergrößerung der heterogen-katalytischen Gasphasen-Reaktoren haben wir durch Veränderung der Form des Reaktors versucht. So gelangten wir zu der planparallelen, bzw. der scheibenförmigen Reaktorform, welche die Parallelschaltung mehrerer Rohrreaktoren mit kleinerem Durchmesser ersetzen, (Abb. 4). Was die Produktionskapazität und die Wärmeübergabe anbelangt, bleiben die Verhältnisse ähnlich; jedoch müssen die Investitionskosten kleinere Summen betragen als die gewohnten.

Gegenüber der mit der Dekarbonylierung (Abb. 5/2) verbundenen Umwandlung des Furfurols zu Furan wird die Reaktionswärme der von uns ausgearbeiteten oxydativen Dekarboxylierung (Abb. 5/3, 4, 5, 6) verzehnfacht, deshalb mußte bei der Planung von Laboratoriums- und Betriebseinrichtungen der Wärmeableitung gesteigerte Beachtung gewidmet werden.

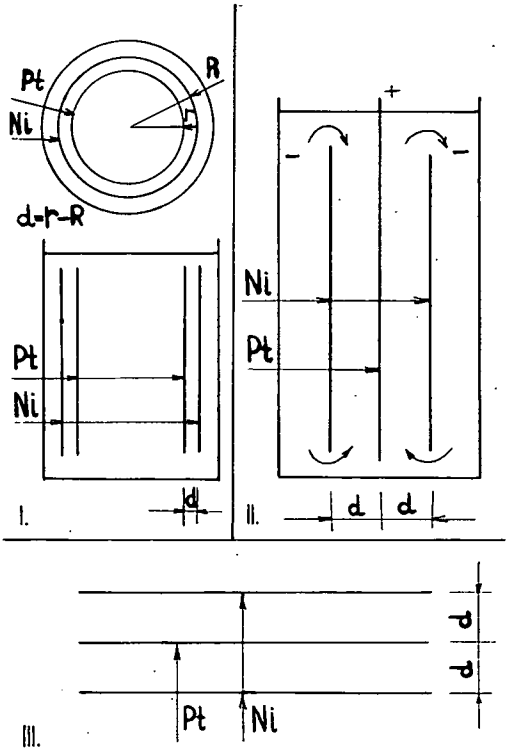

Abb. 3. Elektrolytische Einrichtung zur Alkoxylierung des Furans

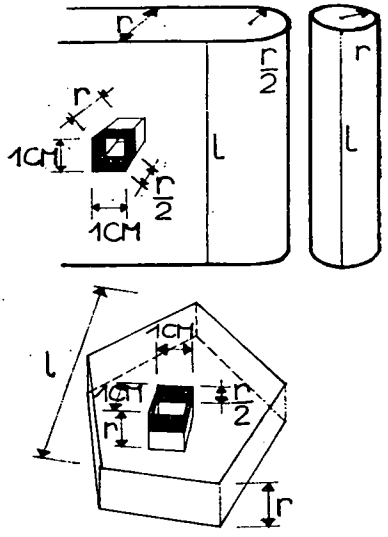

Abb. 4. Entwicklung der Planparallel- und Scheibenreaktorform

Die Vergrößerung des Maßstabes kann folgenderweise geschehen: Das Volumen des zylinderförmigen Reaktors von Radius r und Höhe l (Abb. 4.) sei

$$v = r^2\pi \cdot 1$$

die Oberfläche des wärmeaustauschenden Mantels $f = 2r\pi l$, das auf die wärmeaustauschende Oberflächeneinheit der Reaktorwand entfallende Katalysatorvolumen

$$c = \frac{v}{f} = \frac{r^2\pi l}{2r\pi l} = \frac{r}{2}$$

Wird die Dicke des durch Ebenen begrenzten planparallelen Reaktors als r cm gewählt und das Verhältnis des Volumens r cm³ eines zur Seitenwand senkrechten Prismas von 1 cm² Querschnitt zu seiner Oberfläche 2 cm² bestimmt, so erhalten wir ebenfalls

$$\frac{r}{2} = c.$$

Dies bedeutet, daß wir den Röhrenreaktor in einen Planparallelen Reaktor umwandeln können, denn c, der geometrische Ähnlichkeitsfaktor, ist identisch. Dieses

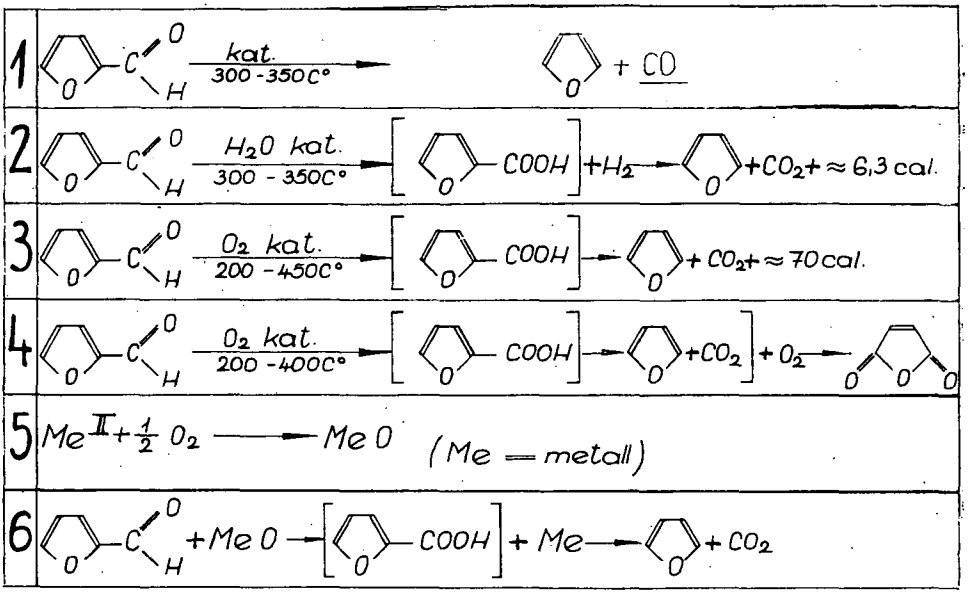

Abb. 5. Reaktionsgleichungen

Ähnlichkeitsprinzip kann zur Vergrößerung oxydativer Reaktionen geeignet sein, d. h., gibt bei einer gewissen organischen Reaktion ein Rohrreaktor vom Radius r und der Höhe l optimale Ergebnisse, so wird dessen betriebsmässige Variante ein durch parallelen Ebenen mit dem Abstand r begrenzter Planparallel-Reaktor mit der Höhe l sein. Die geometrische Ähnlichkeit des Reaktors ändert sich nicht, wenn seine Breite über alle Grenzen wächst. Wenn die Elemente des so „unendlich gemachten" Reaktors mit Halbzylindern vom Radius $r/2$ abgeschlossen werden, so ist das System auch von aerodynamischem Gesichtspunkt als annähernd unverändert zu betrachten, wenn eine Schädigung der organisch-präparativen Ergebnisse nicht beobachtet wird.

Die Planparallel-Reaktoren können parallel miteinander in Salz- oder Metall-Wärmeaustauschbäder gestellt werden, die mechanisch gerührt werden. In diesem Falle dürften die Betriebskosten geringer zu stehen kommen als gewöhnlich.

Werden aus gekrümmten Flächen Streifen der Breite l hergestellt und zwei davon in der Entfernung r voneinander angebracht, so entsteht wiederum ein Krummflächen-Parallelreaktor. Als Parallel-Reaktor ist auch eine Kugelschale der Dicke $r_2 - r_1 = r$ aufzufassen (Abb. 6), deren äußerer Radius r_2 und der innere r_1 ist. Der mittlere Radius der Kugelschale wird am besten so gewählt, daß — wenn das Gas an einem Punkte des Kugelmantels eintritt und am gegenüberliegenden Punkte entweicht — der zurückgelegte Weg gleich der Entfernung l ist. In diesem Falle verdichtet sich der Gasstrom an den Ein- und Austrittspunkten.

Nach dem Patent des VEB LEUNA-Werke läßt sich der Planparallelreaktor der Länge l nach spiralförmig zusammenrollen, (Abb. 7), dann entspricht der Weg der Gasströmung, das heißt die Länge der Spirale, im Sinne der bisherigen Interpretation der Höhe l des Reaktors.

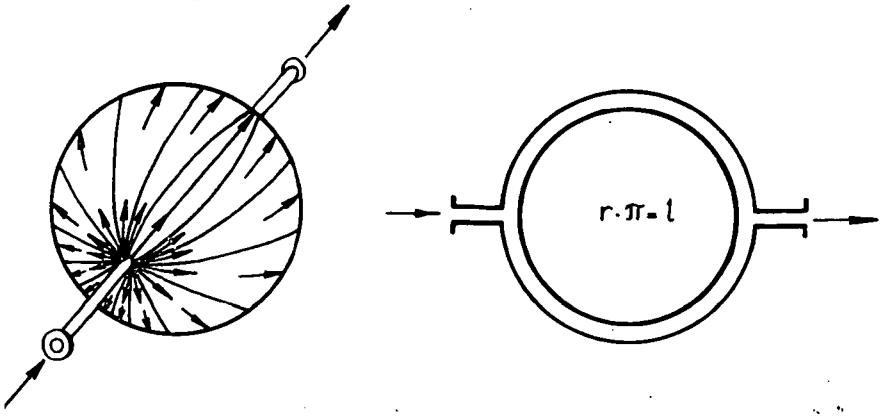

Abb. 6. Prinzipskizze einer Kugelschulenreaktors

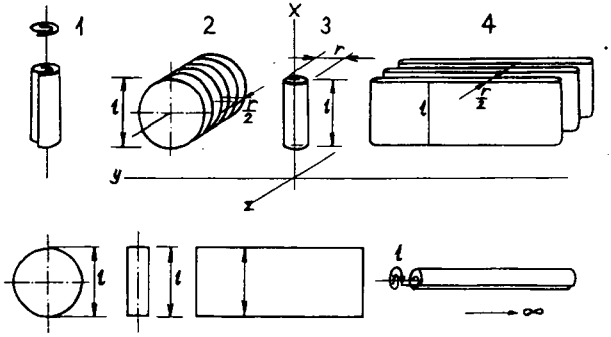

Abb. 7. Prinzipskizze verschiedener Ausmassvergrösserungen

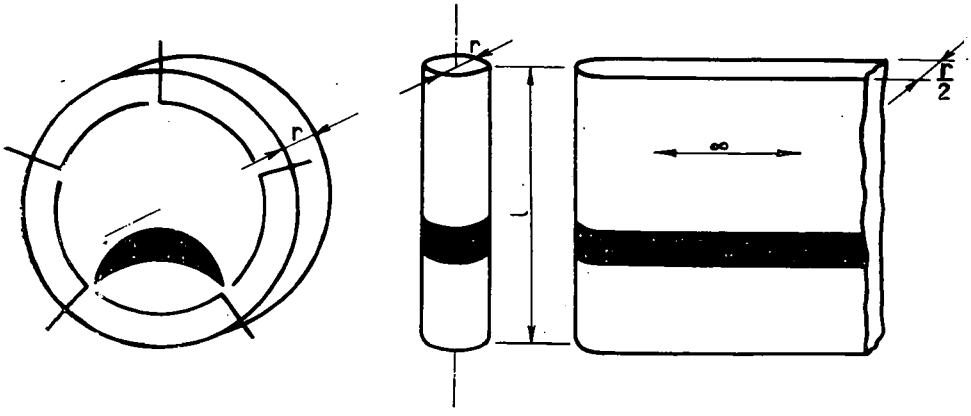

Abb. 8. Wärmegradienten im Rohr-, Planparallel- und Scheibenreaktor

Es läßt sich vorstellen, daß auch dieser Spiralreaktor unbegrenzt vergrößert wurden kann, indem ein unendlich langes Band in Spiralform zu einem Zylinder gerollt wird, d. h. seine „Verunendlichung" erscheint ausführbar.

Beim Planparallelreaktor treten ebenso Wärmegradienten in der Längsrichtung auf wie im Falle des Rohrreaktors (Abb. 8); werden die gleichen Abmessungen angenommen, so liegt der optimale Raum im Planparallelreaktor ebenso wie im Rohrreaktor.

Oft sind die Reaktionsbedingungen nur in 1/10 bis 1/20 des Katalysatorraumes optimal, an den übrigen Stellen verbrennt das Material oder die Produktion ist ungünstig, da die Temperatur unter der Reaktionstemperatur bleibt. Diesem Mißstand sucht man durch Verwendung von Reaktoren mit beweglichem Katalysatorbett abzuhelfen. Bei schwebenden Katalysatoren wird der gesamte Reaktionsraum ausgenutzt, doch ist die Veränderung der Raumgeschwindigkeit begrenzt, weil Altern und Abnutzung des Katalysators gleichzeitig entgegengesezte Operationen beanspruchen.

Wir halten die Planparallelisierung für ein verallgemeinerungsfähiges und nützliches Prinzip der Dimensionsvergrößerung, das sich besonders bei der Vergrößerung von Laboratoriumsapparaten verwenden läßt. Durch Berechnungen und Gedankenversuche haben wir die Vergrößerung mehrerer Laboratoriumsapparate durchgefährt, so wurden z. B. ein mit Rückflußkühler versehener, 1 Liter fassender Grignard—Rotoapparat und Destilliervorrichtungen vergrössert. Die mittels Planparallelisierung auf diese Weise für Betriebsausmaße ausgebauten Prozesse haben wir patentieren lassen, sie sollen in den weiteren Kapiteln unserer Artikelserie erörtert werden.

Scheibenreaktor

Der in planparalleler Form entwickelte Reaktor mit kreisförmigen Querschnitt ist der Scheibenreaktor, dessen Durchmesser der Höhe l des Rohrreaktors und des Planparallelreaktors gleich ist (Abb. 7).

Die im Reaktor herrschenden Strömungsverhältnisse haben wir an einem Prisma studiert, dessen Querschnitt ein gleichseitiges Sechseck ist, das sich in einen Kreis von 80 cm einschreiben läßt und dessen Dicke 4 cm betrug. An den sechs Ecken wurden Glashähne angebracht. Eine der sechseckigen Deckplatten des Prismas bestand aus Glas und wurde mit feuchten Phenolphtalein-Filterpapier belegt. An der einen Ecke strömte feuchte Ammoniak-Luft von konstanter Zusammensetzung mit unveränderter Dosierungsgeschwindigkeit ein, die dann an einer Stelle oder an mehreren in verschiedener Kombination abgeführt wurde. Bei den ersten, zur Untersuchung eines Reaktors mit homogener Phase dienenden Versuchen ließen wir den Reaktorraum frei (Abb. 9).

In den weiteren Versuchen wurden die aerodynamischen Verhältnisse des mit festem Katalysator gefüllten Raumes modelliert (Abb. 10). Die Katalysatorenträger waren Keramikzylinder von 5×5 mm. Die Ammoniak-Luft färbte das weiße Filterpapier — in Abhängigkeit von der Strömungszeit — in immer größeren Flecken rot. Durch alle Minuten vorgenommenes Photographieren der weißroten Flecken durch die Glaswand wurden die aerodynamischen Gradienten registriert. Die längste Versuchsdauer war 10 Minuten.

Wie zu erwarten, war in dem Modell mit homogener Phase den gestreckten Strömungslinien entsprechend die Bewegung der Gase weniger behindert als in dem Modell mit heterogener Phase, wo der Katalysator die Strömung stark beeinträchtigt.

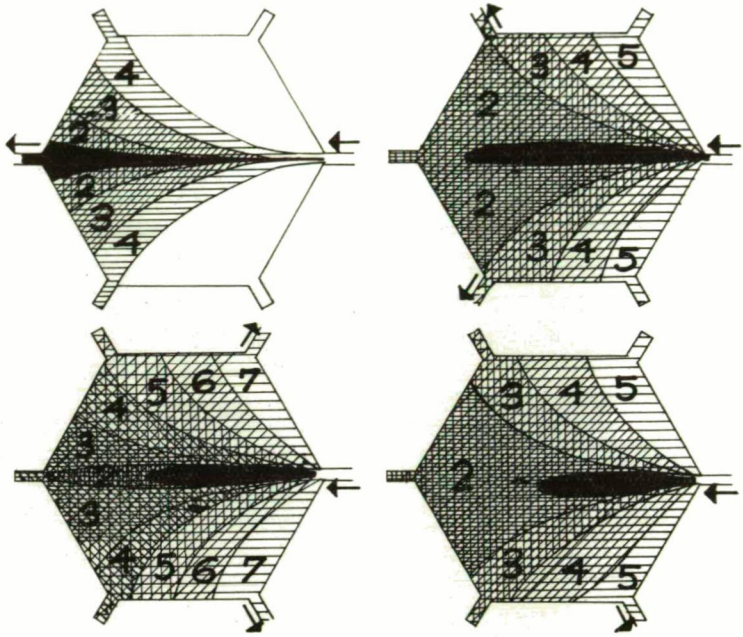

Abb. 9. Strömungsverhältnisse im Scheibenreaktor (homogene Phase)

Diesen Versuch haben wir — anstatt der punktförmigen Ein- und Ausführung der Gase — unter Ein- und Ausströmenlassen derselben auf der Ganzen Seitenlänge wiederholt. Anstatt an den Ecken wurde das Gas durch an den Seiten eines Fünfecks angebrachte, perforierte Rohre eingeführt bzw. abgeleitet.

Das Modellergebnis war bei diesen Versuchen am günstigsten. Es ist anzunehmen, daß auch die Gestaltung der Wärmegradienten an die Strömungslinien des Gases erinnert (Abb. 11).

Auch mit fixem Katalysatorenbett konnten wir im Scheibenreaktor günstige thermische Verhältnisse erzielen, wobei das gasförmige Material durch den Ecken eines Fünfecks entsprechende Öffnungen eintrat bzw. entwich (Abb. 12). Die Möglichkeit einer lokalen Überhitzung läßt sich weiter herabzusetzen, wenn die Ein- und Ausführungsstellen mittels einer Steuerungsvorrichtung mit verstellbarer Periode der Reitze nach gewechselt werden.

Bei allen Reaktionen, Katalysatoren und Reaktorgrößen soll eine minimale Anzahl von periodischen Umschaltungen gesucht werden, bei der die thermischen Bedingungen noch günstig sind. Die optimalen bzw. überhitzten Reaktionsstellen wechseln mit jeder Umschaltung. Durch entsprechende Einstellung der Umschaltperioden der Steuerung kann in Scheibenreaktoren selbst bei exothermen oxydativen

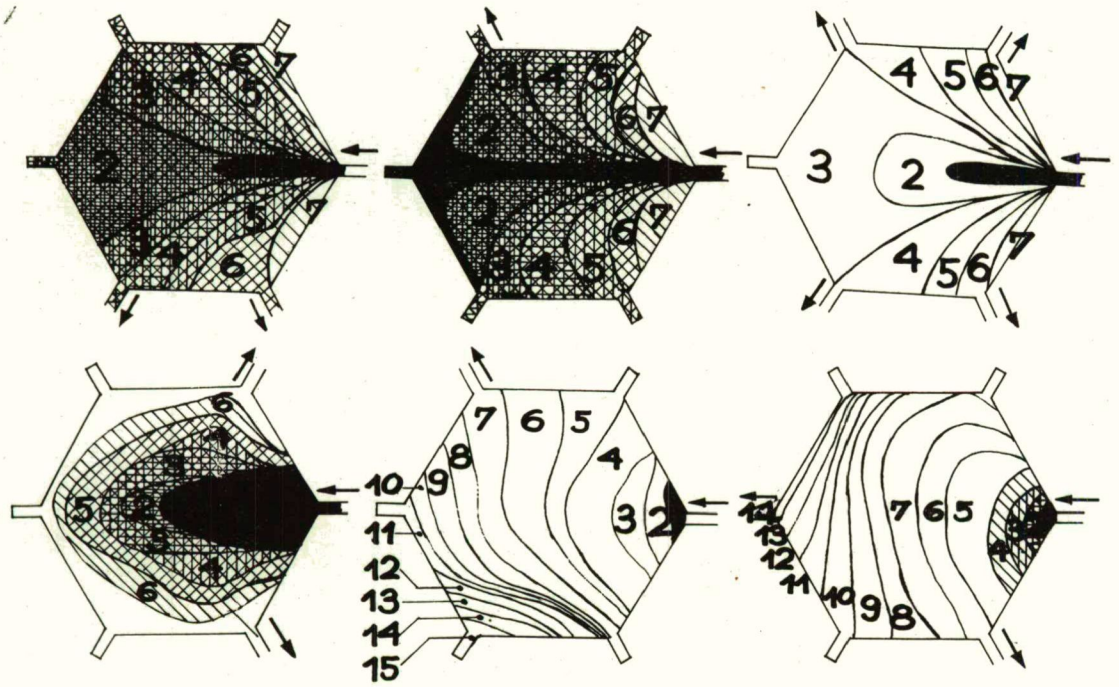

Abb. 10. Strömungsverhältnisse im Scheibenreaktor (heterogene Phase)

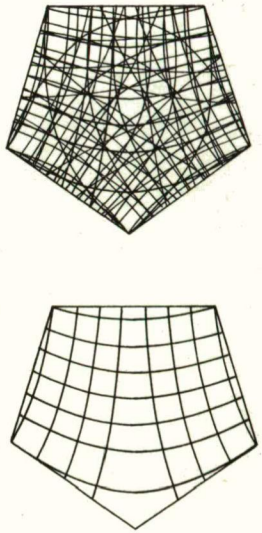

Abb. 11. Konstruierte Wärmegradienten und Strömungslinien im Scheibenreaktor

Prozessen die Temperatur an allen Punkten annähernd gleichmäßig gestaltet werden. Auf diese Weise ist eine gute Annäherung an die idealen oxydativen Reaktionsverhältnisse zu erreichen. Bei Reaktoren mit flüssigem Bett bleibt die Strömungsrichtung des Gases unverändert, der Katalysator bewegt und vermischt sich;

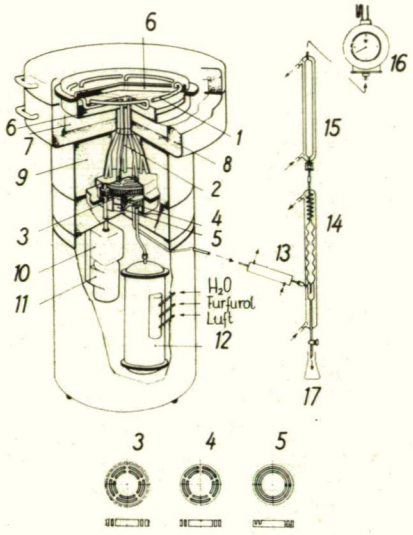

Abb. 12a. Schema des Scheibenreaktors 1 Perforierte Ein- bzw. Abführungsrohre; 2 Verbindungsrohre; 3 Drehbare Verteilungsscheibe; 4 Abführkammer; 5 Einführkammer; 6 Deckplatte; 7 Luftdichtung; 8 Perlitdichtung; 9 Untere Perlitdichtung; 10 Nortonschrank; 11 Motor; 12 Verdampfer bzw. Vorwärmer; 13 Metallener Liebig-Kühler; 14 Kondensbürette; 15 Aktivkohlen-Turm; 16 Gasmesser; 17 Sammler.

beim Scheibenreaktor ist der Katalysator unbeweglich und die Richtung der Gase wechselt. Es ist anzunehmen, daß es gelingen wird, die günstigen Verhältnisse des Flüssigkeits reaktors ohne Abnutzung des Katalysators und den damit verbundenen Nachteilen der aerodynamischen Fehlerquellen zu erreichen.

Die mit den Scheibenreaktoren unternommenen Versuche haben die daran geknüpften Hoffnungen gerechtfertigt. Die Weiterentwicklung des Themas sehen wir in parallelgeschalteten, mit einer Steuerung gleichzeitig betätigten Scheibenreaktoren (Abb. 7, 2).

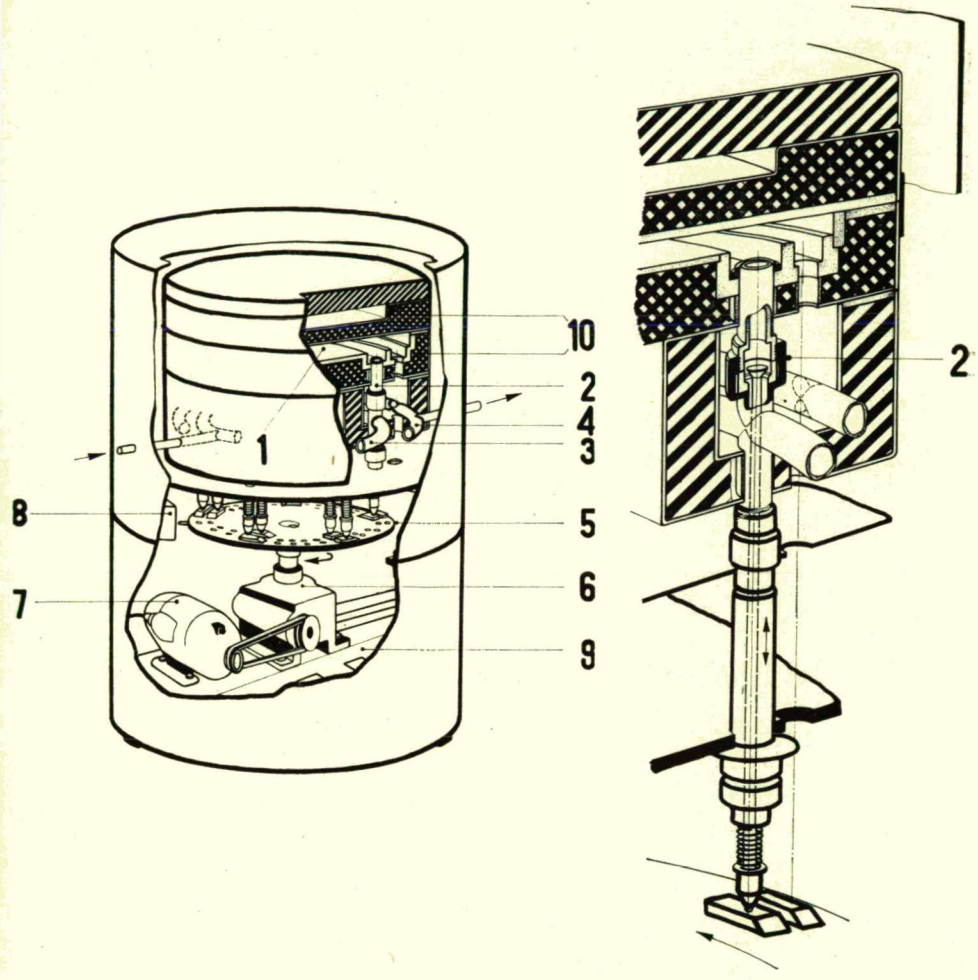

Abb. 12b. Ventile und Steuerung des Scheibenreaktors 1 Scheibenförmiger Katalysatorraum; 2 Ein- und Ausführventil des Reaktorraumes; 3 Ringförmiges Einleitungrrohr; 4 Ringförmiges Ableitungsrohr; 5 Steuerscheibe der Ventile; 6 Drehzahlreduktor; 7 Elektrischer Antriebmotor; 8 Programm-Schaltuhr; 9 Triebwerk-Haltevorrichtung; 10 Geheizte Metallblöcke des Scheibenreaktors.

Mit der gleichen Steuerungsvorrichtung können auch Würfel- (Abb. 13) oder Kugelreaktoren gesteuert werden (Abb. 14), bei denen das Reaktionsgas durch stellen weise perforierte Flächen eingeführt wird und entweicht. Der Vorteil dieser Methode ist, daß die Wärmequellendichte des Raumes entweder unverändert gelassen oder herabgesetzt werden kann, im Gegensatz zu den früher von Z. CIMBALNIK und Mitarbeitern beschriebenen Kugelreaktoren, in denen das Reaktionsgas zwischen der Oberfläche und der Mitte der Kugel strömt und nur zwei Richtungsänderungen zu verwirklichen sind. Auf diese Weise erhalten wir räumlich — u. Zw. vielleicht noch gesteigert — jene Vorteile, die wir beim Scheibenreaktor in der Ebene gefunden haben.

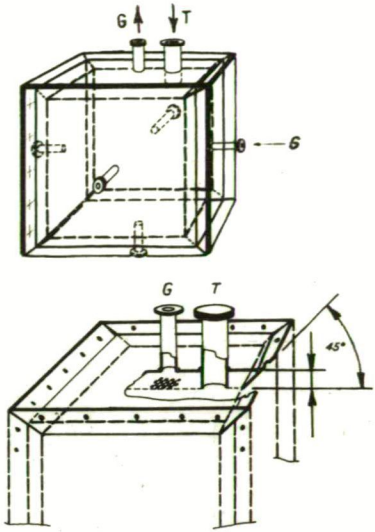

Abb. 13. Würfelförmiger Reaktor

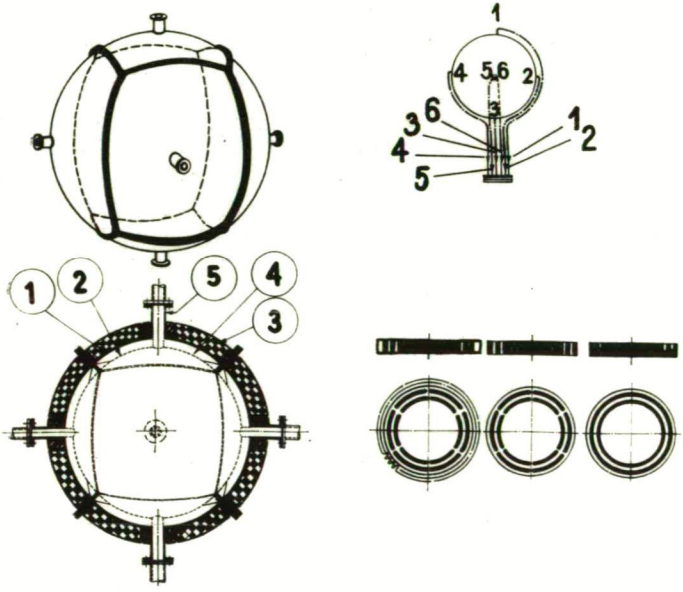

Abb. 14. Kugelreaktor

Experimenteller Teil

Zur Beweisführung unserer Vergrößerungstheorie haben wir außer den Modellversuchen den Planparallel- und den Scheibenreaktor entwickelt. Unsere Einrichtungen eignen sich zur Durchführung heterogener Reaktionen mit ruhenden Katalysatorbetten.

Die Planparallel- und Scheibenreaktoren wurden so geplant, daß der Katalysatorraum das Zehn- bzw. Achtfache desjenigen des klassischen Rohrreaktors beträgt. In diesem Falle soll nach unseren Berechnungen die Kapazität unserer Reaktoren das Zehn bzw. Achtfache jener der Rohrreaktoren betragen. Die Versuche haben unsere Annahmen bestätigt.

Als Modellreaktion diente die Umwandlung von Furfurol in Furan (Abb. 5/3) unter Anwendung von PbO als Katalysator. Diesen stark exothermen Prozess (70 Kcal) haben wir bereits mit Anwendung verschiedener Katalysatoren in verschiedenen Einrichtungen untersucht, so schien derselbe auch zur Bewertung unserer Vergrößerungsversuche geeignet.

Ausgangsmaterial: Destilliertes Furfurol, (Siedep. 161 °C) Oxydationsmittel: Luft, so dosiert, dass das Molverhältnis Furfurol: Sauerstoff 1:2 betrage. Katalysator: 40% PbO enthaltendes, mit Schamott und Wasserglas bereitetes Granulat. Durchschnittliche Katalysatorkorngrösse: $\varnothing = 2—4$ mm.

Temperatur der Reaktorwand bei der Durchführung der Reaktionen: 280 °C.

Planparallel-Reaktor (Abb. 15).

Zur Sicherung identischer Temperaturverhältnisse haben wir den zu vergrößernden und zugleich als Vergleichsbasis dienenden Rohrreaktor und dem vergrößerten Planparallel-Reaktor in den gleichen Heizblock gestellt. Durchmesser des Rohrreaktors 45 mm, Höhe 750 mm, Katalysatorvolumen 1,2 l.

Dicke des Planparallelreaktors 22,5 mm (identisch mit dem Radius des Rohrreaktors), Breite 720 mm (32 r), Höhe 750 mm (identisch mit der Höhe des Rohrreaktors, Katalysatorvolumen: 12 Liter.

Zunächst wurde der Prozess im Rohrreaktor untersucht. Mit Hilfe der Feindosierungsbürette (2) wurde Furfurol, und durch die Speiseforrichtung (1), den Stabilisierungsreduktor (3) und ein Differenzialmanometer (4) Luft in berechneter und gemessener Menge in den Verdampfer (5) eingeführt. Der Reaktor wurde so reguliert, daß das Reaktionsgemisch den Rohrreaktorteil (11a) passiert. Hier spielte sich die chemische Reaktion ab. Die Reaktionspodukte — zusammen mit dem nicht umgewanderten Furfurol — gelangten durch den Liebigschen Kühler (6) und die Kondensbürette (4), von der die flüssigen Produkte abgelassen werden konnten, in den Aktivkohlen-Turm (9a), wo das Furan adsorbiert wurde. Das Furan wurde von der Kohle mittels Wasserdampf-Desorption gewonnen.

Die Ergebnisse der im Rohrreaktor ausgeführten Versuche sind in Tabelle I zusammengefasst.

Nun wurden die Versuche im planparallelen Teil fortgeführt.

Die Dosierung der Reaktionskomponenten geschah auf die beim Rohrreaktor beschriebene Weise, doch wurde der Reaktor so reguliert, dass das Reaktionsgemisch den planparallelen Teil (11b) passieren mußte. Die Gewinnung der Reak-

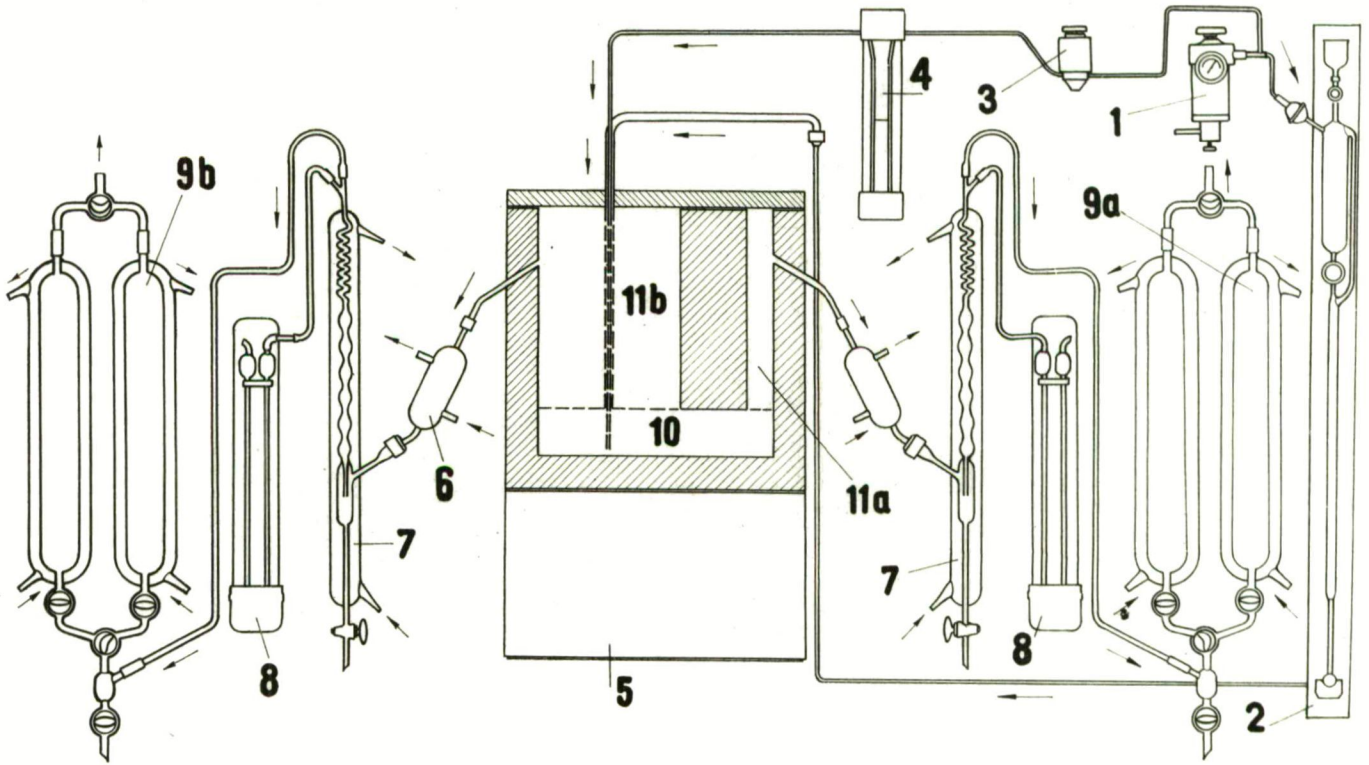

Abb. 15. Der Porozeß un Planparallelreaktor 1 Luft-Einspeisevorrichtung; 2 Feindosierungsbürette zur Furfuroldosierung; 3 Stabilisierungs-Reduktor; 4 Differentialmanometer; 5 Reaktorkörper; 6 Metallener Liebig-Kühler; 7 Kondensbürette; 8 Quecksilbermanometer; 9a und 9b Adsorptions-Kohlenturm; 10 Verdampfer; 11a Rohrreaktorteil; 11b Planparallelreaktorteil

Tabelle I

Dosierungsgeschwindigkeit		Konversion *K* (Mittelwert) %	Produktion *P* (Mittelwert) %	Ausbeute *A* (Mittelwert) %
Furfurol ml/Std.	Luft Liter/Std.			
10	28	98,9	15,3	15,4
15	40	89,8	17,1	19,0
20	56	81,2	16,2	19,4

tionsprodukte geschah auch hier auf die beschriebene Weise, doch erfolgte die Adsorption des Furans jetzt in dem mit 9b bezeichneten Kohlenturm.

Die Versuche haben unsere Theorie gerechtfertigt, da die zehnfache Vergrößerung gleichzeitig eine zehnfache Kapazitätssteigerung des Reaktors ergab. Wir haben auch untersucht, wieweit die Furfuroldosierungsgeschwindigkeit im Falle unseres Reaktors gesteigert werden kann.

Die Ergebnisse der Versuche sind in Tabelle II zusammengefaßt.

Tabelle II

Dosierungsgeschwindigkeit		Konversion *K* (Mittelwert) %	Produktion *P* (Mittelwert) -%	Ausbeute *A* (Mittelwert) %
Furfurol ml/Std.	Luft Liter/Std.			
101	280	97,9	16,0	16,5
143	400	97,4	19,9	20,4
188	550	94,2	28,6	30,3
237	680	95,3	30,9	31,8
294	810	97,6	35,0	35,8
349	960	96,9	32,9	34,0
386	1080	87,9	30,4	34,5

Aus der Tabelle und den graphischen Darstellungen (Abb. 16, 17) der Ergebnisse ist ersichtlich, daß unser Reaktor sich für den gegebenen chemischen Prozess vergrößer läßt und sogar günstiger angewandt werden konnte als der Rohrreaktor. Während in unserem Rohrreaktor auch bei einer Dosierungsgeschwindigkeit von 15 ml/Std. optimal nur eine Produktion von 17,1% zu erreichen war, betrug dieselbe im planparallelen Teil von zehnfachem Katalysatorvolumen bei einer Dosierungsgeschwindigkeit von 143 ml/Std. 19,9%. Unsere Einrichtung erreicht den optimalen Produktionswert erst bei einer doppelt so hohen Belastung, bei einer Dosierungsgeschwindigkeit von 300 ml/Std.

Scheibenreaktor (Abb. 12 und Darstellung des Prozesses Abb. 18).

Aus dem vergrößerten Planparallelreaktor haben wir einen sowohl in der Form, als auch in der Betriebsweise neuen Reaktortyp — den Scheibenreaktor — entwickelt. Der Katalysator ist in dem scheibenfärmigen Reaktorkörper untergebracht, welcher einen Durchmesser von 750 mm hat, der mit der Höhe des Rohr- und Planparallelreaktors übereinstimmt. Die Dicke des Scheibenreaktors ist 22,5 mm, wie der Radius des Rohrreaktors und die Dicke des Planparallelreaktors. Das Katalysatorvolumen beträgt 10 Liter, was eine achtfache Vergrößerung des Rohr-

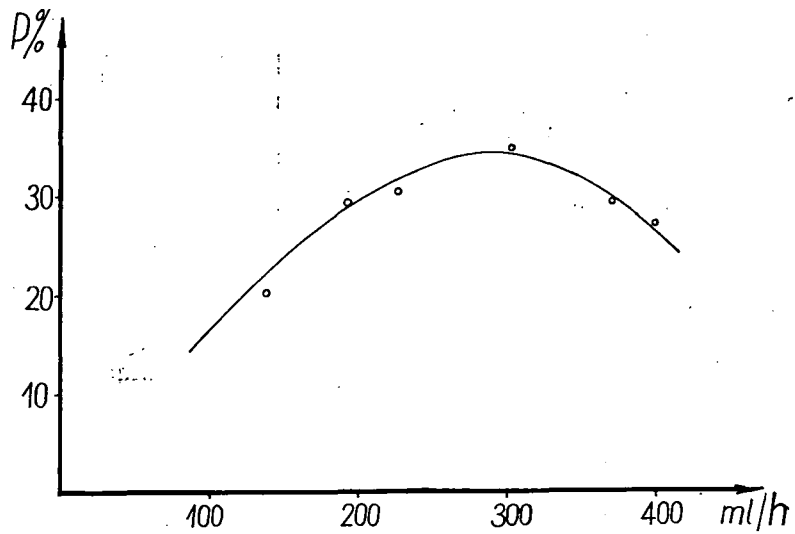

Abb. 16. Produktion im Planparallelreaktor in Abhängigkeit von der Dosierungsgeschwindigkeit

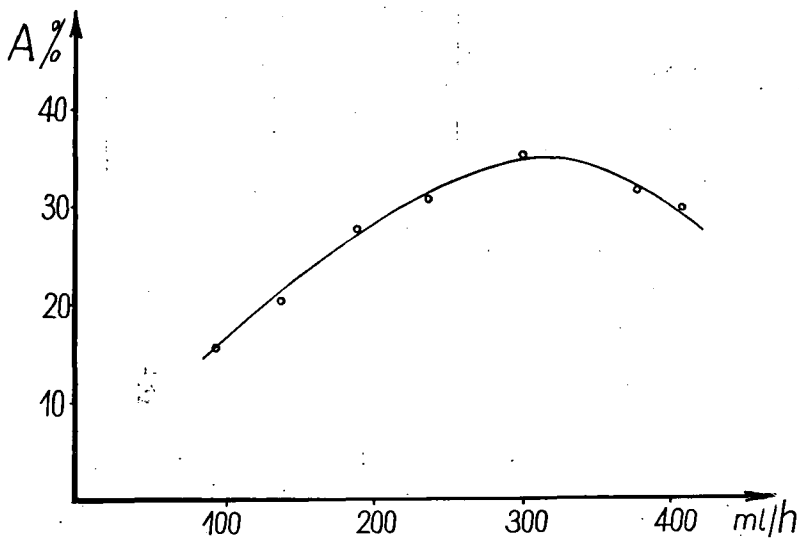

Abb. 17. Ausnutzung im Planparallelreaktor in Abhängigkeit von der Zeit

reaktors bedeutet. Die Verringerung der infolge der Vergrößerung entstehenden lokalen Überhitzung wurde beim Planparallelreaktor durch die Geometria des Reaktors gesichert. Auch der Scheibenreaktor verfolgt dasselbe ziel, doch wird bei letzterem die lokale Übernitzung durch den periodischen Wechsel der Einfüh-

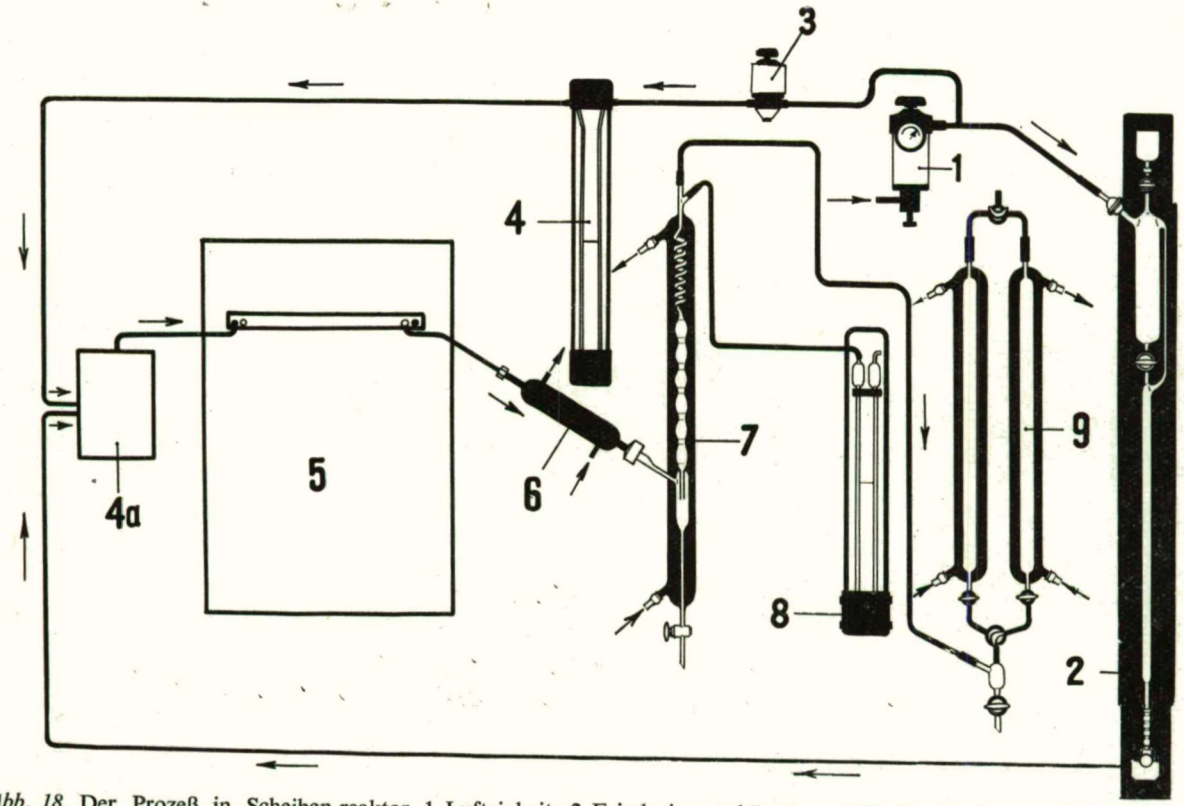

Abb. 18. Der Prozeß in Scheiben-reaktor 1 Lufteinheit; 2 Feindosierungsbürette zur Furfuroldosierung; 3 Stabilisierungsreduktor; 4 Differentialmanometer; 4a Verdampfer; 5 Reaktor; 6 Metallener-Liebig Kühler; 7 Kondensbürette; 8 Quecksilbermanometer; 9 Adsorptions-Kohlenturm

rungsstelle des Reaktionsgemisches und der Ableitungsstelle des Reaktionsproduktes sprungweise herabgesetzt.

Das Einspeisen des Reaktionsgasgemisches und die Abführung der Reaktionsprodukte geschieht durch zwei, den Reaktorumfang in fünf gleiche Teile teilende, voneinander unabhängige, perforierte Röhrensysteme. Das äussere System ist dem Verdampfer, das innere dem Liebigschen Kühler angeschlossen. Die einzelnen Röhrenabschnitte werden mittels Ventilen verschlossen bzw. geöffnet. Das Schließen und Öffnen der Ventile wird durch die entsprechend programmierte Steuerung gesichert.

In der ersten Versuchsreihe wurde die Steuerung so eingestellt, dass ein Rohrabschnitt der Speissystems und das entfernteste Abfährungsrohr gleichzeitig offen waren. Alle 5 Minuten wurde die Ein- bzw. Abführung auf die nächstfolgenden Rohrabschnitte verlegt. — In der zweiten Versuchsreihe wurden die Ein- und Abführstellen alle 10 Minuten gewechselt. Die Versuche wurden mit den gleichen Dosierungsgeschwindigkeiten durchgeführt, wie beim Planparallelreaktor.

Aus der Feindosierungsbürette (2) wurde Furfurol, und durch die Speisevorrichtung (1), den Stabilisierungsreduktor (3) und Rotameter (4) Luft in regulierten und gemessenen Mengen in den Verdampfer (4a) eingeführt. Die mit der vorgewärter Luft vermischten Furfuroldämpfe gelangten in der Reaktor, dann passierten die Reaktionsprodukte den metallenen Liebigschen Kühler (6), die Kondensbürette (7) und den Kohlenturm (9). Das nichtumgewandelte Furfurol und das Wasser sammelten sich in der Kondensbürette. Das im Kohlenturm adsorbierte Furan wurde mit Wasserdampf desorbiert.

Die Ergebnisse sind in Tabelle III Zusammengefaßt und in Abb. 19—21 graphisch dargestellt.

Tabelle III

Dosierungsgeschwindigkeit		Konversion *A* (Mittelwert) % bei 5 Min. — Perioden %		Produktion *T* (Mittelwert) % bei 5 Min. — Perioden %		Ausbeute *K* (Mittelwert) % bei 5 Min. — Perioden %	
Furfurol ml/Std.	Luft Liter/Std.	5 Min.	10 Min.	5 Min.	10 Min.	5 Min.	10 Min.
101	208	83,3	84,3	16,0	21,0	19,2	24,8
148	400	84,0	86,1	19,2	27,3	22,8	31,7
198	550	85,3	87,0	25,6	31,1	30,0	35,7
249	680	87,2	90,2	30,3	33,7	34,7	37,3
299	810	86,9	87,3	34,8	34,1	40,1	39,0
351	960	83,9	83,7	36,1	32,9	43,3	39,4
398	1080	80,1	82,0	31,2	28,2	38,7	38,3

Die Meßergebnisse haben bewiesen, dass die Vergrößerung im Falle des Scheibenreaktors bessere Ergebnisse lieferte, als beim Planparallelreaktor. Die Kapazität des auf das Axhtfache des Rohrreaktors vergrößerten Scheibenreaktors beträgt das Zehnfache derjenigen des Rohrreaktors.

Außer der richtigen Wahl der Geometrie des Reaktors spielt also die Einführung bzw. Ableitung an verschiedenen Stellen eine äußert wichtige Rolle. Mit der kürzeren Schaltzeit ließ sich bei größerer Furfuroldosierungsgeschwindigkeit ein höheres Produktionsmaximum erreichen als mit den längeren Schaltperioden.

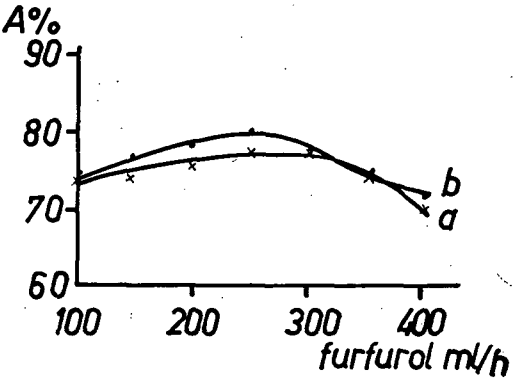

Abb. 19. Konversion im Scheibenreaktor in Abhängigkeit von der Dosierungsgeschwindigkeit: *a* 5 Min.-, *b* 10 Min.-Perioden

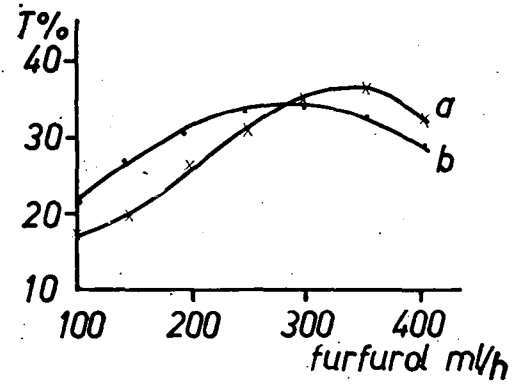

Abb. 20. Produktion im Scheibenreaktor in Abhängigkeit von der Dosierungsgeschwindigkeit: *a* 5 Min.-, *b* 10 Min.-Perioden

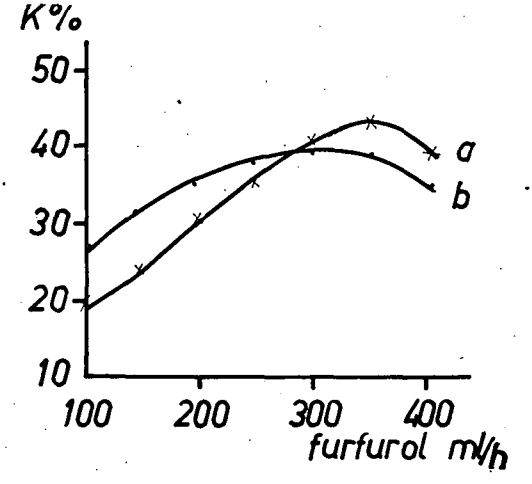

Abb. 21. Ausnutzung im Scheibenreaktor in Abhängigkeit von der Dosierungsgeschwindigkeit: *a* 5 Min.-, *b* 10 Min-Perioden

Bei längeren Umschaltperioden waren dagegen in einem breiteren Bereich der Furfuroldosierungsgeschwindigkeit höhere Produktionswerte zu erzielen.

Im weiteren sollen andere exotherme Prozesse untersucht werden, da die bisherigen Versuche zeigen, dass unsere Vergrößerungtheorie erfolgreich anwendbar ist.

Literatur

[1] *Mészáros, L., Gy. Schöbel:* Acta Phys. et Chem. Szeged **13**, 77 (1967).
[2] *Mészáros, L.:* Observation sur l'agrandissement des dimensions des reacteurs de différents types. XXXIVe Congres International de Chimie Industrielle. Belgrade, 22—29. Sept. 1963; Chimie et Industrie **90**, 175 (1963).
[3] *Benedek P., A. László:* A vegyészmérnöki tudomány alapjai (Műszaki Könyvkiadó, Budapest, 1964).
[4] A Magyar Tudományos Akadémia Műszaki Kémiai Kutató Intézete Kiadványai, 1960—1968.

ИЗУЧЕНИЕ РЕАКТОРОВ ЭКЗОТЕРМИЧЕСКИХ КАТАЛИТИЧЕСКИХ ПРОЦЕССОВ I

Л. Месарош и Ш. А. Гильде

Увеличение размера трубчатых печей было осуществлено путем сохранения их высот, поместив площадь катализаторов между параллельными поверхностями. Расстояние поверхностей было меньше толщины трубчатой печи. Такой метод увеличения размеров не повредило специфическим значениям выхода и в то же время размер прибора мог быть увеличен линеарным расчётом. Метод имеет общий характер.

Таким же методом изготовили полосовой и занавесный реактор из пряжного реактора и зазорные и кругловато-зазорные распылители из распылителя. Потом из планпараллельного реактора изготовился дискообразный реактор и устроили в него пять пробивных дуговых труб для впуска и выпуска реакционных газов. Место ввода и вывода изменилось автоматически и тогда местные перенагревания не могли повредить так как они непрерывно переместились с одного места на другое.

Полезность этой семьи приборов оценилась и была утверждена реакцией изготовления фурана из фурфурола, имеющей очень высокую реакционную температуру.

INDEX

TOMI PRIORES

Acta Chemica, Mineralogica et Physica,	Tom.	I,	Fasc.	1—2,	1928—29.
Acta Chemica, Mineralogica et Physica,	Tom.	II,	Fasc.	1—2,	1932.
Acta Chemica, Mineralogica et Physica,	Tom.	III,	Fasc.	1—3,	1934.
Acta Chemica, Mineralogica et Physica,	Tom.	IV,	Fasc.	1—3,	1934.
Acta Chemica, Mineralogica et Physica,	Tom.	V,	Fasc.	1—3,	1937.
Acta Chemica, Mineralogica et Physica,	Tom.	VI,	Fasc.	1—3,	1938.
Acta Chemica, Mineralogica et Physica,	Tom.	VIII,	Fasc.	1—3,	1939.
Acta Chemica et Physica,	Tom.	I,	Fasc.	1—2,	1942.
Acta Chemica et Physica,	Tom.	II,	Fasc.	1—6,	1948—50.
Acta Physica et Chemica, Nova series	Tom.	I,	Fasc.	1—4,	1955.
Acta Physica et Chemica, Nova series	Tom.	II.	Fasc.	1—4,	1956.
Acta Physica et Chemica, Nova series	Tom.	III,	Fasc.	1—5,	1957.
Acta Physica et Chemica, Nova series	Tom.	IV,	Fasc.	3—4,	1958.
Acta Physica et Chemica, Nova series	Tom.	V,	Fasc.	1—2,	1959.
Acta Physica et Chemica, Nova series	Tom.	V,	Fasc.	3—4,	1959.
Acta Physica et Chemica, Nova series	Tom.	VI,	Fasc.	1—4,	1960.
Acta Physica et Chemica, Nova series	Tom.	VII,	Fasc.	1—2,	1961.
Acta Physica et Chemica, Nova series	Tom.	VII,	Fasc.	3—4,	1961.
Acta Physica et Chemica, Nova series	Tom.	VIII,	Fasc.	1—2,	1962.
Acta Physica et Chemica, Nova series	Tom.	VIII,	Fasc.	3—4,	1962.
Acta Physica et Chemica, Nova series	Tom.	IX,	Fasc.	1—2,	1963.
Acta Physica et Chemica, Nova series	Tom.	IX,	Fasc.	3—4,	1963.
Acta Physica et Chemica, Nova series	Tom.	X,	Fasc.	1—2,	1964.
Acta Physica et Chemica, Nova series	Tom.	X,	Fasc.	3—4,	1964.
Acta Physica et Chemica, Nova series	Tom.	XI,	Fasc.	1—2,	1965.
Acta Physica et Chemica, Nova series	Tom.	XI,	Fasc.	3—4,	1965.
Acta Physica et Chemica, Nova series	Tom.	XII,	Fasc.	1—2,	1966.
Acta Physica et Chemica, Nova series	Tom.	XII,	Fasc.	3—4,	1966.
Acta Physica et Chemica, Nova series	Tom.	XIII,	Fasc.	1—2,	1967.
Acta Physica et Chemica, Nova series	Tom.	XIII,	Fasc.	3—4,	1967.
Acta Physica et Chemica, Nova series	Tom.	XIV,	Fasc.	1—2,	1968.
Acta Physica et Chemica, Nova series	Tom.	XIV,	Fasc.	3—4,	1968.

A kiadásért felelős: Budó Ágoston
1969
A kézirat nyomdába érkezett: 1969. február. Megjelenés 1969 június.
Példányszám: 480 Ábrák száma: 42 Terjedelem: 8,1 (A/5) ív
Készült monoszedéssel, íves magasnyomással, az MNOSZ 5601—54 és az MNOSZ 5602—50 A szabványok szerint

69-7149 — Szegedi Nyomda